Federal Ministry of Education and Research

UNIVERSITE D'ABOMEY - CALAVI (UAC)

INSTITUT NATIONAL DE L'EAU

WASCAL
West African Science Service Center on Climate Change and Adapted Land Use

Registered under N°: 5221-17/UAC/VR-AARU/SA

A DISSERTATION

Submitted in partial fulfillment of the requirements for the degree of
DOCTOR of Philosophy (PhD) of the University of Abomey-Calavi (Benin Republic)
In the framework of the
Graduate Research Program on Climate Change and Water Resources (GRP-CCWR)

By

Fati Aziz

Public defense on: 11/07/2017

======

ASSESSING THE IMPACT OF CLIMATE AND LAND USE/LAND COVER CHANGE ON STREAMFLOW AND SEDIMENT YIELD IN THE BLACK VOLTA RIVER BASIN USING THE SWAT MODEL

======

Supervisors

Abel A. Afouda, Professor, Laboratoire d'Hydrologie Appliquée Faculté des Sciences de l'Université de Abomey-Calavi (Benin)
Emmanuel Obuobie, Dr., Senior Research Scientist, Water Research Institute, Accra (Ghana)
Jaehak Jeong, Associate Professor, Spatial Science Laboratory, Texas A&M University, (United States of America)

======

Reviewers

Sounmaila Moumouni, Professor, Université Nationale des Sciences Technologies, Ingénierie et Mathematiques d'Abomey (Benin)
Sylvie Galle, Professor, Institut des Géosciences de l'Environment (France)
Albert Goula, Professor, Universite Nangui Abrogoua-Abidjan (Côte d'Ivoire)

======

Jury

Norbert Hounkonnou, Professor, Université de Abomey-Calavi, **President**
Joshua A. Odofin, Professor, Federal University of Technology, Minna- Nigeria, **Examiner**
Kwasi Preko, Associate Professor, Kwame Nkrumah University of Science and Technology, Kumasi (Ghana), **Examiner**
Julien Adounkpe, Professor, Université de Abomey-Calavi (Benin), **Examiner**
Sounmaila Moumouni, Professor, Université Nationale des Sciences Technologies, Ingénierie et Mathematiques d'Abomey (Benin), **Reviewer**
Sylvie Galle, Professor, Institut des Géosciences de l'Environment (France), **Reviewer**
Abel A. Afouda, Professor, Université de Abomey-Calavi (Benin), **Supervisor**

Dedication:

To my dad, Abdel-Aziz Farouk and mum, Memuna Musah

Alhamdulillah, we made it!!!

ACKNOWLEDGEMENTS

This PhD work is realized in the framework of the West African Science Service Center on Climate Change and Adapted Land use (WASCAL) and funded by the **German Ministry of Education and Research (BMBF) in collaboration with the Benin Ministry of High Education and Scientific Research (MESRS).**

I'm extremely grateful to my supervisors Prof. Abel Afouda, Dr. Emmanuel Obuobie and Dr. Jaehak Jeong for their support and guidance throughout this research. To Dr. Mouhamadou Bamba Sylla, Prof. Joulien Adounkpe and Prof. Emmanuel Lawin, thank you for your assistance.

My special thanks go to the German Federal Ministry of Education and Research (BMBF) for providing the funds for this research through the West African Science Service Centre on Climate Change and Adapted Land Use (WASCAL). I am also grateful to the staff of the Graduate Research Program (GRP) Climate Change and Water Resources at the University of Abomey Calavi for the training and to my colleagues in the group for the support.

I would like to express my appreciation to Mr. Aaron Bundi Aduna, Basin Officer of the White Volta River Basin, Ghana, for his immeasurable help and support during fieldwork. I will forever remain indebted to you, Sir.

I would like to thank Dr. Raghavan Srinivasan, Director of the Spatial Science Laboratory, Texas A&M University, USA for providing me office space and expert advice during my sojourn at the University. Many thanks go to Dr. Prasad Daggupati of the Spatial Science Laboratory, Texas A&M University for supervising the thesis during my research stay at Texas A&M University. Thanks to Dr. Yihun Dile and Dr. James Kiniry for their assistance in the research.

My appreciation goes to Mr. Samuel Guug and Mr. Kwasie, for the great help during sampling and for holding the fort whenever I was engaged in other aspects of the research. Many thanks go to Mr. Ben and all my field workers who worked tirelessly to ensure the realization of this research. Monica, you made fieldwork interesting, I'm grateful.

My sincere gratitude goes to Dr. Benjamin Kofi Nyarko, a Senior Lecturer at the University of Cape Coast - Ghana and Coordinator of the WASCAL Doctoral program on Climate Change and

Agriculture, for providing me with office space and a GIS tutor at the University of Cape Coast. Special gratitude to Mr. Osman Adams for opening for me the doors to the Geographic Information Systems (GIS) world.

I would like to thank Professor Ousmane Seidou, of the University of Ottawa, Canada, for providing the CORDEX downscaling tool used in the climate downscaling aspect of this research, and for his prompt response to my e-mails concerning the use of the tool.

Many thanks to Mr. Collins Kissi and Mr. Appiah of Water Research Institute, Ghana for guiding me throughout my field and laboratory work. My gratitude goes to Dr. Kwabena Kankam-Yeboah, Dr. Barnabas Amisigo, Dr. Emmanuel Bekoe, Madam Saada Mohammed, Mr. Abdul-Razak Iddrisu, Mr. and Mrs. Gown, Mr. Peter Baako, and Mr. Mahmud Mohammed, for taking special interest in the progress of my work.

Special thanks go to the Banguras, the Bibilazus, the Affuls, Emma, Isaac, Sintayehu and Fikirte for making life and work comfortable and fun during my PhD working visit to the Spatial Science Laboratory at the Texas A&M University, USA.

To all friends who supported and encouraged me throughout this research, thank you for being there for me.

Thank you to my wonderful parents and siblings, for the love and support. I'm also grateful to the entire Cofie family, for their encouragement.

I will forever be grateful to my husband, Mr. Abdul Razak Mohammed Cofie for his massive support throughout the research and for being the greatest "backing vocalist" ever.

ABSTRACT

The Black Volta River Basin (BVRB) in West Africa plays a vital role in supporting the life in and around it. However, the availability and use of the water resource of the basin is threatened by population growth, changes in land use/land cover (LULC) and climate change. This study aimed at assessing the impact of climate change on the flow and sediment yield of the BVRB and investigating the sensitivity of the flow to changes in LULC in order to provide recommendations to inform sustainable planning and management of the water resources.

Prior to the impact study, trends in historical (1981-2010) extreme events over the basin were analyzed using the RClimDex 1.0 software package. Projections of rainfall and mean temperature for 2051-2075 (late 21st century) and 2076-2100 (end of the 21st century) under the RCPs 4.5 and 8.5 for the basin (relative to the historical period) were made using downscaled and bias corrected data from the CORDEX West African project. The model simulation data consisted of precipitation and temperature projections from two RCMs (RCA4 and RACMO22T) driven by three GCMs (MPI-ESM-LR, ICHEC-EC-EARTH, CCCma-CanESM2) for a total of three RCM/GCM pairs. The Soil and Water Assessment Tool (SWAT) model was calibrated and validated for simulation of the basin's flow and sediment yield. After assessing the model's performance in the simulations, projections were made to ascertain the future (2051-2075 and 2076-2100 under the RCPs 4.5 and 8.5) direction of flow and sediment yield in the basin. Finally, the sensitivity of streamflow to changes in LULC in the basin was assessed based on 2 LULC maps (1990 and 2000) developed for the basin.

The results of the extreme event analysis showed a warming trend in temperature, and increasing trends in amounts and intensity of rainfall events over the basin during the historical period. Analyses of average annual, intra-annual and seasonal rainfall indicated high uncertainty regarding the direction of the future rainfall. Mean annual rainfall change for the late 21st century ranged between -16% and +6% under the RCP4.5 scenario and between -27% and +14% under the RCP8.5 scenario. The end of the 21st century projections showed changes ranging between -23% and +2% and between -33% and +13% under the RCP4.5 and RCP8.5 scenarios, respectively. With regards to temperature, average annual projections by the ensemble runs showed increases over the basin under both RCP scenarios and for both time periods. Warming over the basin is projected to be higher under the RCP8.5 scenario than under the RCP4.5 scenario, with the end of the 21st century being warmer than the late 21st century. Average annual mean temperature increase across the model runs ranged between 2.2^{o}C and 2.6^{o}C under the RCP4.5 scenario and between 3.5^{o}C and 3.7^{o}C under the RCP8.5 scenario for the end of the 21st century. The SWAT model's performance in reproducing monthly streamflow and sediment yield of the basin during calibration was rated as "good". The Nash-Sutcliffe efficiency (NSE), coefficient of determination (R^2), percent bias (PBIAS) and root mean square error (RSR) values for streamflow calibration were 0.85, 0.86, 8.1% and 0.38 respectively. Sediment calibration results yielded NSE of 0.68, R^2 of 0.76, PBIAS of 27.5% and RSR of 0.57. In general, the model validation results were "satisfactory" for both flow and sediment yield. The NSE, R^2, PBIAS and RSR values for streamflow validation were 0.60, 0.62, 20.1% and 0.64 respectively while that

for sediment yield were 0.65, 0.74, 39.1% and 0.59 respectively. The p- and r-factor values for the model calibration and validation indicated that low levels of uncertainties existed in the model results. Analysis of dry - (November to March) and wet - (August to October) period streamflow and sediment yield showed mainly increases for the late- and end of the 21st century under both scenarios. Mean annual streamflow is projected to range between +40% and +42%, and between +100% and +143% for sediment yield during the late 21st century under the RCP4.5 scenario. For the end of the 21st century, the projected change ranges between -6% and +78% while sediment yield is between +100% and +216%. Under the high emission RCP8.5 scenario, streamflow is projected to range between +48% and up to +148% across the models. For sediment yield the projected change ranges from +249% to +335%. The end of century projections of flow is between +69% and +243% while total sediment ranges between +358% and 412% across models. Sensitivity analysis of streamflow in the basin based on a 10-year land use/land cover change showed statistically insignificant changes. Recommendations for coping with the projected changes in BVRB have been made based on the findings of the study.

Key words*:* Climate Change, Land use/land cover change, streamflow, sediment yield.

SYNTHÈSE DE LA THÈSE

RÉSUMÉ

Situé en en Afrique de l'Ouest, le Bassin de la Volta Noire (BVRB) joue un rôle essentiel dans le maintien de la vie. Cependant, la disponibilité et l'utilisation des ressources en eau du bassin sont menacées par la croissance démographique, le changement dans l'occupation et utilisation des sols (OUS) et le changement climatique. L'objectif de cette étude était d'évaluer l'impact du changement climatique sur le débit d'écoulement et sur l'apport en sédiments de la BVRB, et de déterminer la sensibilité du débit d'écoulement aux changements dans l'OUS afin de formuler des recommandations pour la planification et la gestion des ressources en eau.
Avant l'étude d'impact sur le changement climatique, les tendances des événements extrêmes de température et de précipitation du BVRB ont été détectées à l'aide du logiciel RClimDex 1.0 pour la période historique (1981-2010).
Le modèle hydrologique SWAT (en raison de sa grande flexibilité) a été utilisé pour l'analyse de l'impact du changement climatique sur le débit d'écoulement et l'apport en sédiments du bassin. Le programme SUFI-2 de SWAT- CUP a été utilisé pour la calibration et la validation de SWAT pour les sous-bassins de Bui et de Chache pour les analyses relatives au débit d'écoulement et à l'apport en sédiments respectivement. En outre, les données journalières de précipitation, de température minimale et maximale de 11 stations climatiques couvrant les périodes 1985-2005 (période de référence) et 2051-2100 (simulations pour le futur) ont été réduites à l'échelle locale et corrigées avant d'être utilisées comme entrée du modèle hydrologique SWAT pour simuler les débits d'écoulement et les apports en sédiments. Les données incluent des projections de deux (02) modèles climatiques régionaux (MCR), RCA4 et RACMO22T pilotés par trois (03) modèles de circulation générale (MCG), MPI-ESM-LR, ICHEC-EC-EARTH, et CCCma-CanESM2 pour les scénarios du GIEC RCP4.5 et RCP 8.5. La sensitivité du débit d'écoulement aux changements dans l'OUS a été évaluée en alimentant le modèle SWAT avec de deux (02) cartes OUS (1990 et 2000) établies pour le bassin.
Le modèle hydrologique SWAT (en raison de sa grande flexibilité) a été utilisé pour l'analyse de l'impact du changement climatique sur le débit d'écoulement et l'apport en sédiments du bassin. Le programme SUFI-2 de SWAT- CUP a été utilisé pour la calibration et la validation de SWAT pour les sous-bassins de Bui et de Chache pour les analyses relatives au débit d'écoulement et à l'apport en sédiments respectivement. En outre, les données journalières de précipitation, de température minimale et maximale de 11 stations climatiques couvrant les périodes 1985-2005 (période de référence) et 2051-2100 (simulations pour le futur) ont été réduites à l'échelle locale et corrigées avant d'être utilisées comme entrée du modèle hydrologique SWAT pour simuler les débits d'écoulement et les apports en sédiments. Les données incluent des projections de deux (02) modèles climatiques régionaux (MCR), RCA4 et RACMO22T pilotés par trois (03) modèles de circulation générale (MCG), MPI-ESM-LR, ICHEC-EC-EARTH, et CCCma-CanESM2 pour les scénarios du GIEC RCP4.5 et RCP 8.5. La sensitivité du débit d'écoulement aux changements dans l'OUS a été évaluée en alimentant le modèle SWAT avec de deux (02) cartes OUS (1990 et 2000) établies pour le bassin.
Les résultats de l'analyse des événements extrêmes révèlent une tendance à la hausse de la température dans l'ensemble du bassin, couplée à une tendance à la hausse de la hauteur et de l'intensité des précipitations pour la période historique.

Les valeurs des critères de validation tels que « NSE », « R^2 », « RSR » et « PBIAS » montrent une bonne performance du modèle SWAT à simuler les débits d'écoulement et l'apport en sédiments du bassin à l'échelle mensuelle. Cependant, les valeurs de « p-factor » et « r-factor » obtenues durant la calibration et la validation du modèle montrent un certain degré d'incertitude dans les simulations. En comparaison à la période de calibration, l'incertitude est moindre pour la période de validation et le degré d'incertitude est meilleur pour la simulation du débit d'écoulement que pour l'apport en sédiments.

Les projections de précipitation sur le bassin montrent des tendances positives et négatives statistiquement non significatives. L'analyse de la moyenne des précipitations annuelles, interannuelles et saisonnières indique une grande incertitude quant à l'évolution des précipitations dans le futur. La variation du cumul de pluie annuel oscille entre -16 % et +6 % sous le scenario « RCP4.5 » et entre -27% et +14% sous le scenario « RCP8.5 » pour la période 2051-2075. Cette variation oscille entre -23% et +2% et entre -33% et +13% sous les scenarios « RCP4.5 » et « RCP8.5 » respectivement pour la période 2076-2100. Concernant les températures, la projection des moyennes annuelles montre une augmentation sous les deux scénarios et pour les deux périodes considérées (2051-2075 et 2076-2100). Par ailleurs, le réchauffement est plus grand sous le scenario « RCP8.5 » que sous le scenario « RCP4.5 » avec la fin du XXIe siècle (2076-2100) plus chaude que la période la précédant (2051-2075). La hausse de la température annuelle est comprise entre 2.2 ^{o}C et 2.6 ^{o}C sous le scenario « RCP4.5 » et 3.5 ^{o}C et 3.7 ^{o}C sous le scenario « RCP8.5 » pour la fin du XXIe siècle.

L'analyse des débits et des apports en sédiments pour les saisons sèche (novembre-mars) et pluvieuse (aout-octobre) montre une tendance à l'augmentation pour les décennies 2060s et 2080s sous les deux scenarios (Figures A1, A2, A3 and A4). De même, le débit d'écoulement moyen annuel et l'apport moyen annuel en sédiments connaissent une augmentation comprise entre + 40% et 42%, et entre 100% et 143% pour la période 2051-2075 sous le scénario « RCP4.5 » respectivement. Pour la période 2076-2100, la variation est comprise entre -6% et +75% pour le débit et entre +100% et 216% pour l'apport en sédiments. Sous le scenario d'émission élevée « RCP8.5 », la variation de débits est comprise entre 48% et 148% et celle de l'apport en sédiments entre 249% et 335%. La projection pour la fin du siècle est comprise entre 69% et 243% pour le débit et 358% et 412% pour l'apport en sédiments. L'analyse des projections des débits et des apports en sédiments indique que les augmentations mises en exergue sont statistiquement signifiantes avec un niveau de confiance de 5%.

La prise en compte des changements dans l'OUS sur 10 ans (1990-2000) montre que les débits d'écoulement ne seraient pas influencés par l'OUS, particulièrement pour les changements en savanes et terres cultivées. Se basant sur les résultats susmentionnés, des recommandations ont été formulées pour la BVRB.

Mots clés. Changement climatique, couverture/utilisation du sol, débits d'écoulement production de sédiment

INTRODUCTION

Les ressources en eau jouent un rôle capital dans le développement socio-économique de l'Homme. La disponibilité et l'accessibilité de l'eau ont un effet considérable dans la croissance économique de plusieurs régions du monde, en particulier l'Afrique (Odada, 2006). La démographie galopante, l'expansion de l'agriculture irriguée et de l'industrialisation ont augmenté la demande en eau provenant des biens et services dans le monde entier, mettant ainsi cette ressource à risque. Les changements climatiques constituent un danger supplémentaire pour les ressources en eau. Selon le Groupe Intergouvernemental sur les changements climatiques, les températures des océans et de l'atmosphère augmentent à un rythme incomparable à celui d'autres périodes (IPCC, 2007). Les changements du climat affectent les pluies et les températures qui provoquent des bouleversements dans le comportement hydrologique des bassins versants, dégradent les cours d'eau et modifient les caractéristiques du transport sédimentaire (Tu , 2009). En Afrique de l'Ouest, les impacts des changements climatiques couplés avec la réduction de la pluviosité and l'augmentation du taux d'évapotranspiration potentiel dans le bassin de la Volta menace d'accroitre les défis liés à l'insuffisance des ressources en eau dans le bassin (Kasei, 2009). L'utilisation /couverture du sol est un autre facteur qui affecte les ressources en eau (Stonestrom et al., 2009).

Les ressources en eau du bassin versant de la Volta Noire supportent d'importantes activités économiques telles que l'agriculture, l'hydro-électricité et l'approvisionnement en eau potable au Ghana, Burkina Faso et Cote d'Ivoire. Les bénéfices hydrologiques du bassin pourraient cependant être menacés par les changements globaux (Kasei, 2009). Il est prouvé que les variabilités /changements climatiques peuvent changer les débits de pointe et le volume d'eau dans les cours d'eau (Prowse et al., 2006), tandis que les changements d'utilisation du sol peuvent changer la fréquence des inondations, l'infiltration, la recharge des aquifères, l'écoulement de base, le ruissellement et le débit moyen annuel (Brath et al., 2006 ; Coasta et al., 2003 ; Crooks and Davies, 2001 ; Lin et al., 2007). Des sécheresses ont touché le bassin à l'étude dans les années 1980s et 1990s (IIED, cité dans Kasei, 2009) et avaient été aggravées par l'augmentation dans la saisonnalité hydrologique (Kasei, 2009). L'exacerbation de la pluie saisonnière avec les changements climatiques et d'utilisation/couverture du sol pourraient avoir des impacts plus sévères sur les ressources en eau.

L'objectif général de cette étude est de contribuer à la gestion durable des ressources en eau et de la production d'hydroélectricité dans le bassin de la Volta Noire en explorant les impacts des changements climatiques sur les débits d'écoulement et la production sédimentaire et en évaluant la sensitivité du bassin au changement d'utilisation/occupation du sol.

ZONE D'ETUDE

Le Bassin de la Volta Noire (Figure 2.8) est un sous bassin majeur du bassin de la Volta en Afrique de l'Ouest avec une superficie totale d'environ 142 056 km^2 (Kasei, 2009). Il est situé entre les latitudes $7^o00'00"$N et $14^o30'00"$ N et les longitudes $5^o30'00"$W et $1^o30'00"$ W (Annor, 2012). Il est partagé par le Ghana, le Burkina Faso, la Côte d'Ivoire et le Mali. La population du bassin a été estimée à 4,5 million en 2000 et selon les projections, elle pourra atteindre 8 millions en 2025 (Annor, 2012). Le taux de croissance de la population dans le bassin est d'environ 3 % par an (Green Cross International, 2001). Selon la classification du climat de Köppen-Geiger, le bassin a un climat tropical humide au Sud et un climat semi-aride chaud au Nord (Peel et al.,

2007). La quantité moyenne annuelle de pluie est comprise entre 1,043 mm et 1,270 mm. Le bassin appartient aux zones écologiques savanes guinéennes et soudanaises.

MATERIELS ET METHODES

Les données utilisées pour l'évaluation des impacts des changements climatiques comprennent : 3 RCMs (le model climatique régional de Rossby Center, RCA4 et le modèle climatique régional de l'atmosphère) . Le logiciel RclimDex a été utilisé pour l'analyse des événements extrêmes et le model SWAT pour l'analyse de l'impact des changements climatiques sur les débits d'écoulement et la production sédimentaire et l'évaluation de la sensitivité de l'utilisation /couverture du sol sur le débit dans le Bassin de la Volta Noire.

Onze (11) des 27 principaux indices définis par l'équipe d'expert de l'Organisation Mondiale de la Météorologie sur les indices de détection des changements climatiques ont été considérées pour l'analyse des événements extrêmes. Cinq de ces indices sont basés sur la température et 6 sont basés sur la pluie. Le contrôle de la qualité des données a été faite selon la procédure indiquée dans le logiciel.

Pour les projections de changement de température et de précipitations dans le Bassin de la Volta Noire, l'approche « stepwise » impliquant la réduction d'échelle et la correction des erreurs, la formulation des scenarii du model et les projections futures a été suivie tandis que les méthodes de réduction d'échelle « Quantile-Quantile » et la transformation « Quantile-Quantile » (Marraun et al., 2011) ont été utilisées.

La mise au point du model SWAT pour le bassin de la Volta Noire s'est faite à travers plusieurs processus dont la délimitation du bassin, la détermination des unités de réponses hydrologiques, la définition des données météorologiques et l'écriture des données d'entrées. Le modèle a été calibré et validé en utilisant SUFI-2 dans SWAT –CUP (Abbaspour, 2007). Le modèle a été calibré d'abord à un pas de temps mensuel pour les débits et après pour les sédiments (aussi à un pas de temps mensuel) tels que recommandé par Abbaspour (2015). Le processus de calibration a cessé lorsque des valeurs satisfaisantes des fonctions objectives utilisées (coefficient de Nash (NSE), RSR, le coefficient de détermination (R^2), pourcentage de biais (PBIAS), p-factor, r-factor) ont été obtenues . Après la calibration pour les débits, le model a été calibré pour la production sédimentaire. Ensuite, le model a été validé pour le débit et la production sédimentaire en utilisant le model calibré pour d'autres périodes autres que celles utilisées pour la calibration et sans changer encore les paramètres.

Les impacts de changement climatique sur les débits d'écoulement et la production sédimentaire ont été évaluées en simulant le model SWAT avec 16 scenarii de climat future et en comparant la tendance saisonnière et la quantité annuelle de production sédimentaire et de débit avec celles des périodes de références (1984-2010). Trois années de « warm-up » (1981-1983) ont été faites durant les simulations.

L'analyse de sensitivité de changement dans l'utilisation et la couverture du sol sur le débit d'écoulement dans le bassin de la Volta Noire a été conduite à partir d'autres simulations en utilisant la carte d'utilisation et d'occupation de sol de 1990. Ceci a été fait en utilisant le model hydrologique SWAT calibré après avoir simulé le model avec la carte d'utilisation et de couverture du sol de 2000. Pour cette analyse de sensitivité, toutes les variables d'entrée à l'exception des données d'utilisation et de couverture de sol étaient restées inchangées. La carte de 1990 a été utilisée plutôt que celle de 2000. Les débits de sortie à la station de Bamboi ont été comparés avec ceux provenant des données d'utilisation et de couverture de sol de 2000. Avant

les tests de sensitivité, les détections de changements d'utilisation et d'occupation de sol du bassin ont été conduites en utilisant les cartes d'utilisation et d'occupation de sol de 1999 et 2000. En utilisant la fonction overlay dans ARCGIS 10.2.2 et Microsoft Excel 2010, les taux de changements dans l'utilisation et la couverture du sol ont été calculés pour une période de 10 ans.

RESULTATS ET DISCUSSION

L'évolution des indices liés à la température du temps présent montre un réchauffement du bassin de la Volta Noire. D'une manière générale, tous les 5 indices liés à la température montre une évolution positive dans le bassin indiquant que le bassin de la Volta Noire a subi un réchauffement durant la période 1981-2010. Ces tendances au réchauffement sont consistantes avec les résultats de New et al. (2006) qui ont montré une augmentation des hautes températures diurnes et nocturnes en Afrique de l'Ouest au cours des périodes 1961-2000. Mouhamed et al. (2013) ont aussi suggéré une tendance générale au réchauffement au Sahel Ouest africain de 1960 à 2010. Par ailleurs, l'analyse des séries temporelles d'indices liées aux pluies extrêmes montrent une augmentation globale dans le bassin pour les périodes 1981-2010. En général, l'analyse montre une augmentation des pluies totales et intensités dans le bassin de la Volta Noire de 1981 à 2010. Alexander et al. (2013) ont trouvé que les pluies extrêmes à travers le globe ont augmenté au cours de la période 1951-2003. Bien que les résultats de Mouhamed et al. (2013) ont montré une diminution de la pluie totale annuelle pour le Sahel Ouest Africain, en particulier au Burkina Faso de 1961-2010, une augmentation des pluies des jours extrêmement humides et des nombres maxima des jours humides consécutifs ont été observés dans leurs études pendant la fin des années 1980, comparée à la période 1961-1990.

Les courbes des pluies intra-annuels de la simulation des pluies historiques montre que RCMs RCA4/MPI-ESM-LR et RACM022T/ICHEC-EC-EARTH ont bien simulé l'évolution des pluies dans le bassin, captant le début de la saison des pluies (Avril-Mai-Juin) de même que la saison humide (Juillet-Aout-Septembre). L'analyse des pluies moyennes annuelles dans le bassin pour les dernières années et la fin du XXIe siècle a montré un haut niveau d'incertitudes, avec des signaux mélangés d'augmentation et de diminution des quantités de pluies dans les modèles. Des observations similaires ont été faites par Sylla et al. (2016). Une diminution des pluies peut causer des sécheresses, affecter le développement de l'agriculture et provoquer une chute de la production de l'énergie hydroélectrique tandis que qu'une augmentation des pluies peut provoquer des inondations dans le bassin. Consistants avec le dernier rapport du groupe d'experts intergouvernemental sur les changements climatiques (IPCC 2013), les résultats des projections de température dans le bassin de la Volta Noire indiquent un climat chaud au cours des dernières années et à la fin du XXIe siècle sous les deux scénarii RCP par rapport à la période de référence.

L'évaluation quantitative de la performance via les méthodes statistiques pendant la calibration du model a donné un R^2 de 0.86, un RSR de 0.38 et un NSE de 0.85. Ce qui indique que le modèle a bien simulé les débits. Le model a été capable de simuler un peu bien les basses eaux et de capter la majorité des pointes de débit. En comparaison avec les performances statistiques générales données par Moriasi et al. (2007) et Santhi et al. (2001), les résultats globaux de la calibration des débits sont « très bons ». Les résultats de validation des débits sont généralement « satisfaisants » (NSE : 0,6 ; R^2 : 0,62 ; RSR : 0,64 ; PBIAS : 20,1 %). L'évolution des simulations pendant la calibration et la validation a suivi celle des observations hormis quelques

différences pour certaines années. Beaucoup d'études ont démontré l'incapacité du modèle hydrologique SWAT à simuler les débits de pointe convenablement (e.g. Chu et al., 2004 ; Wang et al., 2015 ; Himanshu et al., 2017). En général, les productions sédimentaires simulées par le modèle sont concordantes avec les observations pendant la calibration et la validation. Globalement, les résultats de l'évaluation (NSE : 0,68. R^2 : 0,76 et RSR : 0,57 °indiquent une « bonne » performance du model. Pour la période de validation, le rapport de la production sédimentaire simulée avec les observations a été maintenu. Les résultats de la validation obtenus (NSE : 0,65 ; R^2 : 0,74 ; RSR : 0,59 et PBIAS : 39,1) étaient satisfaisants.

Par rapport à la période de référence, les scénarii des modèles projettent une augmentation des débits et de la production sédimentaire pendant les périodes sèches pour les années 2060s et sous le scénario RCP 4.5. La seule exception à cette évolution était une projection de diminution des écoulements en périodes humides avec une augmentation de production sédimentaire par le RACMO22T/ ICHEC-EC-EARTH. Cette diminution des écoulements et augmentation de production sédimentaire est identique avec les résultats de Phan et al. (2011) and Shrestha et al. (2013). La diminution des écoulements avec une augmentation correspondante de la production sédimentaire peut être parfois possible avec une diminution des précipitations et une augmentation de température (Shresta et al., 2013). Sous le scénario RCP 8,5, tous les modèles ont projeté une augmentation des écoulements et des sédiments pendant les périodes sèches et humides (Figures A1 et A2). Une forte production sédimentaire suivant une augmentation des écoulements dans les bassins versants peut être due aux pluies intenses, à l'érosion et au défrichage des bancs de rivières. Les bancs des cours d'eau dans le bassin sont majoritairement sableux et pourraient contribuer aux valeurs de production sédimentaires élevées obtenues. En général, le cycle saisonnier de la production sédimentaire suit celui des écoulements avec une augmentation des écoulements conduisant à une augmentation de la production sédimentaire. Une augmentation des écoulements peut entrainer des inondations dans le bassin et affecter ainsi la sécurité alimentaire. L'augmentation de la charge sédimentaire dans le bassin peut entrainer une augmentation de la turbidité des cours d'eau et causer une perte de capacité de stockage des réservoirs (Walling, 2008).

Le changement le plus visible dans l'utilisation et la couverture du sol au cours des 10 années (1990 à 2000) était une augmentation des terres cultivées et des terres couvertes d'herbes et une diminution des savanes. Durant cette période, le taux moyen de croissance de la population dans le bassin occupé par le Burkina Faso et le Ghana étaient de 2,38% et 2,5% respectivement (Barry et al., 2005). Au Burkina Faso, près de 78% de la population totale vivent dans le bassin de la Volta en 2000 et les aires cultivées représentaient 82,5% des terres cultivées au Burkina Faso (ibid). L'augmentation des terres cultivées peut ainsi être attribuée à une augmentation de la population dans le bassin au cours de cette période car une augmentation de la population demande plus de terre à cultiver pour vivre. Les aires de forêts ont montré une légère diminution (309 km^2) entre 1990 et 2000. Cette diminution peut être due à la coupe des arbres pour des cultures de fourrage pour nourrir les bétails. Comparés aux autres types d'utilisation/couverture de sols, les terres couvertes d'arbustes ont montré moins de changement (diminution de 19 km^2).

Les totaux des débits d'écoulements annuels basés sur les simulations de 1984-2010 ont montré une diminution légère des débits suite à un changement dans l'utilisation de sols de 1990 à 2000.

CONCLUSION

L'analyse des événements extrêmes ont montré que le bassin de la Volta Noire devient plus chaud et humide (révélée à travers les augmentations dans les volumes et intensités de pluies) au cours de la période 1981-2010. La performance du modèle SWAT à simuler les débits et les productions de sédiments historiques du bassin de la Volta Noire, évaluée à l'aide de méthodes statistiques (NSE, R^2, RSR et PBIAS) et des calibrations/ validations à pas de temps mensuels montrent que le modèle simule raisonnablement les deux variables. Les résultats de la calibration pour les débits d'écoulement étaient : R^2 de 0,86 ; NSE de 0,85 ; RSR de 0,38 et PBIAS de 8,1. Pour la production de sédiments, les résultats étaient : R^2 de 0,76 ; NSE de 0,68 ; RSR de 0,57 et PBIAS de 27,5. Les deux résultats montrent une « bonne » performance du model. Les résultats de la validation étaient « satisfaisants » pour les écoulements et la production sédimentaire, avec R^2 de 0,62 ; NSE de 0,60 ; RSR de 0,64 et PBIAS de 20,1 % pour les écoulements et R^2 de 0,74 ; NSE de 0,65 ; RSR de 0,59 et PBIAS de 39,1% pour la production sédimentaire.
Les courbes des moyennes mensuelles des données de pluie et de température simulées non corrigées, simulées corrigées et observées ont montré que les méthodes de réduction d'échelle quantile-quantile et transformation quantile-quantile ont une bonne performance dans la réduction des biais du RCM. Les RCMs individuels affichaient des biais dans la simulation des pluies historiques du bassin. Tous les modèles simulent bien les températures historiques du bassin. Par rapport à la période de référence, les volumes annuels de pluies ont montré des signaux positifs et négatifs à travers les modèles.
Pareillement pour les pluies annuelles, l'analyse des pluies intra-saisonnières et saisonnières a montré une grande incertitude dans les volumes de pluies futurs, avec une grande variabilité dans les saisons humides par rapport aux saisons sèches. Les projections de températures par les modèles montrent unanimement un réchauffement du bassin au cours des années 2060s et 2080s avec des augmentations comprises entre 2 °C (dernières années du XXIe siècle sous RCP 4,5) et 3,7 °C (fin du XXI e siècle sous RCP 8,5). L'analyse de l'évolution de futures pluies annuelles montrent des directions positives et négatives. Ces tendances étaient cependant statistiquement insignifiantes à 5% du niveau de confiance. Les évolutions des températures moyennes annuelles ont montré quant à elles une augmentation statistiquement signifiante des températures futures dans le bassin. Les hautes températures pourraient affecter la disponibilité de l'eau dans le bassin. Puisque la majorité de la population du bassin dépend de l'agriculture, les problèmes liés au manque d'eau pourraient aggraver la pauvreté dans le bassin. Des mesures d'adaptation aux hautes températures doivent alors explorées et développées bien en avance. L'analyse saisonnière des débits moyens annuels et de la production sédimentaire a montré une augmentation des débits d'écoulements et de la production sédimentaire pendant les périodes sèches et humides au cours des dernières années et à la fin du XXIe siècle sous les scénarios RCP4,5 et RCP 8,5. L'analyse des débits moyens annuels et de la production sédimentaire a montré des augmentations statistiquement signifiantes. L'analyse des changements d'utilisation et de couverture de sol a montré qu'entre 1990 et 2000, la couverture en terre cultivées et en herbes a augmenté considérablement, avec une réduction correspondante en savanes. Ces changements pourraient être dus à la croissance démographique et l'utilisation des savanes pour le bois énergie dans le bassin. L'analyse de sensitivité des débits dans le bassin en lien avec les 10 années de changement d'utilisation de sol ont montré des changements légers. Les statistiques des simulations de débits ont montré cependant, que ces changements sont insignifiants. Considérant le rôle de l'utilisation et de la couverture de sol dans les écoulements, l'analyse de sensitivité en utilisant différents scénarios hypothétiques extrêmes peut être utile pour conclure

de façon forte en la sensitivité ou non des écoulements dans le bassin de la Volta Noire aux changements d'utilisation de sol.

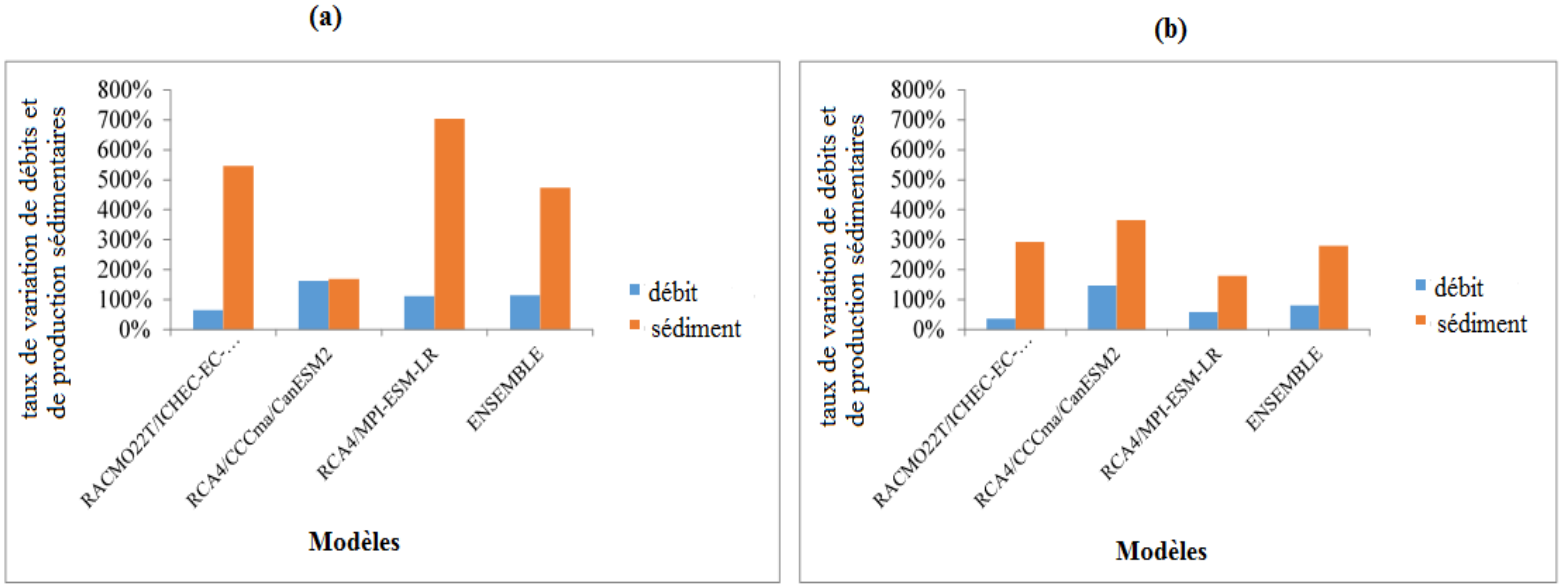

Figure A1 : taux de variation de débits moyens saisonniers et de production sédimentaires pour la fin du XXI siècle (2060s) sous le scenario RCP8.5 : (a) pendant la saison sèche (Janvier-Mars) et (b) pendant la saison humide (Août- Octobre)

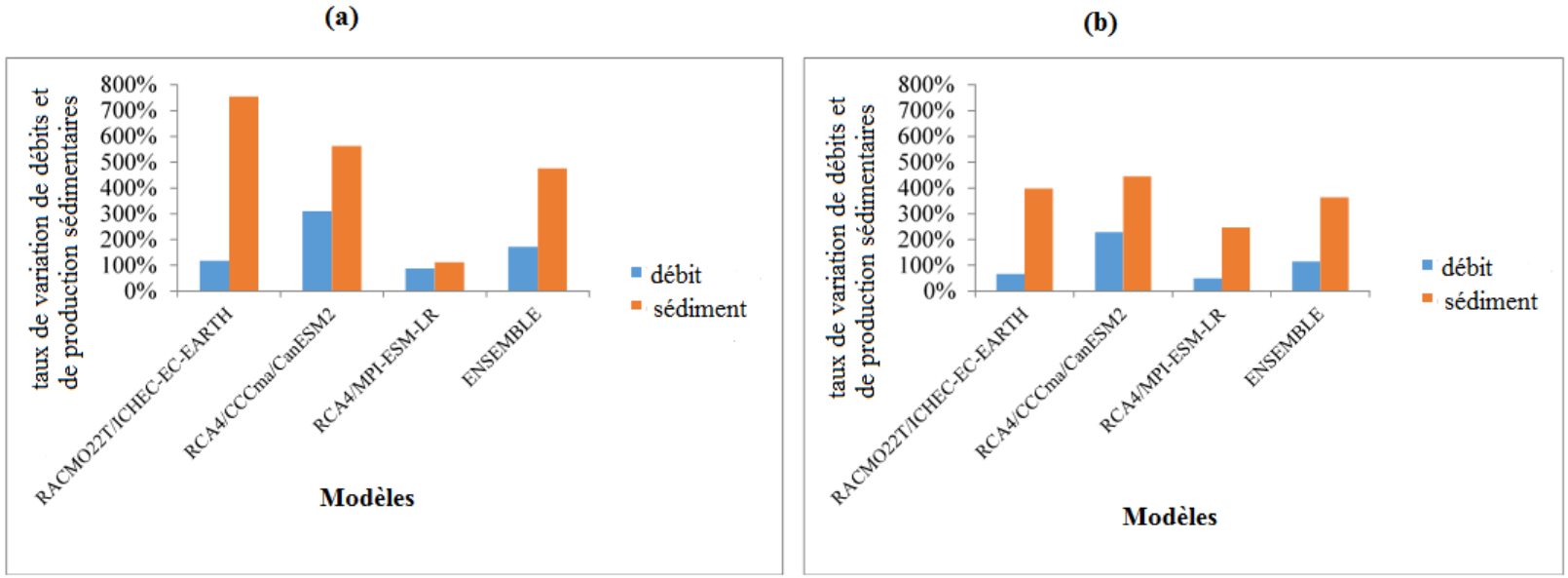

Figure A2 : taux de variation de débits moyens saisonniers et de production sédimentaires pour la fin du XXI siècle (2080s) sous le scenario RCP8.5 : (a) pendant la saison sèche (Janvier-Mars) et (b) pendant la saison humide (Août- Octobre)

TABLE OF CONTENTS

LIST OF ACRONYMS

BVRB	Black Volta River Basin
CC	Climate Change
CFSR	Climate Forecast System Reanalysis
CMIP5	Coupled Model Intercomparison Project Phase 5
CORDEX	Coordinated Regional Climate Downscaling Experiment
CREAMS	Chemicals, Runoff, and Erosion from Agricultural Management Systems
DEM	Digital Elevation Model
EPIC	Erosion Predictability Impact Calculator
GCM	Global Climate Model
GIS	Geographic Information System
GLEAMS	Groundwater Loading Effects on Agricultural Management Systems
GLUE	Generalized Likelihood Uncertainty Estimation
HRU	Hydrologic Response Unit
IPCC	Intergovernmental Panel on Climate Change
LULC	Land use/land cover
MCMC	Markov Chain Monte Carlo
MDG	Millennium Development Goal
MUSLE	Modified Universal Soil Loss Equation
NGO	Non-governmental Organization
NSE	Nash-Sutcliffe-Efficiency
Parasol	Parameter Solution
PBIAS	Percent Bias
PET	Potential Evapotranspiration
R^2	Coefficient of determination
RCM	Regional Climate Model
RCP	Representative Concentration Pathway
RMSE	Root Mean Square Error
RSR	RMSE-observations standard deviation ratio
SCS	Soil Conservation System
SRTM	Shuttle Radar Topographic Mission
SUFI-2	Sequential Uncertainty Fitting, version 2
SWAT	Soil and Water Assessment Tool
SWAT-CUP	Soil and Water Assessment Tool- Calibration and Uncertainty Programs
UN	United Nations
UNEP	United Nations Environment Programme
USDA	US Department of Agriculture
USDA-ARS	United States Department of Agriculture-Agricultural Research Service
USLE	Universal Soil Loss Equation
VRB	Volta River Basin
WMO	World Meteorological Organization

LIST OF FIGURES

LIST OF TABLES

CHAPTER 1: GENERAL INTRODUCTION

This chapter provides a general introduction of the research and presents the research background, problem statement, objectives, hypothesis and significance of the study. The chapter also reviews literature on the subject matter. Definitions and concepts of key terminology of the research have been defined and explained in this chapter. Further, the effects of soil erosion and sedimentation as well as climate and land/use land cover (LULC) change in West Africa and the Volta basin are discussed. The chapter also highlights possible conflicts that may arise from sharing the river basin in the absence of proper management.

1.1. Context and Problem Statement

Water resources are indispensable in every living system, playing a key role in various economic and social developments. Water is also important in addressing issues of hunger, health and poverty. Its availability and accessibility has huge effects on patterns of economic growth for many regions of the world, especially the African region (Odada, 2006).

Rapid population growths, expansion of irrigated agriculture and industrialization have increased the demand for water related goods and services worldwide, putting the resource at risk. Climate change is undeniably occurring and poses additional risks to water resources. The Intergovernmental Panel on Climate Change (IPCC, 2007) reports that global average surface air and ocean temperatures are increasing at rates unequivocal to any other period on record. Changes in climate affect rainfall and temperature which causes changes in the hydrology of river basins, alters streamflow and modifies the transport characteristics of sediments (Tu, 2009). In West Africa, climate change impacts coupled with the anticipated reduction in rainfall and an increase in potential evaporation rates over the entire Volta River Basin threaten to increase the challenges associated with insufficient water resources in the basin region (Kasei, 2009). Studies

by Obuobie (2008) and Awotwi et al. (2015) revealed that the White Volta Basin is sensitive to changes in climate, with increases in temperature and rainfall resulting in increases in annual surface runoff, annual baseflow and evapotranspiration.

Land-use/land-cover (LULC) is another important factor that affects water resources (Stonestrom et al., 2009). Studies by Elfert and Bormann (2010), Ghaffari et al. (2010) and Li et al. (2009) for example, have shown that LULC change affects hydrological processes. Land-use/land-cover is linked directly with the hydrological cycle and influences the partitioning of rainfall into runoff, evapotranspiration, infiltration (Foley et al., 2005) and sediment yield (Walling, 1994). To this end, changes in LULC constitute an important human interference that affects the quality and quantity of water resources (Dwarakish and Ganasri, 2015).

Lahmer et al. (2001) have shown that although the hydrological effects of land use/land cover and climate variation/change happen at all spatial scales, studies conducted at smaller scales, (e.g. regional level) tend to be more beneficial for the provision of key information for local developments.

The water resources of the Black Volta River Basin support important economic activities such as agriculture, hydro-power generation and domestic water supply in Ghana, Burkina Faso and Cote D'lvoire. The hydrological benefits of the basin could however be threatened by global change (Kasei, 2009). It is established that climate variability and/change can cause changes in peak-flows and volume of water in rivers (Prowse et al., 2006), whereas changes in land use can cause changes in flood frequency, infiltration, groundwater recharge, base flow, runoff and annual mean discharge (Brath et al., 2006; Costa et al., 2003; Crooks and Davies, 2001; Lin, et al., 2007).

A number of drought events affected the water resources of the studied basin in the 1980s and 1990s (IIED, 1992 *cited in* Kasei, 2009) and were worsened by increases in hydrologic seasonality (Kasei, 2009). The exacerbation of seasonal rainfall together with climate change and land use/land cover change may have some more profound effects on the water resources.

1.2. Literature Review

1.2.1. Climate Change

According to the United Nations Framework Convention on Climate Change (UNFCCC), climate change is "a change of climate which is attributed directly or indirectly to human activity that alters the composition of the global atmosphere and which is in addition to natural climate variability observed over comparable time periods" (IPCC, 2007b).

1.2.2. Land use

Land use refers to how mankind use land and land resources, for example for agricultural purposes, mining and urban development. The FAO (1997a) defines land use as the human action, which alters land cover.

1.2.3. Land cover

Land cover is the physical undisturbed state of the surface of the land. It includes categories like forests, roads, cropland and urban areas. Land cover has also been defined by several other authors (Di Gregorio and Jansen, 1998; Jansen and Di Gregorio, 1998) as the observed (bio) physical cover on the surface of the earth.

1.2.4. Land use/land cover change

Land use/land cover (LULC) change can be classified into two; conversion and modification (Butt and Olson, 2002). Land use/land cover conversion occurs when there is a complete change

from one cover/use to another. In such a situation, one land cover type completely replaces another, and changes its classification e.g. conversion of forest land to urban settlement. In the case of land use/land cover modification there is a slight change which alters the characteristics of the land cover. In this instance even though the land cover is modified the original is retained giving rise to the maintenance of the original classification e.g. fragmented forest or overgrazed grassland. According to Butt and Olson (2002), key LULC changes include desertification, wetland drainage, deforestation and agricultural extensification. Land use/land cover changes are caused by both natural and human driving forces (Meyer and Turner, 1994). Human beings however, play a key role in contributing to land use/land cover change. At the same time, they are equally affected by the changes (Lambin and Geist, 2006).

1.2.5. Soil erosion and sediment yield

Sediment yield is the amount of sediment supplied at the outlet of a catchment at a specific time (Patra, 2001) and result from erosion and deposition processes within a basin (Jain and Das, 2010). It is the sum of sediments generated by overland flow, gully, and stream channel erosion in a catchment (Duru, 2015). Transport of sediment in the channel network is a function of degradation and aggradation (Neitsch et al., 2005).

Runoff transport capacity is the main factor which controls sediment yield (Mutchler et al., 1988). As such, whenever runoff transport capacity is insufficient to sustain transport, the bulk of the sediment gets deposited at intermediate locations (Julien, 2010). Only a small fraction of eroded sediment within a drainage basin usually finds its way to the outlet. Sediment yield from catchments are usually slightly lower than the rates of soil erosion measured from plots of hillslope (Edwards, 1993 and Wasson et al., 1996). This shows that most sediments move only short distances (Parsons and Stromberg 1998) and then gets deposited. Varying proportions of

the eroded materials are deposited between the source and the outlet, with a large proportion usually remaining in lakes or reservoirs.

In the Volta River Basin, erosion occurring upstream of the basin causes sediments to fill river channels and reservoirs, thereby reducing the quality of the water in the process. A major source of degradation of the water resource is thus the transport of sediment among the riparian countries of the Basin (Barry et al., 2005). Sedimentation also affects the storage capacity and life span of reservoirs and dams in the Volta Basin (Mul et al., 2015) and may lead to floods and hamper the fight against food insecurity in the region.

According to Nagle (2000), materials which make up sediment yield are of three different types: dissolved load (soluble materials carried as chemical ions); suspended load (made up of clay and silt held up by the turbulent flow), and bed load (includes larger particles moved by saltation, rolling and sliding). The quantity of sediments transported by streams usually contain between 70 and 99% suspended load (Babiński, 2005). The rest of the sediment materials are transported by saltation or intra-sediment movement (Yves, 2008). Sediment yield in a catchment reflects soil type, land cover/use, hydrology, topography, runoff, drainage network, sediment characteristics and geologic formation (Stand and Pemberton, 1982 *cited in* Duru, 2015).

1.2.6. Climate Change and evidence of global warming in West Africa

There is an overwhelming scientific agreement that humans are contributing to global warming. The Intergovernmental Panel on Climate Change (IPCC) has since its establishment provided evidence in support of the warming of the climate system. The IPCC is a scientific international body set up by the World Meteorological Organization (WMO) and by the United Nations Environment Programme (UNEP) in 1988 to assess the science related to Climate Change. In its

Fifth Assessment Report, the IPCC highlights that successively warming trends have been recorded over the Earth's surface in the last three decades than any preceding decade since 1850 (IPCC, 2014a). For major parts of Africa, warming could go beyond 2 °C by 2050 and rise by as much as 2.6–4.8 °C by the end of the century under both medium and high emission scenarios (IPCC, 2013). Temperatures in West Africa are expected to rise by between 3 °C and 6 °C by the end of the 21 century under a range of scenarios. Unlike temperature, projections for rainfall in West Africa are less certain. Many global models however project a wetter main rainy season with a slight delay in the onset of the rainy season by the end of the 21 century (CDKN, 2014). Although Africa's contribution to greenhouse gas emissions has not been as much as the emissions by other regions of the world, the costs it faces, for example in terms of health issues, will continue to be huge due to the low adaptive capacity (Boko et al., 2007). Due to the projected mean changes in rainfall, temperature and increases in the frequency of extreme events (Rosenzweig et al., 2002) climate change is expected to amplify the pressure on water availability, affect food security and impact on human health significantly in the Africa region (IPCC 2013, IPCC 2014b).

1.2.7. Land use/land cover change in West Africa and the Volta Basin

The West African land cover has seen some changes in the past forty years as a result of increase in population, increases in the use of land for agriculture and economic development as well as the spread of settlement (Braimoh and Vlek 2005; Abbas et al., 2010; Ouedraogo et al., 2010). Land cover change analysis within the Volta Basin for the years 1990, 2000 and 2007/8, for instance showed that 36% of the 400,000 km^2 Volta Basin area saw some changes over the 18 years (1990-2008), with 64% remaining unchanged (Liebe et al., 2010).

1.2.8. Climate Change effects on water-related disasters in the Volta Basin

The Volta Basin has experienced loss of lives, severe damage and large economic and societal losses resulting from unexpected weather conditions in the region over the past 40 years. Extreme weather or climate event, popularly termed extreme event, is one of the key manifestations of climate change in a region or an area. It occurs when the "value of a weather or climate variable exceed (or go below) a threshold value near the upper (or lower) ends ('tails') of the range of observed values of the variable" (IPCC, 2012). The high spatial and temporal variability of rainfall intensities and amount within and between the countries that share the Volta River has greatly exacerbated local water shortages and competition in the basin. In the past few decades, the region has recorded significant increases in the frequency of heavy rainfall events and a common occurrence of droughts (Oyebande and Odunuga, 2010), resulting in several instances of water-related disasters. In 2007, for instance, a massive rainfall in the Basin caused severe flooding which resulted in the death of 56 people in Ghana (OCHA, 2007). Severe flooding also occurred in Northern and Central Burkina Faso over a 30-year period (1988,1992, 1994, 2007, and 2009) after drought events (World Bank, 2011), with the 2007 and 2009 floods inundating about 33,000 ha and 22,220 ha of farmlands respectively. In addition, the 2009 floods destroyed 15 dams and 42,000 homes (Burkina Faso Post-Disaster Needs Assessment, 2010).

1.2.9. Water uses in the Volta Basin

The water resources of the Volta basin are used mainly for hydro-power generation, agriculture and domestic water supply. Ghana, which is located downstream of the Volta basin relies heavily on the Volta river for hydro-power production as opposed to Burkina Faso, which has invested in water infrastructure upstream of the basin mostly for irrigated agriculture. The different uses can

lead to conflicts between countries if water infrastructure investments in the Volta basin are not optimized for mutual benefits. Most often than not, Ghana blames upstream Burkina Faso when there is too much or too little water downstream as is usually the case between riparian countries. For instance, the 2007 flood in Northern Ghana which caused severe economic losses was linked to the spilling of water from the Bagre dam in Burkina Faso (Armah et al., 2010).

1.3. Research Questions

The main research questions addressed in this thesis included the following;

- What has been the trends in extreme rainfall and temperature events in the BVRB?
- How will the future climate (precipitation and temperature) of the BVRB change with respect to the present?
- How can the SWAT model be adapted to simulate the flow and sediment yield of the BVRB? and
- How will changes in climate and land use/land cover impact on streamflow and sediment yields in the Black Volta River Basin?

1.4. Thesis Objectives

1.4.1. Main Objective

The overall objective of the study is to contribute to the sustainable water resources management and hydropower generation in the Black Volta River Basin by investigating the impacts of climate change on streamflow and sediment yield and assessing the sensitivity of the basin's flow to land use/land cover change in the basin.

1.4.2. Specific objectives

The specific objectives were to:

1. Analyze historical trends in extreme rainfall and temperature events in the BVRB;

2. Develop and analyze local climate scenarios through statistical downscaling of projections from regional climate models;

3. Adapt the Soil and Water Assessment Tool (SWAT) hydrological model to simulate streamflow and sediment yield in the BVRB;

4. Assess the impacts of climate change on streamflow and sediment yield; and

5. Assess the sensitivity of streamflow to changes in LULC in the BVRB.

1.5. **Research Hypothesis**

This research hypothesizes that change in climate and land use/land cover will impact negatively on the streamflow and sediment yield in the BVRB, the largest sub-basin of the Volta River Basin in West Africa.

1.6. **Novelty**

Climate change is expected to have severe impacts on both human and natural systems worldwide and Africa in particular (Boko et al., 2007; Chinowsky et al., 2011). The Volta basin of West Africa is by no means exempted from the impacts of climate change (Kankam-Yeboah et al., 2013). Very few studies have been conducted to assess the impact of climate change on the hydrology of the Volta basin and some of its sub-basins, namely, the White Volta, Black Volta and Pru (Kankam-Yeboah et al., 2013; Sood, 2013; Obuobie et al., 2013; Obuobie et al., 2012; Obuobie, 2008; Andah et al., 2004; Opoku-Ankomah, 2000). However, nearly all the studies used climate projections from a single Regional Climate Model (RCM) driven by one Global Climate Model (GCM) and based on one IPCC Scenario experiment. Therefore, these studies were unable to adequately quantify the uncertainties associated with the climate projections used in their analysis. To overcome this drawback this study makes use of a number of RCM/GCM combinations. Regarding land use/land cover, its impact or sensitivity to streamflow in the

studied basin has not been researched. Such information is important for sustainable water resources management including reliable hydropower generation in the Black Volta Basin.

1.7. Scope of Thesis

The study covers analysis of trends in past extreme events in the BVRB and makes projections of future precipitation and temperature. A detailed analysis of climate change impact on the basin's flow and sediment yield is carried out using the multimodel ensemble approach. The study does not cover in-depth analysis of potential impact of land-use/-cover change on the basin's hydrology. Only sensitive analysis is conducted.

1.8. Expected Results and Benefits

This study will generate impact specific information and data for informing water management decisions, climate change adaptation and land-use/-cover planning in the Black Volta Basin. The results from the study can contribute to attaining the UN Sustainable Development goals 1, 2, 3, 6 and 7 which all have linkages to water.

1.9. Outline of the Thesis

This thesis has 8 chapters, each of which contains information, data, and knowledge that contribute to addressing the overall objective of the research.

Chapter 1 provides a general introduction of the research. The chapter also contains review of literature on the subject matter. Definitions and concepts of key terminology of the research have been defined and explained in this chapter. The research background, problem statement, objectives, hypothesis and significance of the study are presented in this chapter.

Chapter 2 describes the study area, starting with a general description of the main Volta River Basin and narrowing it down to the Black Volta River Basin. The physical features, climatic conditions, hydrology and surface water use and development are presented.

Chapter 3 deals with the data sets, materials and methodology used in achieving the objectives of this research. The procedure used in analyzing the extreme events in the BVRB for the 1981-2010 period is described. The details of the modelling process with the Soil and Water Assessment Tool (SWAT) model are also provided. A description of the downscaling technique and the bias correction methods used are presented, together with the procedure used in the climate change projects. The methodology used in the sensitivity analysis of land use/land cover change on the flow of the basin is also presented.

Chapter 4 presents and discusses the results of the extreme event analysis. The results of the hydrological modelling with SWAT are presented and discussed in Chapter 5. In particular, the model sensitivity analysis, calibration and validation results are discussed. The results of the climate downscaling and bias correction aspect of this research are presented and discussed in Chapter 6 together with the projected changes in rainfall and temperature. Chapter 7 discusses the impact of climate change on streamflow and sediment yield in the basin as well as the sensitivity of flow to changes in LULC.

Chapter 8 presents the conclusion and perspective of the study and provides recommendations for the sustainable management of the water resources of the basin informed by the results of this study.

CHAPTER 2: THE STUDY AREA

2.1. Introduction

This chapter first presents a general description of the Volta River Basin (VRB) and goes further to provide detailed description of the Black Volta River Basin where the study was conducted.

2.2. General overview of the Volta River Basin

The 400,000 km² Volta River Basin is located in West Africa and stretches between latitudes 5 ^{o}N and 14 ^{o}N and longitudes 2 ^{o}E and 5 ^{o}W. The Basin is shared by six West African countries, namely, Benin, Burkina Faso, Côte d'Ivoire Ghana, Mali, and Togo (Figure 2.1). The major part of the Basin is shared by Burkina Faso and Ghana (about 82%) with the remaining 18% shared by the other four countries (Rodgers et al., 2007). The basin had an estimated population of 18.6 million in 2000, projected to reach 33.9 million by 2025 (Biney, 2010). A highly variable geographic distribution exists within the basin, with densities ranging from 8 to 104 persons/km^2 (Barry et al., 2005).

The Volta Basin has 4 main sub-basins, namely, Black Volta (147,000 km^2), White Volta (106, 000 km^2), Oti (72,000 km^2) and Lower Volta. The Lower Volta is formed through the joining of the Black and White Volta Rivers in the north of Ghana. The Volta Basin is largely flat with a mean elevation of about 257 m (Obuobie, 2008). The lowest point is found in the Lower Volta (elevations of about 1 m) and the highest point in the Oti Basin (elevations of about 920 m) (Barry et al., 2005). Agriculture is the main economic activity in the Volta basin with about 70 to 90% of the population depending on subsistence farming (Rodgers et al., 2006, *cited in* Obuobie, 2008). The population also exploits the natural resources for survival (Barry et al., 2005).

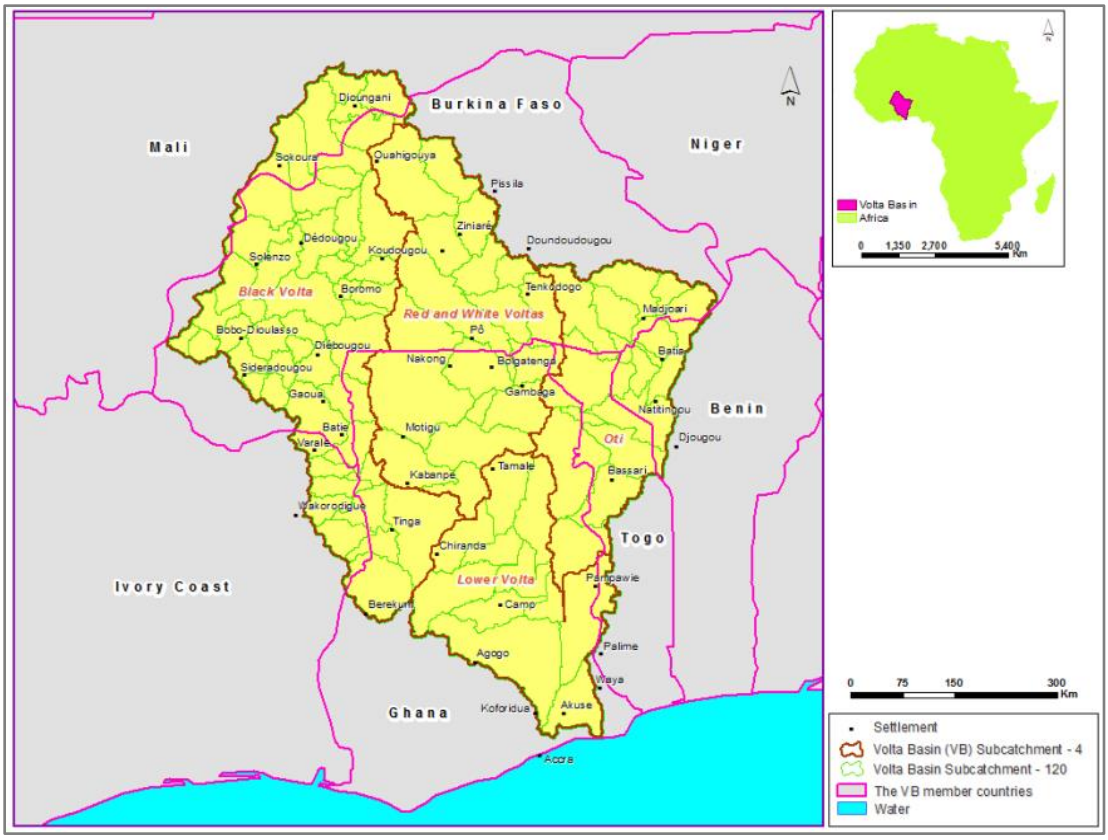

Figure 2.1: Map of Volta River Basin showing the four major sub-catchments (Geoportal of Volta Basin Authority, 2015)

2.3. **Climate and hydrology**

The climate of the Volta Basin is largely dependent on the movement of the dry North-East Trade winds from the interior of the African continent and the moist South-West Trade winds that blow from the seas (Amisigo, 2005 *cited in* Obuobie, 2008). The basin area has three climate zones; the humid south, the tropical transition zone and the tropical zone. The humid south and tropical transition zones each experience two rainfall seasons. While the rainfall seasons in the humid south are strongly bi-modal (peaking in June and September), those in the tropical transition zone are weakly bi-modal (Figures 2.2 and 2.3). The tropical zone on the other hand has just one rainfall season (Figure 2.4) which peaks in August/September (Barry et al., 2005).

Rainfall is distributed evenly in the humid zone throughout the year but poorly distributed in the tropic north zone. Over 70% of the total annual rainfall in the tropic north zone falls between June and September (Amisigo, 2005).

In general, higher rainfall amounts are experienced in some parts of the basin (e.g. 1600mm in the south-eastern section in Ghana) with smaller amounts in other parts (e.g. approximately 360 mm in the northern part of Burkina Faso). There have been some changes in the rainfall patterns in some of the Volta Basin's sub-catchments since the 1970's with a reduction in rainfall and runoff (Opoku-Ankomah, 2000). The beginning of the rainy season has also become difficult to predict (Obuobie, 2008).

Mean annual temperature in the Basin is higher in the northern half of the basin than in the southern half. According to Oguntunde (2004), mean daily temperature is about 36 ^{o}C in the north and 27 ^{o}C in the south. Humidity is between 6% and 83% (Barry et al., 2005). Mean annual potential evaporation is about 1,500 mm in the south and above 2,500 mm in the north of the Basin (Kasei, 2009). Annual mean potential evapotranspiration ranges from 1,800 mm in the coastal zone to 2,500 mm in the northern portions of the Basin (Green Cross International, 2001). Oguntunde (2004) estimated that about 80% of the rain which falls in the Basin during the rainy season is lost to evapotranspiration. Potential evapotranspiration exceeds rainfall for most parts of the year (Obuobie, 2008).

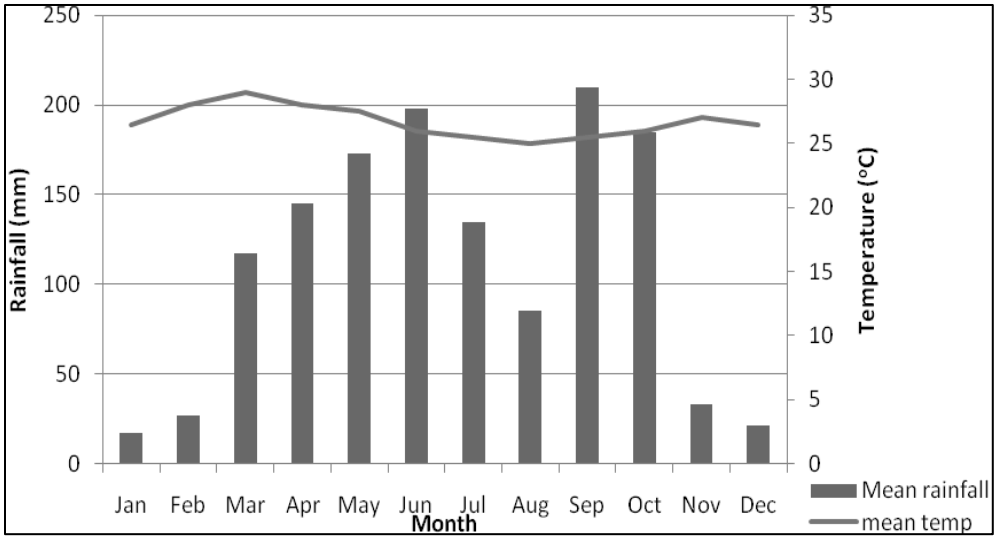

Figure 2.2: Mean monthly rainfall and temperature (1970-2000) at Ejura-Ghana (Kasei, 2009)

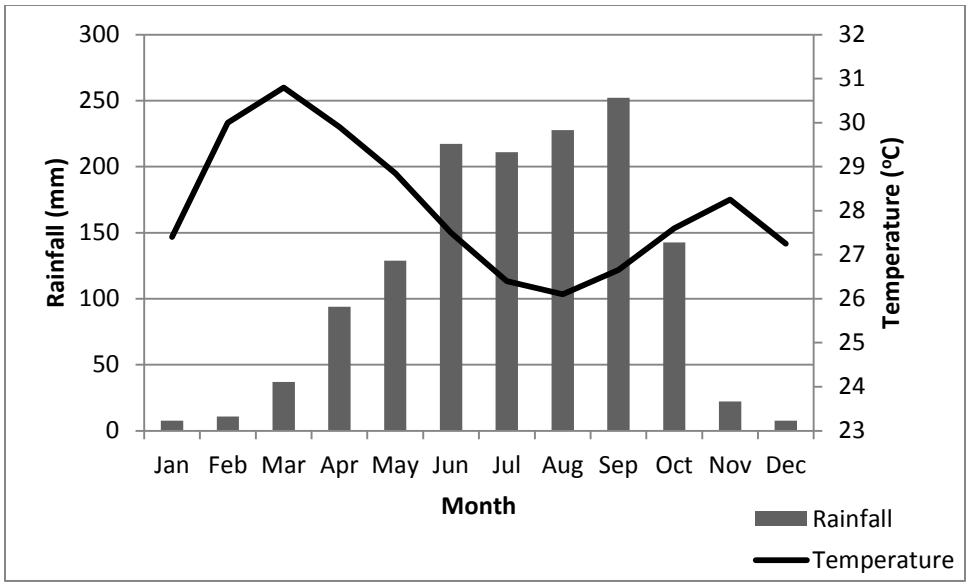

Figure 2.3: Mean monthly rainfall and temperature (1981-2010) at Kete Krachi – Ghana

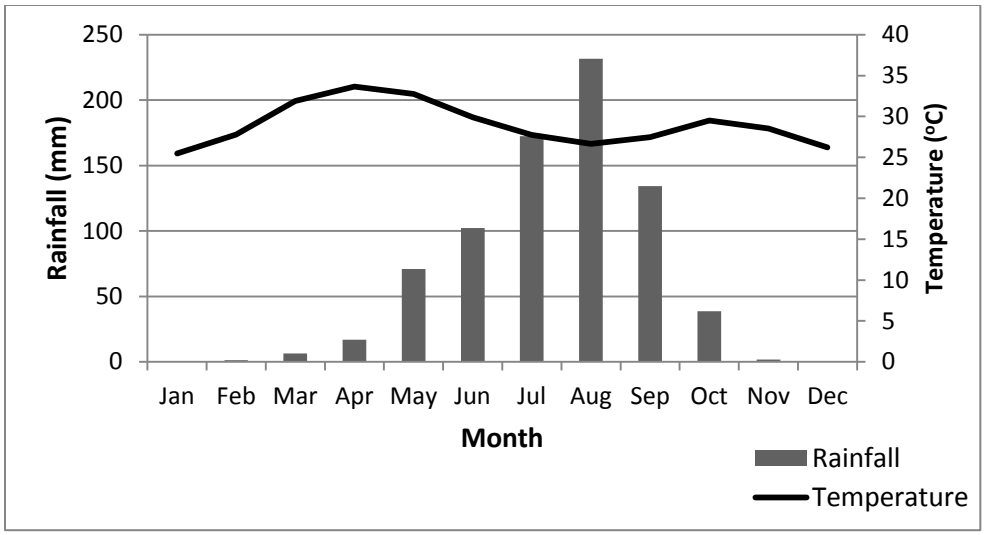

Figure 2.4: Mean monthly rainfall and temperature (1981-2010) at Dedougou, Burkina Faso

2.4. **Geology and soils**

The geology of the Volta Basin (Figure 2.5) is largely (over 90%) comprised of the Precambrian basement crystalline formation that are related to the West African Craton and the Proterozoic to Paleozoic consolidated sedimentary formation (Obuobie et al., 2016; Mul et al., 2015). According to Key (1992) and MWH (1998), both *cited in* Mul et al. (2015), the basement crystalline formation consists of igneous rocks, metamorphic rocks, granite-gneiss-greenstone rocks, and anorogenic intrusions while the consolidated sedimentary formation consists of shales, mudstones, arkose, limestones, sandstones and sandy and pebbly beds. Other geological formation of importance in the basin is the unconsolidated sedimentary formation that consists of the recent tertiary sandstones and thick layers of sandstones together with schists, conglomerate and dolomite (Martin 2006; Obuobie and Barry 2012). Further information on the geology of the Volta Basin can be obtained from Obuobie et al., (2016), Mul et al. (2015), Obuobie and Barry (2012) and Martin (2006). The soils of the Basin (Figure 2.6) are derived from weathered parent material of the mid Palaezoic age (Andah et al., 2005 *cited in* Obuobie, 2008) with the topsoil

characterized by the buildup of organic matter (Kasei, 2009). The soils in the north of the basin (Burkina Faso) are mostly of lateritic type while that in the south (Ghana) is mainly lixosols. These weathered soils are mostly kaolinite clays high in iron, aluminium and titanium oxide. The soils in the northern savannah part of the Basin have less organic matter and lower nutrient content than the forest soils in the south (Kasei, 2009). The arenosols, mostly found in the arid northern portion of the basin, constitute the other main group of soils in the basin (Jung, 2006). These soils have high infiltration rates and are red in colour due to the sand being coated with iron oxides (Jung, 2006).

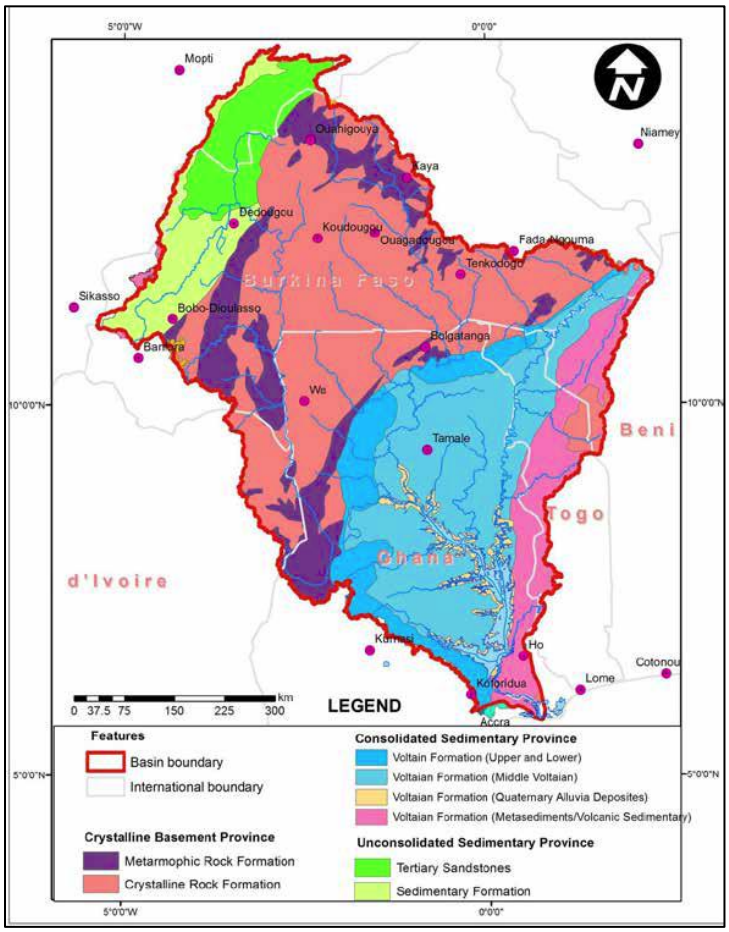

Figure 2.5: Volta Basin Geology (Glowa Volta Project, obtained from Mul et al., 2015)

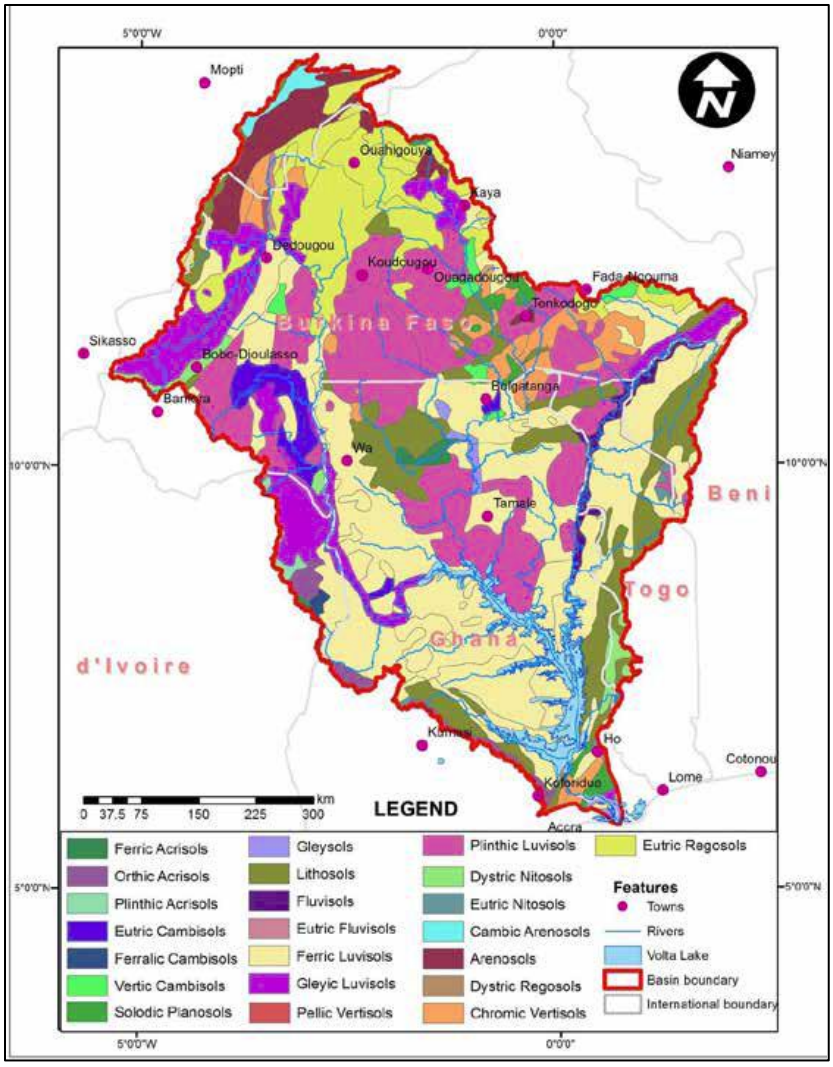

Figure 2.6: Volta River Basin soil map (Mul et al., 2015)

2.5. **Land cover and land use**

Land cover in the Volta Basin is dominated by the savannah land cover (Figure 2.7), which covers about 86% of the basin (Obuobie 2008). The remaining (14%) land cover is made up of croplands and natural vegetation wetland, forest cover and urban/industrial areas (WRI, 2003 *cited in* Obuobie 2008). Cultivated crops include cereals such as maize and millet, root crops and vegetables (Obuobie, 2008). Land cover type has a major influence on runoff processes including infiltration (Chevallier and Planchon, 1993; Giertz, 2004).

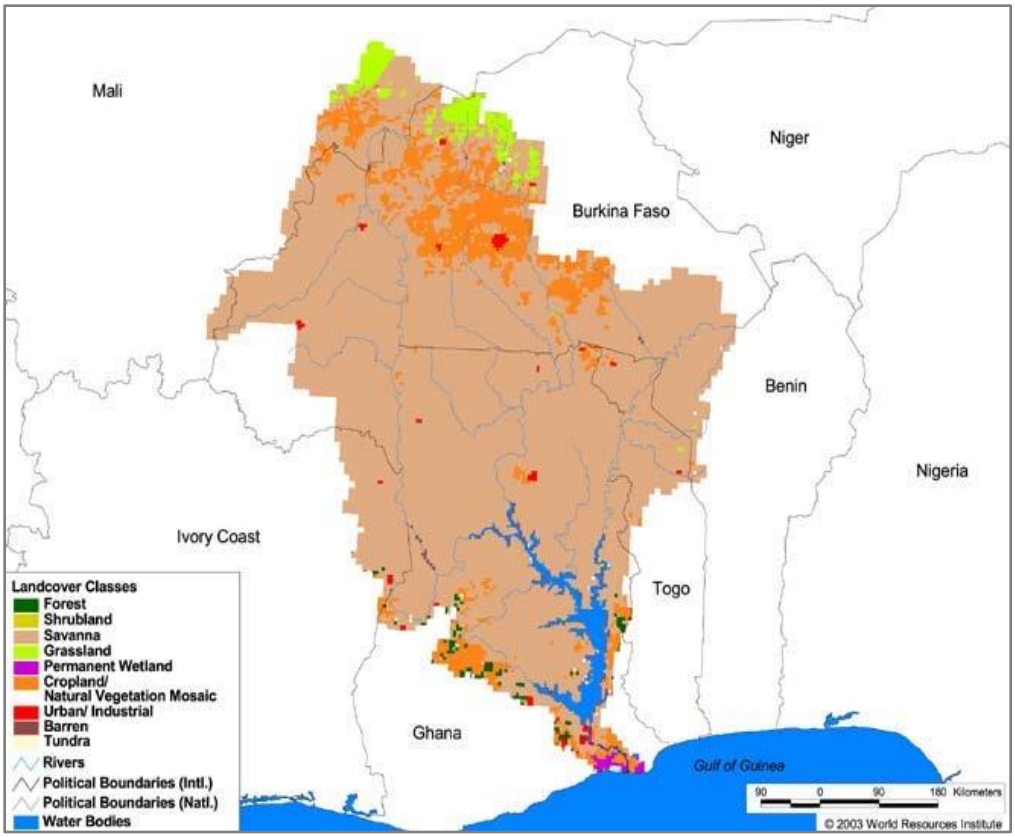

Figure 2.7: Land cover map of the Volta River Basin (Barry et al., 2005)

2.6. Surface water development and use

The Volta River Basin has a number of reservoirs constructed to mobilize water for agriculture, energy generation and water supply. The basin houses one of the world's largest man-made lakes, the Volta Lake, which resulted from the construction of the Akosombo Dam in Ghana in 1964 for hydropower generation. The lake has a surface area of 8,500 km^2 and a storage capacity of 148 km^3 (FAO, 1997b). The Kpong Headpond is a relatively smaller hydroelectric dam constructed in 1981 at Kpong, 20 km downstream of Akosombo with an area of about 40 km^2 (WRC, 2016). Together the Akosombo dam and Kpong headpond generate about 1,180 MW of hydropower (Ghana Energy Commission, 2015). The ever increasing energy demands and high energy costs in the country has, however, led to the establishment of a third dam, the Bui, located

in the Bui Gorge of the Black Volta Basin, approximately 150 km upstream of Lake Volta (Environmental Resources Management, 2007). The construction of the dam began in 2009 and started operation in May 2013 with a hydropower generation of about 400 MW.

A number of other small and large dams have also been constructed by governments, local populace and Non-Governmental Organizations (NGOs) in the other 5 riparian countries of the basin. These constructions occurred after the severe droughts of 1970s and 1980s and are mainly for irrigation and watering of livestock for food security. A typical example is the case of the Nakambé (White Volta) sub-basin in Burkina Faso where more than 600 small dams have been built (Barry et al., 2005). Power generating dams have also been constructed on the Oti River at the border between Togo and Benin and in some of the Volta main tributaries (e.g., Bagre on White Volta and Kompienga on Oti in Burkina Faso). The power generating capacities of the Bagre and Kompienga dams are 16 MW and 14 MW, respectively (Mul et al., 2015).

The mean annual groundwater recharge of the Volta River system is approximately 5-13% of annual rainfall (Martin, 2006). Since surface water is becoming increasingly insufficient for many communities in the basin, most of the people have resorted to the use of groundwater for everyday domestic purposes and for irrigation.

2.7. The Black Volta River Basin

2.7.1. Location and administrative boundaries

The Black Volta River Basin (Figure 2.8) is located between Latitude $7^{o}00'00''N$ and $14^{o}30'00''N$ and Longitude $5^{o}30'00''W$ and $1^{o}30'00''W$ (Annor, 2012). With a total area of about 142,056 km^{2} (Kasei, 2009), it is the largest sub-catchment of the Volta River Basin. It is shared by Ghana, Burkina Faso and Cote D'Ivoire.

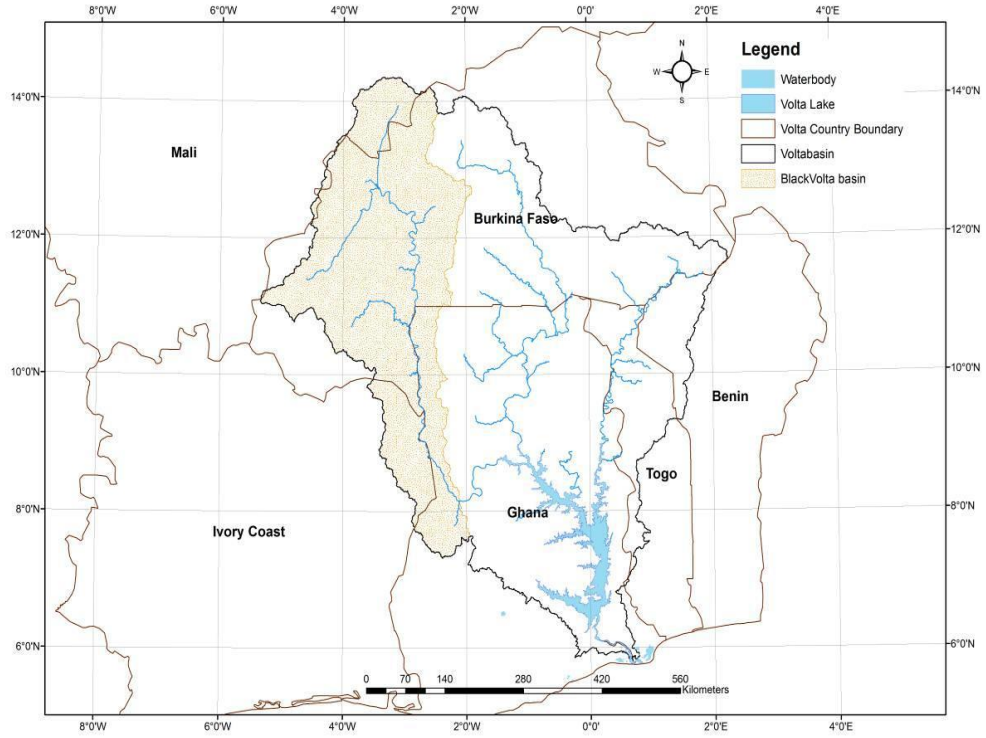

Figure 2.8: The Black Volta sub-catchment within the Volta Basin (Annor, 2012)

2.7.2. Rainfall, temperature and evaporation

The BVRB experiences two contrasting rainfall seasons: the rainy season and the dry season. Rainy season spans from May to September during which over 76% of the total annual rainfall occurs (Amisigo, 2005 *cited in* Obuobie, 2008) with the remaining months being dry and hot. Mean annual rainfall ranges between 1,043 mm - 1,270 mm, with annual evapotranspiration of about 1,450 mm/year to 1,800 mm/year. Mean monthly minimum temperature for the basin ranges between 18 ^{o}C in December to 25 ^{o}C in April while mean maximum temperatures vary from 30 ^{o}C in August to 37 ^{o}C in April (Figure 2.9). The spatial distribution of rainfall in the BVRB is presented in Figures 2.10 and 2.11.

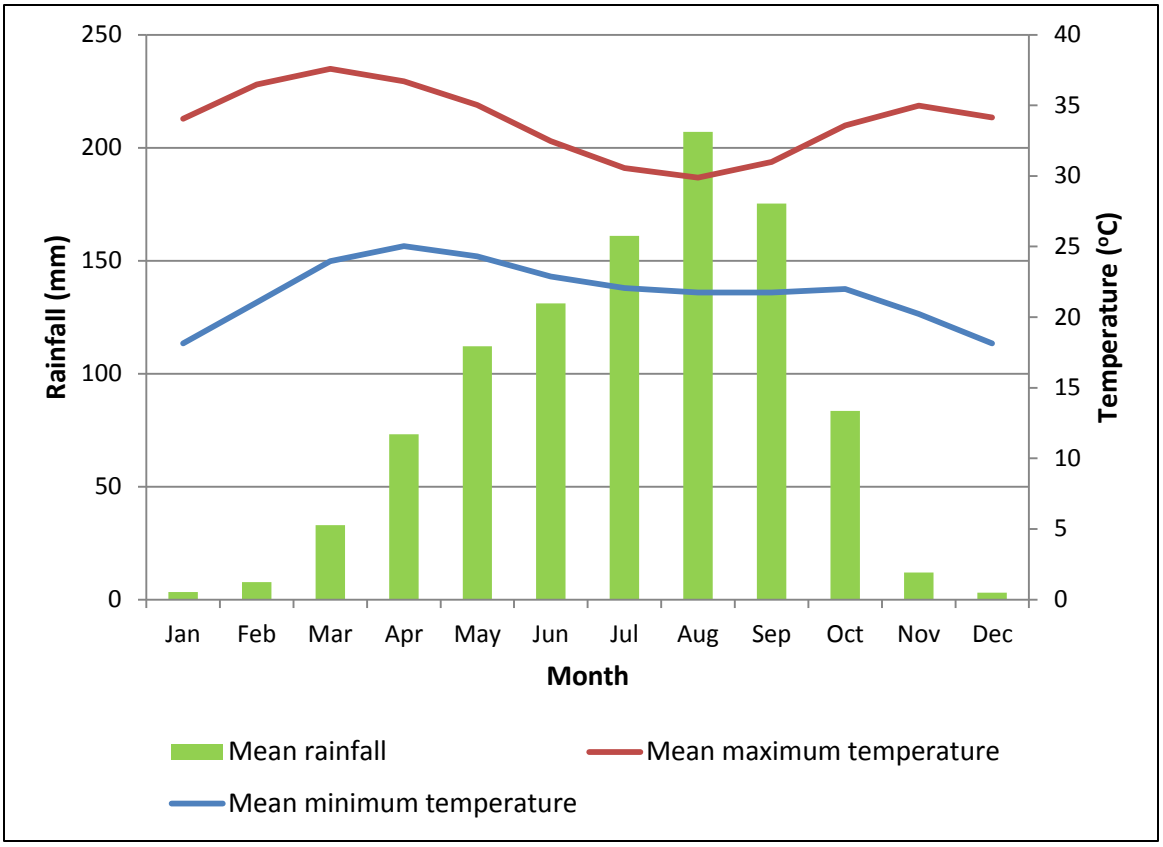

Figure 2.9: Mean monthly rainfall and temperature in the Black Volta Basin (1981-2010)

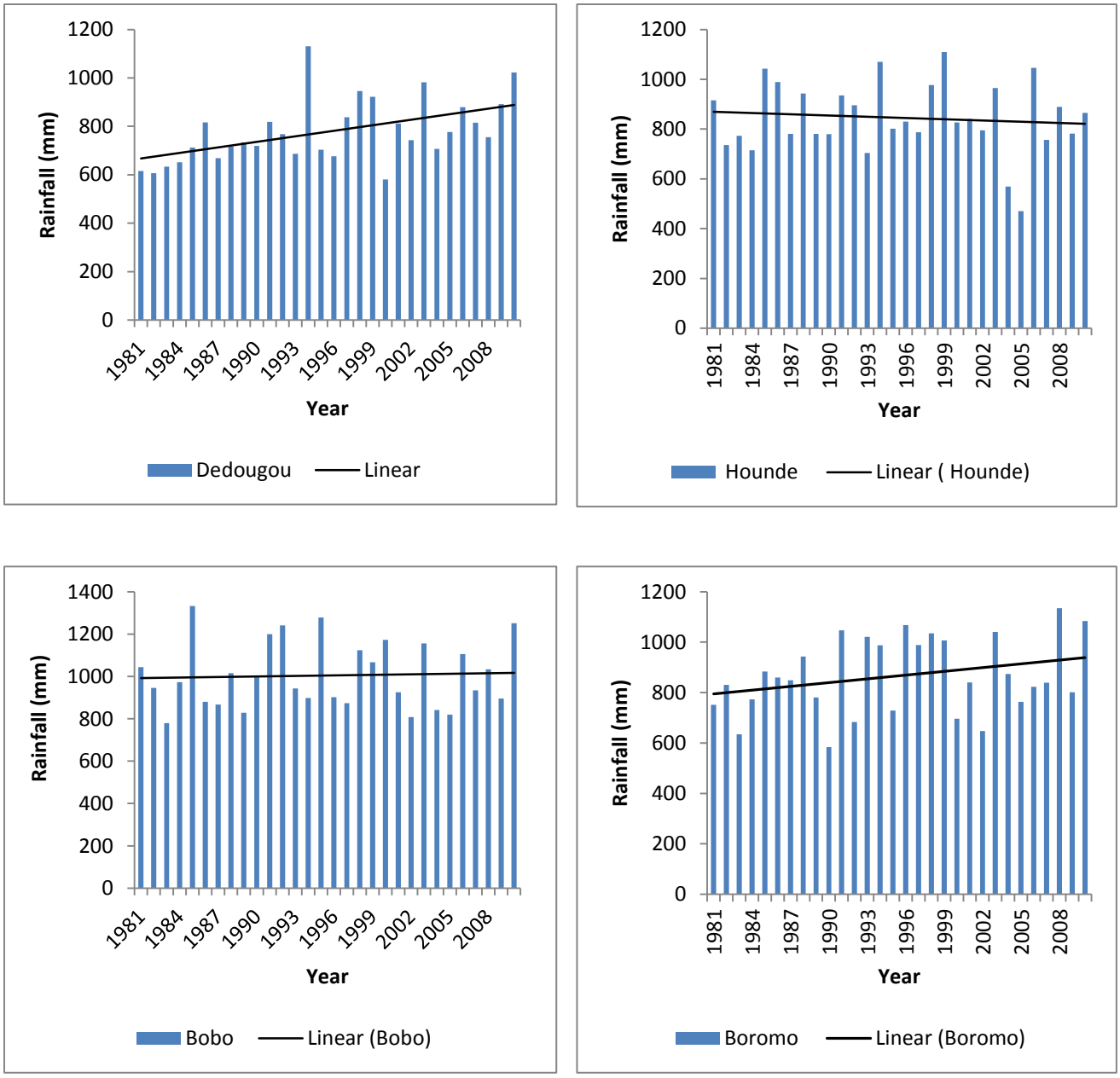

Figure 2.10: Inter-annual rainfall (1981-2010) at 4 gauge stations in the north of the basin in Burkina Faso

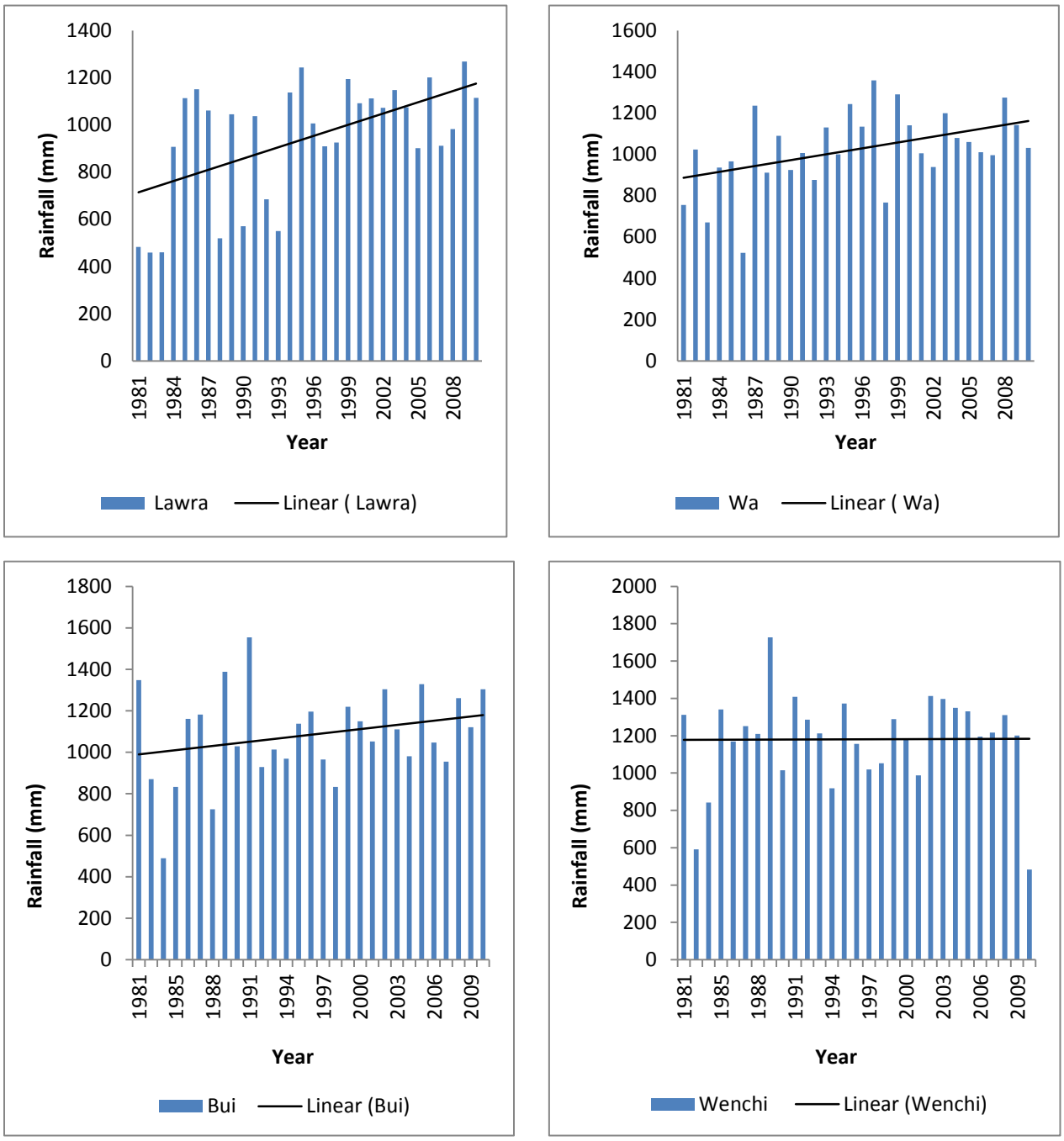

Figure 2.11: Inter-annual rainfall (1981-2010) at 4 gauge stations in the south of the basin in Ghana

2.7.3. Vegetation and land use /land cover

The BVRB belongs to the Guinea and Sudan savannah agro ecological zones. The dominant vegetation is savannah woodland. Majority of the land in the basin is used for agricultural purposes, with most of the crops (e.g. millet, sorghum, rice and maize; cassava, beans, groundnuts and yams) cultivated under rain-fed conditions. During the dry season, some farmers in the region cultivate vegetables. Livestock grazing is usually done on free range. In the dry season, however, herdsmen migrate with their animals in search of feed and water in nearby communities (Barry et al., 2005). Usually, most herdsmen (commonly known as "fulani") migrate from Mali and Burkina Faso to the lower parts of the basin in Ghana (Annor, 2012) where the grass is greener. As this movement places a lot of pressure and burden to Ghanaian communities, there is often big strife between herdsmen and affected community members.

2.7.4. Geology and soil

The Black Volta Basin geology consists mainly of granite, Birimian, Voltaian and Tarkwaian systems (Gordon and Amatkpor, 1999; Barry et al., 2005). The Birimian system is made of gneiss, granite-gneiss, phyllite, migmatite, schist and quartzite (Gyau-Boakye and Tumbulto, 2006). The Voltaian system is made of Precambrian to Paleozoic sandstones, shale and conglomerates. The Tarkwaian system consists of quartzites, phyllites, grits, conglomerates, and schists. The underlying rocks of the basin are without inherent porosity and so groundwater is stored only in fractures in the rocks (Barry et al., 2005). Based on the FAO claissification, the soils of the BVRB are dominantly Luvisols and Gleysols (Figure 2.12).

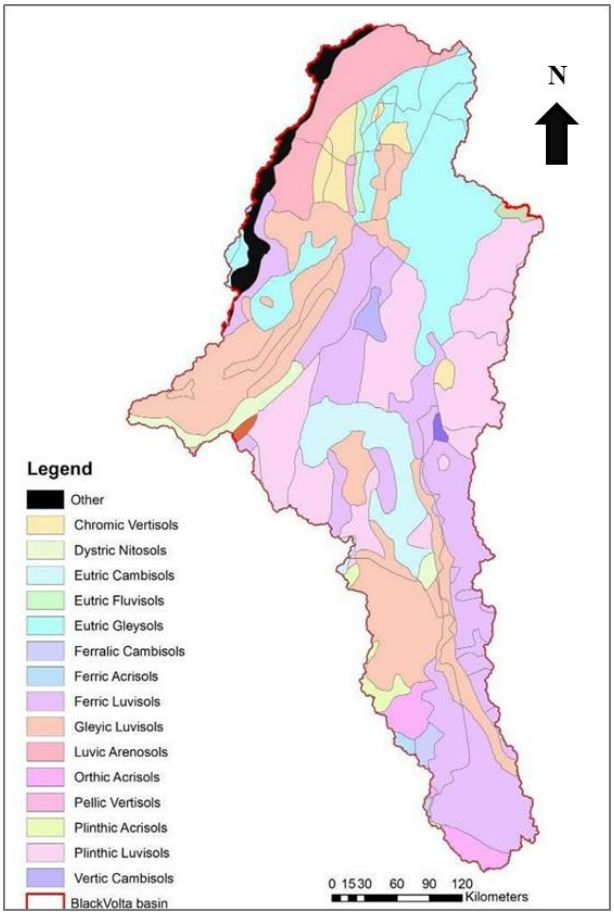

Figure 2.12: Dominant Soil types in the Black Volta River Basin (Annor, 2012)

2.7.5. Population

The population of the BVRB was around 4.5 million as of year 2000 and projected to reach 8 million by 2025 (Annor, 2012). The basin's population density ranges between 8 and 123 people/km^2 (Allwaters Consult, 2012), with a population growth rate of around 3% per annum (Green Cross International, 2001).

2.8. Conclusion

Due to the numerous services it offers, the Black Volta River Basin in West Africa remains an important resource especially for the four countries surrounding it.

CHAPTER 3: DATA, MATERIALS AND METHODS

This chapter describes in detail the data, materials used and procedure followed in achieving the objectives of the study.

3.1. Data

3.1.1. Soil and Water Assessment Tool (SWAT) input data

The input data used for setting up the SWAT model for the Black Volta basin included a digital elevation model (DEM), the year 2000 land-use/land cover (LULC) map, soil map and data, data on climate, plant growth, management and the Bui reservoir. The land use map for the year 1990 was used in the land use sensitivity analysis. Streamflow and sediment yield data covering a period of eleven years (2000-2010) and eight years (2000-2007) respectively, were used for calibrating and validating the model.

3.1.2. Digital elevation model (DEM)

The Shuttle Radar Topographic Mission (SRTM) Digital Elevation Model (DEM) provides reliable global coverage of topography and stream network and was used in this study for watershed delineation. The DEM (Figure 3.1) was obtained from the CGIAR-CSI Consortium for Spatial Information server (http://srtm.csi.cgiar.org/index.asp) and had a resolution of 90 m. All data voids had been filled when the DEM was obtained.

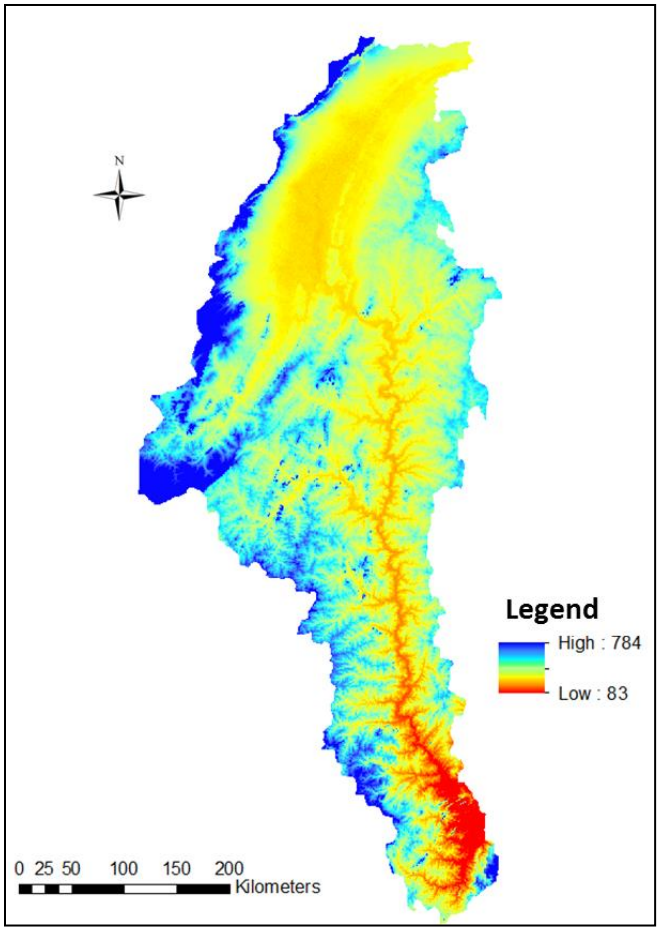

Figure 3.1: SRTM DEM of the Black Volta Basin (Source: The CGIAR-CSI Consortium for Spatial Information server - http://srtm.csi.cgiar.org/index.asp)

3.1.3. Land use/land cover map and data

The year 2000 land-use/-cover map (Figure 3.2) with a resolution of 250 m obtained from the GLOWA Volta project of the Center for Development Research (ZEF), Germany, was used in setting up the SWAT model. The original legend of the map was modified to allow for modelling in SWAT as shown in Table 3.1. The existing SWAT look up table was also modified to include land use/land cover types that were not already present (e.g. savanna) in SWAT 2012.

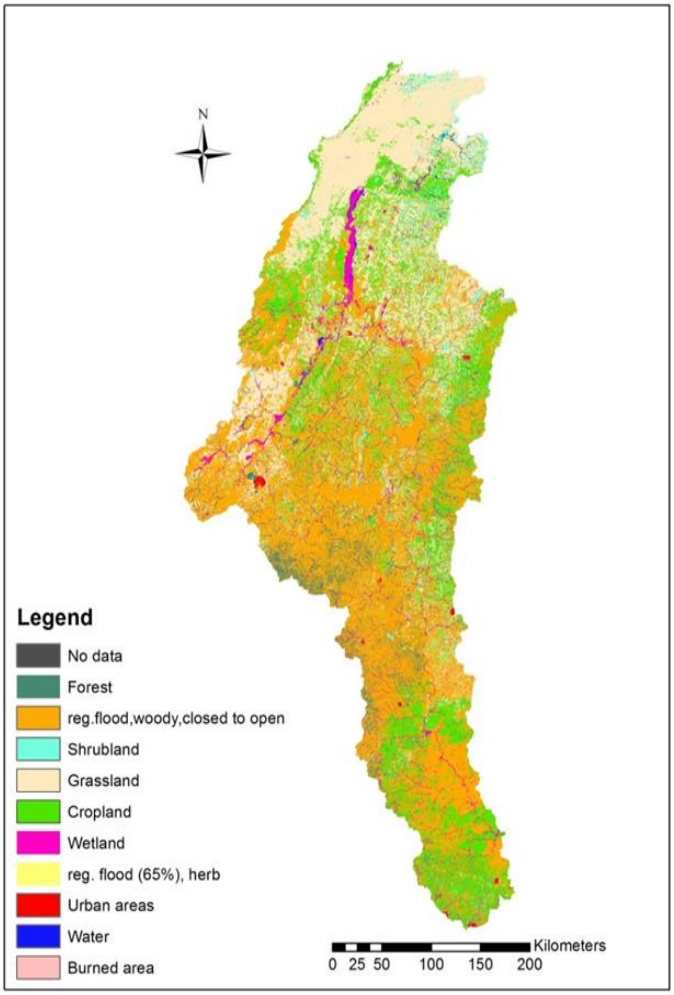

Figure 3.2: Land use/land cover map used as input in SWAT (Data source: Glowa Volta project)

Table 3.1: User-defined SWAT LULC classes for the Black Volta Basin

No.	Land use class	Description
1	SAVA	Savanna
2	FRSE	Forest-Evergreen
3	SHRB	Shrubland
4	GRAS	Grassland
5	AGRL	Agricultural Land-Generic
6	WETN	Wetlands-Non-Forested
7	WEHB	Herbaceous wetland
8	URMD	Urban Medium Density
9	WATR	Water Body
10	BARR	Barren

3.1.4. Soil map and data

The BVRB soil map (Figure 3.3) used in this study was obtained from the FAO digital soil map of the world and derived soil properties (FAO, 1995). Soil properties play an important role in the hydrological process of watersheds. Soil physical characteristics determine the movement of water and air within the HRU and are required for modelling in SWAT. In addition to the digital soil map, the SWAT model requires information on the physical and chemical properties (e.g. soil depth, soil texture, hydraulic conductivity and bulk density, and organic carbon) of each soil layer modeled. These data were obtained from the FAO digital soil map of the world and derived soil properties (FAO, 1995) and the Soil Research Institute (SRI) in Ghana. A user table specific for the Black Volta River basin soil layers was appended to the existing soil table in the SWAT database using Arc toolbox in ArcGIS since the soil types found in the study area are not

included in the US soils database. A list of soil properties required for modelling in SWAT is listed in Table 3.2.

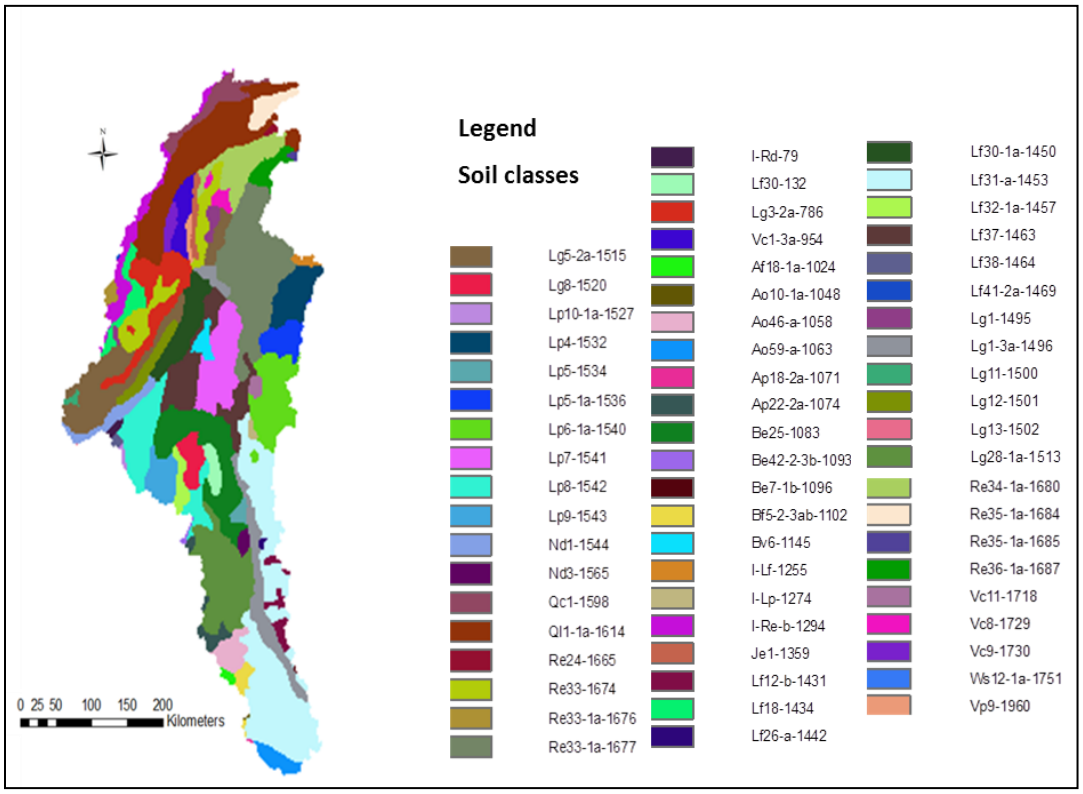

Figure 3.3: Soil map of the Black Volta Basin used as input in SWAT

Table 3.2: Soil physical properties required for modelling in SWAT (Arnold et al., 2012a)

Soil parameter	Description	Unit
NLAYERS	Number of layers in the soil (min 1, max 10)	-
HYDGRP	Soil hydrologic group (A, B, C, D)	-
SOL_ZMX	Maximum rooting depth of soil profile	mm
ANION_EXCL	Fraction of porosity from which anions are excluded	-
SOL_CRK	Potential or maximum crack volume of the soil profile expressed as a fraction of the total soil volume [optional]	-
TEXTURE	Texture of soil layer [optional]	-
SOL_Z	Depth from soil surface to bottom of layer	mm
SOL_BD	Moist bulk density	Mg/m^3 or g/cm^3
SOL_AWC	Available water capacity of the soil layer	mm H_2O/mm soil
SOL_K	Saturated hydraulic conductivity	mm/hr
SOL_CBN	Organic carbon content	% soil weight
CLAY	Clay content	% soil weight
SILT	Silt content	% soil weight
SAND	Sand content	% soil weight
ROCK	Rock fragment content	% total weight
SOL_ALB	Moist soil albedo	-
USLE_K	Soil erodibility factor	0.013 (metric ton m^2 hr)/(m^3-metric ton cm)

3.1.5. Climate data

The observed daily climate data used in this study for the extreme event analysis and for setting up the SWAT model were obtained from the Ghana Meteorological Agency and the Direction Generale de la Météorologie, Burkina Faso. The data included daily rainfall and minimum/maximum air temperature and were from 11 synoptic climate stations (Figure 3.4) in the BVRB and covered the period 1981-2010. During the extreme event analysis, data for only 6 (Bobo-dioulasso, Bole, Boromo, Dedougou, Gaoua and Wa) out of the 11 stations were available so these were used. For the SWAT modelling, all 11 climate station data were used. SWAT requires climate data such as rainfall, maximum and minimum air temperature, solar radiation, wind speed and relative humidity to calculate the water balance of a river basin. The SWAT model reads the values for weather parameters directly from records but in cases where there is missing data in any of the weather data, a weather generator incorporated in SWAT can be used to fill in gaps in data and/or simulate data. Three climate stations (Bobo-Dioulasso, Bole and Dedougou) in the BVRB, with almost complete (> 98%) climate data were used for generating missing records in the data of the other stations (Annex 1).

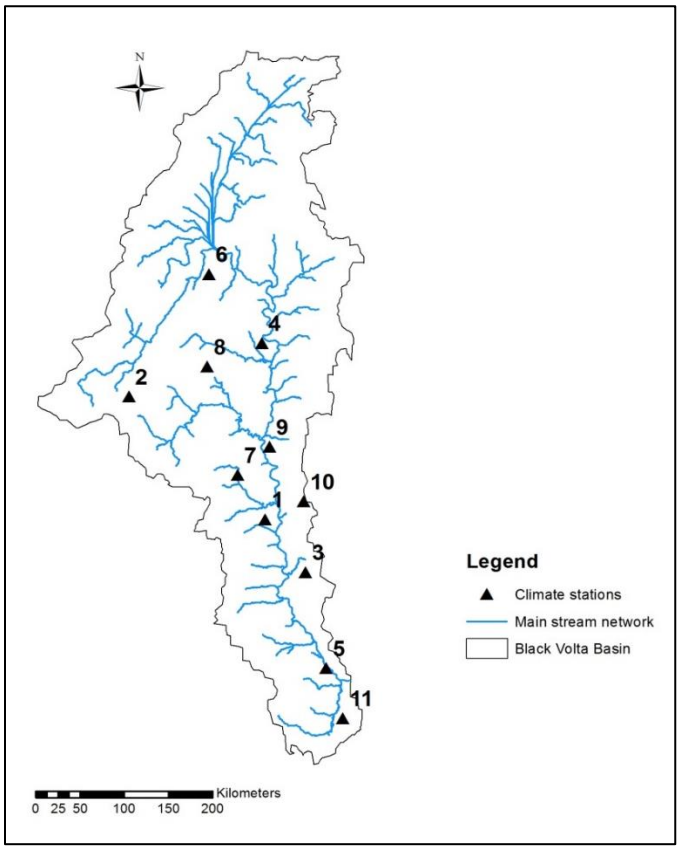

No.	Station Name
1	Batie (BF)
2	Bobo-Dioulasso (BF)
3	Bole (GH)
4	Boromo (BF)
5	Bui (GH)
6	Dedougou (BF)
7	Gaoua (BF)
8	Hounde (BF)
9	Lawra (GH)
10	Wa (GH)
11	Wenchi (GH)

Figure 3.4: Location of synoptic climate stations in the Black Volta River Basin

3.1.6. Discharge data

Monthly discharge data from the streamflow gauge at Bui on the main course of the BVRB (Figure 3.5) was used for calibrating and validating the SWAT model. The discharge data, covering a period of eleven years from 2000 to 2010 was obtained from the Ghana Hydrological Services Department and the Water Research Institute (WRI) of Ghana. Bui has a drainage area of about 127,926 km^2.

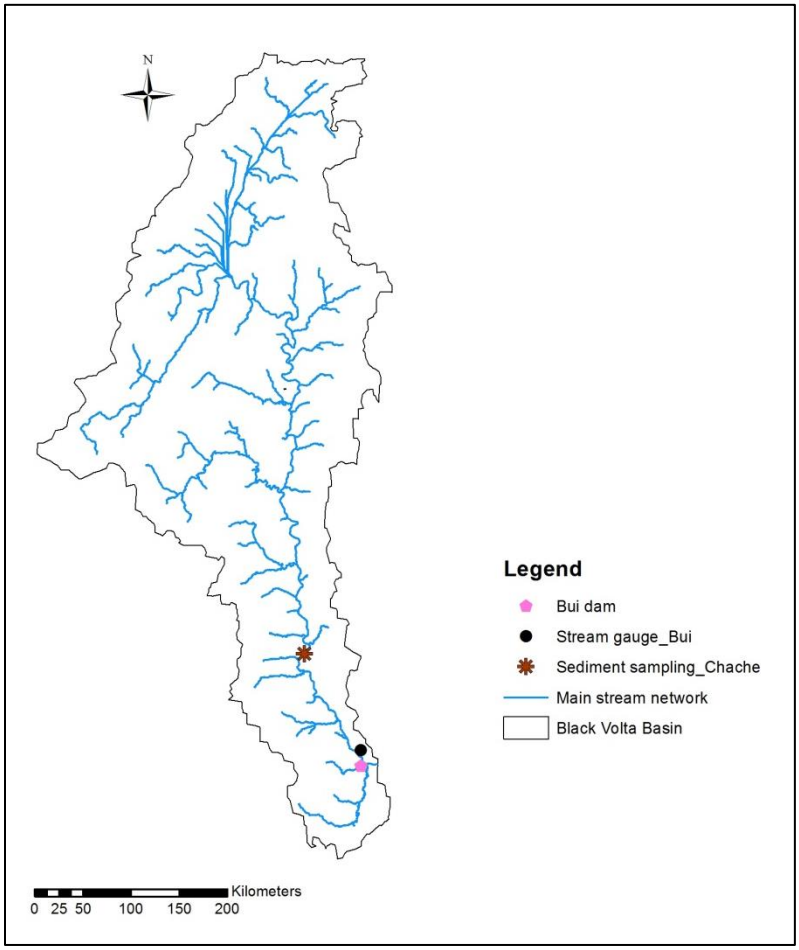

Figure 3.5: Location of sediment sampling site, Bui dam and Bui discharge station in the Black Volta Basin.

3.1.7. Reservoir data

The 400-megawatt Bui dam (Figure 3.5) is the main reservoir located on the main course of the Black Volta River. The data required for reservoir water balance modelling in SWAT (shown in Table 3.3) were obtained from literature, Water Research Institute in Ghana and the Bui Dam Authority in Ghana.

Table 3.3: Characteristics of the Bui dam

Parameter	Description	Value	Unit
MORES	Month the reservoir became operational	May	_
IYRES	Year of the simulation the reservoir became operational	2013	_
RES_ESA	Reservoir surface area when the reservoir is filled to the emergency spillway	44000	ha
RES_EVOL	Volume of water needed to fill the reservoir to the emergency spillway	1257000*10E4	m^3
RES_PSA	Reservoir surface area when the reservoir is filled to the principal spillway	35000	ha
RES_PVOL	Volume of water needed to fill the reservoir to the principal spillway	772000*10E4	m^3
RES_VOL	Initial reservoir volume	694800*10E4	m^3

3.1.8. Sediment data

Measured data on sediment yield are very limited in developing countries including the riparian countries of the Black Volta River Basin. In Ghana, for example, sediment yield data is limited due to the high cost associated with sampling and lack of logistics (Akrasi, 2011). The problems of lack of continuous suspended sediment concentration records and hence sediment load data can be overcome through development of sediment rating curves (e.g.,Walling 1977). In a number of studies (e.g., Walling, 1977 and Zhang et al., 2012) suspended sediment load have

been estimated using sediment rating equations. For this research, sediment yield data for calibrating the SWAT model were generated from sediment rating curve established for the Black Volta Basin at Chache. Chache is located on the lower course of the main BVRB (Figure 3.5) and was chosen for suspended sediment sampling because of the availability of historic flow discharge data for the development of sediment rating curve for the Basin. Sediment (suspended) sampling for laboratory analysis of sediment concentration was done once every month from May 2014 to June 2015 using the depth integration procedure (Guy and Norman, 1970). Flow measurements were also taken with the mobile OTT Qliner 2 each time sampling was done. When maintained in a stationary location in a river, the Qliner measures the water depth and velocities of water passing through the vertical axis of the instrument and calculates the average flow velocity of each vertical as well as the partial discharge of a discharge segment in accordance with the mid-section method (Rantz *et al.*, 1982). The final stream discharge is calculated as the total of all sub discharges when the measurement is completed. Details of the operating principles and instructions of the OTT Qliner 2 can be found in the OTT Hydromet 2011 user manual. Following the evaporation method (Tilrem, 1979) suspended sediment concentration was calculated using equation 3.1 below.

$$\mathrm{Cs} = \frac{\text{sediment weight (total weight of sand+clay+silt)}}{\text{smple weight (weight of water+sediment)}} * 10^6 \quad \text{(3.1)}$$

Cs = sediment concentration (ppm, same as mg/l for sediment concentration between 0 - 15,900 parts per million)

The suspended sediment concentration was converted to values of tons/day using equation 3.2 below:

$$Q_s = k * Q_w * C_S \quad \text{(3.2)}$$

where *Qs* is sediment discharge (tons/day), Q_w is water discharge (m^3/s), C_S is sediment concentration (mg/l), and *k* is 0.0864

Suspended sediments move at a close velocity with flow velocity (McMahon et al., 2004) making sediment load a function of water discharge. After obtaining the sediment discharge (tons/day), the sediment rating curve was developed for suspended sediment load (*Load*) and water discharge (*Q*) for Chache (see Annex 2) using equation 3.3.

$$Load = aQ^b \quad \text{(3.3)}$$

where *a* and *b* are empirical parameters.

The resulting sediment rating equation $\boldsymbol{S = 1.1168Q^{1.342}}$ (where S is the suspended sediment load in tons/day and Q is the discharge in m^3/s) developed for Chache was used together with historic streamflow data to generate historical suspended sediment yield data for the BVRB. Bedload was estimated as 25% of suspended load using Maddock's (1975) ratios for estimation of bedload (Annex 3). The total sediment yield for Chache was obtained by taking the sum of suspended sediment yield and bedload (Annex 4).

3.1.9. Other data

Other data e.g., plant-cover and land use factor, and potential heat unit that were used in setting up the SWAT model for the Black Volta Basin were obtained from literature.

3.1.10. Scenarios data

The scenarios data used for climate change impact assessment were obtained from the archives of the Coordinated Regional Downscaling experiment (CORDEX) for the West African region. The data included daily rainfall and maximum and minimum temperature series for the 11 climate stations used in this study for the period 1981-2005 (control run) and 2051-2100 (future

horizon). The data consisted of projection from 2 RCMs driven by 3 GCMs (Table 3.4) for two of the IPCC Scenarios, RCP 4.5 and RCP 8.5 (Table 3.5). The choice of the RCMs was based on data availability at the beginning of this study. Since majority of the CORDEX datasets consist of control runs and projections based on RCP 4.5 and RCP 8.5, the dataset with these two scenarios were chosen to enable a fair comparison of the results.

Table 3.4: Regional Climate models (RCMs) with driving Global Climate Models (GCMs) used in this study (modified from Nikulin et al., 2012)

RCMs	RCA4 (SMHI)	KNMI Regional ClimateModel, (RACMO22T)	RCA4 (SMHI)
Institute	Swedish Meteorological and Hydrological Institute	Koninklijk Netherlands Meteorologisch Instituut (KNMI) Netherlands	Swedish Meteorological and Hydrological Institute
Short name	RCA4	RACMO	RCA4
Resolution	0.44^{o}	0.44^{o}	0.44^{o}
Reference	Samuelsson et al. 2011; Kupiainen et al. 2011; Strandberg et al., 2014	van Meijgaard et al. 2008	Samuelsson et al. 2011; Kupiainen et al. 2011; Strandberg et al., 2014
Boundary forcing (GCMs)	MPI-ESM-LR (MPI-M) Stevens et al. 2013	ICHEC-EC-EARTH Hazeleger et al. 2010	CCCma-CanESM2 Chylek et al., 2011

Table 3.5: Characteristics of the IPCC Representative Concentration Pathways (Moss et al., 2010)

Name	Radiative Forcing	Concentration (ppm)	Emissions Pathway
RCP8.5	>8.5 W/m^2 in 2100	>1370 eq-CO_2 in 2100	Rising
RCP6.0	~6W/m^2 at the stabilization level after 2100	~850 eq-CO_2 at the stabilization level after 2100	Stabilization without overshoot
RCP4.5	~4.5W/m^2 at the stabilization level after 2100	~660 eq-CO_2 at the stabilization level after 2100	Stabilization without overshoot
RCP2.6	Peak at ~3/Wm^2 before 2100 then decrease	Peak at ~490 eq-CO_2 before 2100 then decrease	Peak and decline

3.1.11. Coordinated Downscaling Experiment (CORDEX)

The CORDEX initiative was founded by the World Climate Research Program of the World Meteorological Organization with the aim of fostering international collaboration to produce an ensemble of high-resolution historical and future climate projections at regional scales to be used as inputs for impact and adaptation studies (Giorgi et al. 2009; Jones et al. 2011). By downscaling different Global Climate Models (GCMs) participating in the Coupled Model Intercomparison Project Phase 5 (CMIP5) (Taylor et al. 2012) in combination with RCPs (Moss et al., 2008, 2010), the CORDEX project has produced projected future climate data for several regions in the world. Specifically, each climate model output from the CORDEX project is made up of an ensemble of RCM runs each one of them based on the output of one CMIP5 multi-model ensemble (Taylor et al. 2012), plus evaluation runs driven by ERA-Interim reanalysis data. The dataset includes rainfall, solar shortwave radiation and minimum and maximum temperature. These datasets are mostly made up of control runs and projections based mostly on the emission scenarios RCP4.5 and RCP8.5. For the Africa domain, the RCM simulations are at a grid resolution of 0.44°x 0.44° (Figure 3.6), approximately 50 km. Studies conducted over the

entire African continent (e.g. Nikulin et al., 2012; Panitz et al., 2014 and Dosio et al., 2015) and at the regional level (e.g. Klutse et al., 2014; Abiodun et al., 2015 and Endris et al., 2015) have shown that CORDEX RCMs simulate well the spatial and temporal distributions of the West African rainfall with some seasonal and sub-regional biases.

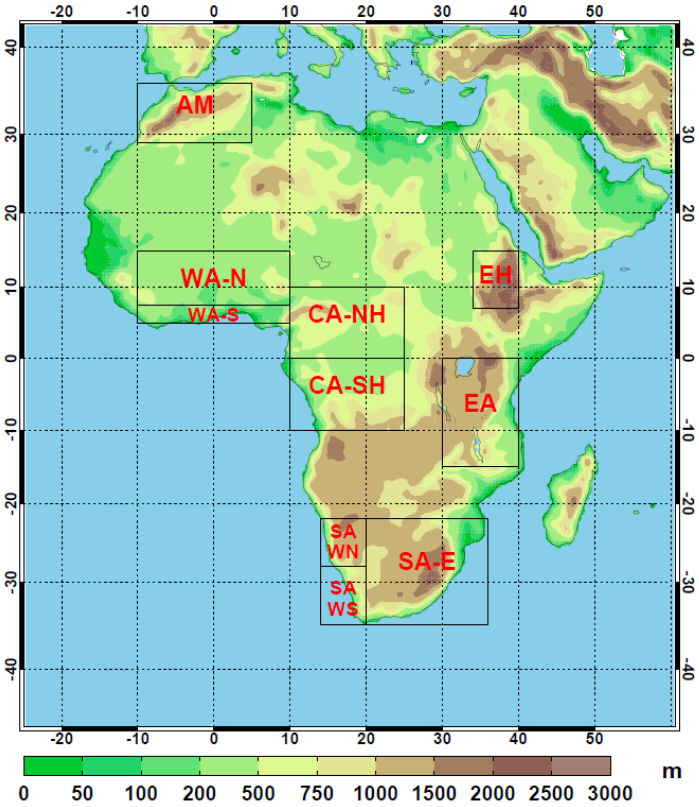

Figure 3.6: CORDEX Africa domain 0.44deg, 50-km (Swedish Meteorological and Hydrological Institute, 2016)

3.1.12. Representative Concentration Pathways (RCPs)

The Representative Concentration Pathways (RCPs) are the latest iteration of the scenario process, superseding the second generation of projections, the Special Report on Emissions Scenarios (SRES). The RCPs include four greenhouse gas concentration trajectories RCP2.6,

RCP4.5, RCP6.0, and RCP8.5 (shown in Table 3.5) and derive their names from a possible range of radiative forcing values in the year 2100 relative to pre-industrial values (+2.6, +4.5, +6.0, and +8.5 W/m^2, respectively) (van Vuuren et al, 2011a; Moss et al, 2010; Rogelji et al, 2012).

Representative Concentration Pathway (RCP) 2.6 scenario is compared to pre-industrial conditions and hence designed to meet the 2°C global average warming target with a peak in the radiative forcing at approximately 3 W/m^2 (~400 ppm CO_2) before the year 2100. This peak is followed by a decline to 2.6 W/m^2 (~330 ppm CO_2) by the end of the 21st century (van Vuuren et al., 2011b). RCP4.5 scenario includes long-term, global emissions of greenhouse gases, short-lived species, and land-use-land cover which stabilize radiative forcing at 4.5 W/m^2 (~650 ppm CO_2) in the year 2100. The third scenario, RCP 6.0 is a medium-end scenario in which greenhouse gas emissions increase gradually, stabilizing radiative forcing at 6.0 W/m^2 (~670 ppm CO_2) in the year 2100 (Moss et al., 2010; van Vuuren et al., 2011c). Compared to the total set of Representative Concentration Pathways (RCPs), RCP8.5 assumes the highest greenhouse gas emissions (business as usual) scenario, with a high rate of radiative forcing increase which peaks at 8.5 W/m^2 (~940 ppm CO_2) in year 2100 (Riahi et al., 2011). The RCP scenarios have the primary purpose of providing time-dependent projections of atmospheric greenhouse gas (GHG) concentrations (IPCC, 2007a) and are neither projections nor predictions but representations of alternative, possible ways in which the future may unfold depending on how much greenhouse gasses are emitted in the years to come. They were released in the year 2000 and have been used in the latest IPCC report - Assessment Report Five (AR5) in 2014**.**

3.2. **Materials**

As mentioned in section 3.1.10, the data used for the climate change impact assessment consisted of projection from the RCMs the Rossby Centre (SMHI) regional climate model, RCA4 and the

Regional Atmospheric Climate Model (RACMO). The RClimDex (1.0) software package was used for the extreme event analysis, and the Soil and Water Assessment Tool (SWAT) model for analyzing the impact of climate change on flow and sediment yield and assessing the sensitivity of land use/land cover change on streamflow of the Black Volta River Basin.

3.2.1. The Rossby Centre (SMHI) regional climate model, RCA4

RCA fourth generation is based on the High Resolution Limited Area Model (HIRLAM), a numerical weather prediction model (Undén et al., 2002). Earlier versions of the model include RCAO, RCA1, RCA2 and RCA3. Detailed descriptions of the earlier versions have been given by Rummukainen et al. (1998, 2001); Räisänen et al. (2003, 2004), Jones et al. (2004), Kjellström et al. (2005) and Samuelsson et al. (2011). The current version, the RCA4, is an improvement of the RCA3 (Samuelsson et al. 2011) and has undergone physical and technical changes to make it applicable for any domain worldwide. In addition, the improvement was aimed at making the model easy to use (Strandberg et al., 2014). Within the CORDEX project framework, the Swedish Meteorological and Hydrological Institute (SMHI) using RCA4 (Strandberg et al., 2014) has downscaled the ERA-Interim Reanalysis (1980-2010) and eight (8) different GCMs from the CMIP5 archives over the African domain (Jones et al., 2011, Nikulin et al., 2012). The data are available for RCP 2.6, RCP4.5 and 8.5 and cover the period 1951(1960) - 2100. The 8 GCMs employed by the SMHI for the dynamical downscaling are shown in Table 3.6.

Table 3.6: GCMs employed by the SMHI for the dynamical downscaling with RCA4

NO.	GCM NAME	INSTITUTE NAME
1	CanESM2	CCCma (Canada)
2	CNRM-CM5	CNRM-CERFACS (France)
3	HadGEM2-ES	MOHC (UK)
4	NorESM1-M	NCC (Norway)
5	EC-EARTH	ICHEC (Europian consortium)
6	MIROC5	MIROC (Japan)
7	GFDL-ESM2M	NOAA-GFDL (USA)
8	MPI-ESM-LR	MPI-M (Germany)

3.2.2. The Regional Atmospheric Climate Model (RACMO)

The Regional Atmospheric Climate Model (RACMO) is a hydrostatic limited-area model developed and maintained by the modeling group at the Royal Netherlands Meteorological Institute (KNMI) (van Meijgaard et al., 2008). The first version of the model, RACMO1 combines the HIRLAM model with the physics of ECHAM4. The second version, RACMO2, was developed based on the ECMWF-NWP release cy23r4 and the Numerical Weather Prediction (NWP) model HIRLAM version 5.0.6 (Lenderink et al., 2003). Climate change simulations of the RACMO22T model, driven by the EC-EARTH for RCP 4.5 and 8.5 within the CORDEX project are used in this study.

3.2.3. The RClimdex (1.0) software

The calculation of indices of climate extremes was done using RClimDex (1.0) software package developed by Zhang and Yang (2004). The software is a Microsoft Excel based program (ClimDex) under R 1.84 and provides a user friendly interface for computing indices of climate extremes. It computes all 27 core indices (described in Annex 5) suggested by the CCl/CLIVAR Expert Team for Climate Change Detection Monitoring and Indices (ETCCDMI).

3.2.4. The Soil and Water Assessment Tool (SWAT) model

Several hydrological models have been developed and used by a wide scientific audience for studying the impacts of climate change on water resources. A hydrological model is a simplified representation of the hydrological system for studying watershed hydrology. Examples of hydrological models include the VIC model (Liang et al., 1994), HEC-HMS (Fleming and Neary, 2004), SWAT (Arnold et al., 1998) model and WaSiM-ETH (Schulla, 1997). The SWAT model is a physically-based medium- to large-scale watershed model developed by the United States Department of Agriculture-Agricultural Research Service (USDA-ARS) and is used for studying long-term impacts of climate, land use and agricultural management on water quality and quantity (Neitsch et al., 2005; Arnold et al., 1998). It is a very flexible and robust tool that can be used for simulating a variety of catchment problems. The model derives many of its modelling processes from some earlier models like: Chemicals, Runoff, and Erosion from Agricultural Management Systems (CREAMS) model (Knisel, 1980), the Groundwater Loading Effects on Agricultural Management Systems (GLEAMS) model (Leonard et al., 1987), and the Erosion Predictability Impact Calculator (EPIC) model (Arnold et al., 1998).

Over the past few years, the SWAT model has gained worldwide recognition for its strengths compared to other hydrological models. It is considered a versatile model for water resource and nonpoint source pollution problems for a wide range of scales and environmental conditions (Gassman et al., 2007). Presently, more than 2,000 peer-reviewed articles on the model have been published with hundreds more published in other formats such as conference proceedings (Gassman, 2015). Globally, SWAT has been used in studying impact of climate change and/or land use change on hydrology of watersheds. Schoul and Abbaspour (2006) used SWAT to model river discharges of Niger, Volta and Senegal rivers in West Africa. Awotwi et al. (2015) used the model to assess the impact of land cover changes on water balance components of the

White Volta Basin and concluded that in such "a poorly gauged rural West African catchment, the model could provide reliable results for stakeholders". In assessing the climate change impact on streamflow in selected river basins in Ghana, Kankam-Yeboah et al. (2013) successfully calibrated and validated the SWAT model for Nawuni (on the White Volta River Basin) and Twifo Praso (on the Pra River Basin). Other SWAT related studies in the Volta Basin includes the works of Lumor (2017), Sood et al. (2013) and Obuobie et al. (2010) respectively.

3.2.5. Watershed simulation in SWAT

The first and basic step in setting up a watershed simulation is the partitioning of the watershed into subunits. SWAT allows the following subunits to be defined within a watershed;

- ✓ Sub-basins
- unlimited number of Hydrologic Response Units (HRUs) [1 per sub-basin required]
- Ponds [optional]
- Wetlands [optional]
- ✓ Reach/main channel segments [1 per subbasin required]
- ✓ Impoundments on main channel network [optional]
- ✓ Point sources [optional]

Sub-basins are the first level of watershed subdivisions. They possess a geographic position in the watershed and are related to one another spatially. Sub-basin delineation may be obtained from watershed boundaries defined by surface topography. In this way the whole area within a sub-basin flows to the sub-basin outlet. Another way to obtain sub-basin delineation is from grid cell boundaries. Generally a sub-basin contains at least one HRU, a tributary channel and a main reach. A wetland and/or pond may also be defined in a sub-basin as additional features.

Hydrologic response units (HRUs) are a further subdivision of the land area in a sub-basin and possess unique land use/management/soil attributes. Since it is often not practical to simulate individual fields with specific land use, management and soil, HRUs are used in most SWAT runs to simplify a run by lumping together all similar soil and land use areas into a single response unit. All calculations in SWAT are performed at the HRU level. The following section provides a summary of SWAT hydrology as well as the sediment component since they are important for this model application. The details of these and all the other components of the model can be found in the SWAT Input/Output Documentation (Arnold *et al*., 2012a).

3.2.6. Hydrology component

Simulation of watershed hydrology can be categorized into the land phase of the hydrologic cycle (Figure 1.2) and the routing phase of the hydrologic cycle. The routing phase involves movement through the channel network. The water balance equation (3.4) is the basic driver of the SWAT model hydrology. The model calculates daily water balances from meteorological, soil and land use data (Arnold et al., 1998).

$$SW_t = SW_o + \sum_{i=1}^{t} \left(R_{day} - Q_{surf} - E_a - W_{seep} - Q_{gw}\right)i \quad \text{..... (3.4)}$$

where SWt is the final soil water content (mm); SW0 is the initial soil water content on day i (mm); t is the time (days), Rday is the amount of rainfall on day i (mm); Qsurf is the amount of surface runoff on day i (mm); Ea is the amount of evapotranspiration on day i (mm); Wseep is the amount of water entering the vadose zone from the soil profile on day i (mm), and Qgw is the amount of return flow on day i (mm).

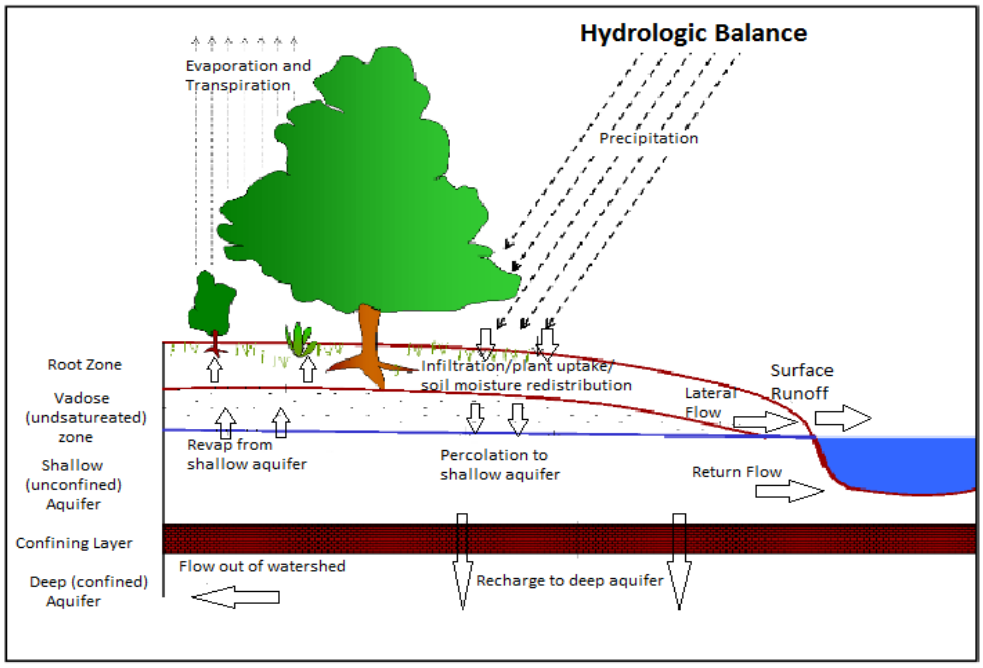

Figure 3.7: Schematic diagram of the hydrologic cycle used in the SWAT Model (Neitsch et al., 2005)

3.2.7. Surface runoff

Surface runoff occurs each time water application rate to the ground surface exceeds infiltration rate. The methods for surface runoff estimation in the SWAT model include the SCS curve number procedure (Soil Conservation Service 1972) and the Green & Ampt infiltration method (Green & Ampt 1911). Compared with the SCS curve number procedure, the Green & Ampt infiltration method is data intensive. For instance, whereas the former uses daily rainfall data, the latter needs hourly rainfall data. The SCS curve number method was thus used since the rainfall data for the study area was available only at the daily timescale.

3.2.8. Percolation

The SWAT model categorizes soil into multiple layers. Percolation of water through these soil layers is allowed when soil moisture content in a layer exceeds its field capacity. The rate of percolation in each of the layers is highest at saturation and reduces to zero when the field

capacity is reached. The flow from one layer to the underlying layer is modeled using the storage routing technique aggregated with crack flow. For dry and cracked soils, percolation of water occurs through the cracked layers without any impact on the water content of the soil. Percolated water through all the soil layers forms part of the groundwater and contributes to a stream as part of baseflow.

3.2.9. Lateral flow

The model uses a kinematic storage technique (Sloan et al., 1983, 1984) to compute lateral flow through each soil layer as a function of soil layer properties (saturated hydraulic conductivity, drainable porosity), soil slope and hill slope length.

3.2.10. Groundwater flow

The groundwater component in the SWAT model is simulated as two aquifers in each sub-basin; a shallow (unconfined aquifer which contributes to the flow in the main channel of the sub-basin) and a deep (confined) aquifer. Shallow aquifer recharge from percolation is also grouped into two; a part that percolates into deep aquifer and never gets to the stream, and a remaining part in shallow aquifer that adds to the stream as base flow and satisfies a portion of evaporative demand in the root zone (revap). Arnold et al., (1993) presume that water that enters the deep aquifer contributes to streamflow somewhere outside the watershed. Groundwater storage loses water either by seepage to the deep aquifer, upward movement from the water table into the capillary fringe or by discharging to rivers and lakes. The model simulates the contribution of groundwater to streamflow by creating shallow aquifer storage rechargeable by percolation from the unsaturated zone. The shallow aquifer storage is reduced by withdrawal, baseflow, deep aquifer recharge and upward flows into the soil zone.

3.2.11. Evapotranspiration

SWAT provides three methods for computing potential evapotranspiration (PET). These are the: Penman- Monteith (Monteith, 1965), Hargreaves (Hargreaves *et al*., 1985) and Priestley-Taylor (Priestley and Taylor, 1972). The model also provides an option to use daily PET values computed with other methods. Due to the lack of long-term good quality data on relative humidity, wind speed, and solar radiation, the Hargreaves method, which requires only minimum and maximum temperature data was used for computing PET in this study.

3.2.12. Transmission loss

According to Lane (1982) many watersheds in the semiarid regions have ephemeral channels that abstract large quantities of streamflow. SWAT calculates all transmission losses using the method by Lane (1983).

3.2.13. Flow routing

Water can be routed though channel network in the SWAT model by selecting the variable storage method or Muskingum River routing method using daily time step. The model estimates the volume of water to be routed (surface runoff + lateral flow + baseflow– transmission loss) first in each HRU and then sums the values up to calculate total volume of water to be routed from a sub watershed. Apart from transmission loss, the channel can also loose water via evaporation, which is a function of water surface area in the channel. Evaporation loss in each channel segment is subtracted from total volume before routing the flow through the next channel segment.

3.2.14. Erosion and sediment yield

The SWAT model estimates erosion and sediment yield for each hydrologic response unit (HRU) using the Modified Universal Soil Loss Equation (MUSLE) (Williams, 1975). The

MUSLE is a revision of the Universal Soil Loss Equation (USLE) developed by Wischmeier & Smith (1965, 1978). The USLE uses the delivery ratios (the sediment yield at any point along the channel divided by the source erosion above that point) since the rainfall factor represents energy used in detachment only. In the MUSLE, the energy factor used in the USLE is replaced with a runoff factor. As a result of this improvement, sediment yield prediction using the MUSLE approach eliminates the need for delivery ratios since the runoff factor represents the energy for detaching and transporting sediment. For comparison purposes SWAT computes the USLE.

The MUSLE (Williams, 1995) is given as:

$$SY = 11.8(Q_{surf} * q_{peak} * area_{hru})^{0.56} * K_{USLE} * C_{USLE} * P_{USLE} * LS_{USLE} * CFRG \quad (3.5)$$

$$CFRG = e^{(-0.053\text{rock})} \quad (3.6)$$

where SY is the sediment yield (t/ha), 11.8 is a unit conversion constant, Q_{surf} is the surface runoff volume (mm), q_{peak} is the peak runoff rate (m^3/s), $area_{hru}$ is the area of the hydrologic unit area (HRU) (in ha), K_{USLE} is the USLE soil erodibility factor (0.013 tm^2 h/m^3t cm), C_{USLE} is the USLE cropping and management factor (dimensionless), P_{USLE} is the USLE erosion control factor (dimensionless), and LS_{USLE} is the USLE slope length (in meter) and steepness factor (no units), and $CFRG$ is the coarse fragment factor (dimensionless) and rock represents the rock fragments in the first soil layer (%).

3.3. **Methods**

3.3.1. Extreme Indices Calculation

The calculation of indices of climate extremes was conducted using the RClimDex 1.0 software package (Zhang and Yang, 2004). Eleven (11) out of the 27 core indices devised by the joint World Meteorological Organization Expert Team on Climate Change Detection Indices

(ETCCDI) were considered. The selected indices included 5 temperature- and 6 rainfall- related (Table 3.7) indices relevant for the BVRB. Data quality control was carried out using the quality control procedure provided in the software.

Table 3.7: List of temperature- and rainfall- related indices used in this study

Index	Indicator Name	Definition	Units
SU25	Summer days	Annual count when TX (daily maximum temperature) >25 °C Days	Days
TR20	Tropical nights	Annual count when TN (daily minimum temperature) >20 °C Days	Days
WSDI	Warm spell duration indicator	Annual count of days with at least 6 consecutive days when TX >90th percentile	Days
DTR	Diurnal temperature range	Monthly mean difference between TX and TN	°C
GSL	Growing Season Length	Annual (1 Jan–31 Dec in NH; 1 July–30 June in SH) count between first span of at least 6 days with daily mean temperature T >5 °C and first span after July 1st (January 1st in SH) of 6 days with T <5 °C	Days
CDD	Consecutive dry days	Maximum number of consecutive days with rainfall <1mm	days
CWD	Consecutive wet days	Maximum number of consecutive days with rainfall ≥1mm	days
PRCPTOT	Annual total wet-day rainfall	Annual total rainfall in wet days with rainfall ≥1mm	mm
Rx5DAY	Max 5-day rainfall	Annual maximum 5 day rainfall	mm
SDII	Simple daily intensity index	Annual total rainfall divided by the number of wet days (defined as PRCP ≥1.0mm) in the year	mm/day
R95p	Very wet days	Annual total PRCP when rainfall>95th percentile	mm

3.3.2. Projected changes in precipitation and temperature over the BVRB

To project changes in precipitation and temperature over the BVRB, a stepwise approach involving climate downscaling and bias correction, model scenario formulation and future projections was followed.

3.3.3. Climate downscaling and bias correction

Firstly, each of the RCM data was corrected using the Quantile-Quantile downscaling technique and Quantile-Quantile transformation (Q-Q) (Maraun et al., 2010; Themeßl et al., 2011) to obtain station-specific future climate scenario data with reduced RCM biases. This was to help improve projections of the future rainfall and temperature (maximum and minimum) data. This empirical statistical technique was applied to adjust the statistical distribution of the RCM data to match the statistical distribution of the observed data. The Q-Q transformation procedure was applied on a monthly basis on each of the data set as described by Amadou et al., (2015) and Sarr et al., (2015), as follows;

The historical data set was split into two, one half for calibration and the other half for validation. In order to avoid issues due to non-stationarity in hydrologic time series, the calibration period consisted of every odd year starting from the beginning of the historical period (i.e. years 1, 3, 5, etc.). The performance of the downscaling was tested on even years (years 2, 4, etc.). The daily time series of the month were extracted for both calibration and validation periods from both observation and RCM simulation data.

Two empirical cumulative distribution functions, F_{obs} and F_{RCM}, were then developed. F_{obs} was generated using observations on the calibration period and F_{RCM}, using RCM outputs on the calibration period.Corrected RCM simulations, X_{CORR}, were generated on the validation period and future periods using the transformation: $X_{CORR} = F_{obs}^{-1}\left(F_{RCM}(X_{RCM})\right)$, where X_{RCM} refers to the variable extracted from raw simulated RCM data.

The probability mass function (PMF) of rainfall occurrence (i.e intensity greater than 1mm/day) and probability density function (PDF) of rainfall intensity on wet/rainy days, maximum and

minimum temperatures were built. The quantile-quantile transformation was applied to produce improved (corrected) future RCM simulations of a variable if it was noticed that the PDF (or (PMF) of a corrected variable was closer to the PDF of the observations than the PDF (or PMF) of the raw non-corrected variable.

Assessment of performance of the models in simulating historical climate is the first and necessary step for model projections. This is to help establish whether a model is credible enough to be used for climate projections. In this regard, the performance of the individual RCMs in simulating the historical (1981-2005) rainfall and temperature of the BVRB was evaluated. The performance of the mean of the RCMs was also assessed. The historical period was set from 1981 to 2005 to allow for comparison among the RCMs since some of the RCA4 generated historical data sets (e.g. rainfall) were only until the end of 2005.

3.3.4. Model scenario formation

The second step was to form sixteen model scenarios consisting of the individual RCM outputs, the ensemble average of the RCMs and two future time horizons, 2051-2075 representing the late 21st century (also the 2060s) and 2076-2100 representing the end of the 21st century (also the 2080s) (Table 3.8). The ensemble mean of the RCMs was considered to account for uncertainties in the projections (especially rainfall) and for more robust results as recommended by several authors (e.g. Owusu and Klutse 2013: Klutse et al., 2014; Panitz et al., 2014; Abiodun et al. 2015 and Endris et al. 2015; Dosio et al., 2015). There is a lot of disagreement in models regarding the trend of change and variability in rainfall over West Africa and indeed the entire continent of Africa (Hewitson and Crane 2006; IPCC-AR4, 2005).

Table 3.8: Model scenarios for climate change impact assessment in the Black Volta Basin

Scenario Number	Model Scenarios
1	RACMO22T/ ICHEC-EC-EARTH (RCP4.5/Late 21st century)
2	RACMO22T/ ICHEC-EC-EARTH (RCP4.5/End of 21st century)
3	RACMO22T/ ICHEC-EC-EARTH (RCP8.5/Late 21st century)
4	RACMO22T/ ICHEC-EC-EARTH (RCP8.5/End of 21st century)
5	RCA4/CanESM2 (RCP4.5/Late 21st century)
6	RCA4/CanESM2 (RCP4.5/End of 21st century)
7	RCA4/CanESM2 (RCP8.5/Late 21st century)
8	RCA4/CanESM2 (RCP8.5/End of 21st century)
9	RCA4/MPI-ESM-LR (RCP4.5/Late 21st century)
10	RCA4/MPI-ESM-LR (RCP4.5/End of 21st century)
11	RCA4/MPI-ESM-LR (RCP8.5/Late 21st century)
12	RCA4/MPI-ESM-LR (RCP8.5/End of 21st century)
13	ENSEMBLE (RCP4.5/Late 21st century)
14	ENSEMBLE (RCP4.5/End of 21st century)
15	ENSEMBLE (RCP8.5/Late 21st century)
16	ENSEMBLE (RCP8.5/End of 21st century)

3.3.5. Precipitation and temperature projections

Finally, projections of the direction of temperature and precipitation over the basin were made using Microsoft Excel software and following the model scenarios formed. The Mann-Kendall test (Mann, 1945; Kendall 1975; Gilbert 1987) was used in analyzing the trends of the projected changes while the magnitude (slope) of the trends were estimated using the Sen's slope estimator (Sen, 1968). The details of the Mann-Kendall test and the Sen's slope estimator are presented in Annex 7 and 8 respectively.

3.3.6. Hydrological modelling with SWAT

The processes followed to setup the SWAT model for the Black Volta included watershed delineation, determination of hydrological response units, weather data definition and finally the writing of input tables. The details of each of the processes is described below.

3.3.7. Watershed delineation

The SRTM DEM was used to delineate the BVRB watershed and to analyze the drainage pattern of the land surface in ArcGIS with ArcSWAT extension. The BVRB watershed was divided into 167 sub-basins (Figure 3.8) to allow for capturing of the heterogeneity in the catchment's physical properties.

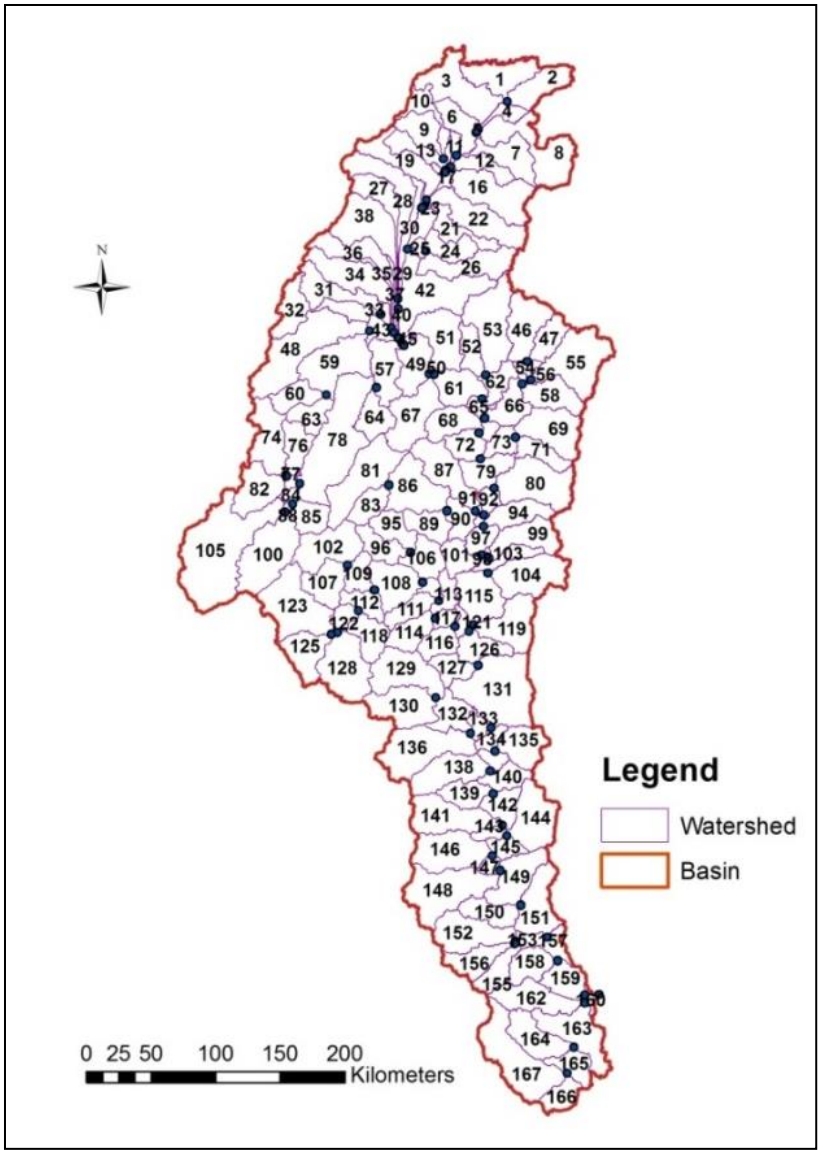

Figure 3.8: SWAT-delineated sub-basins in the Black Volta Basin

3.3.8. HRU definition

To account for differences in hydrologic conditions and evapotranspiration, the delineated sub-basins were further divided into 2,539 hydrologic response units (HRUs) based on differences in land use, soil and slope. To achieve this, the modified land use dataset was loaded and reclassified based on the land use SWAT code assigned to the map. In a similar manner, the soil map was also loaded and reclassified by linking it to the SWAT soil database information.

Finally the the slope characteristics were identified based on the DEM. The reclassification processes yielded 7 LULC classes (Table 3.9), 56 soil classes (Annex 6) and 3 slope classes (Figures 3.9 and 3.10). The BVRB is largely flat resulting in over 50% of the watershed falling within the slope class 0-2%. The overlay operation was carried out after the reclassification process.

The final step in the HRU analysis was the definition of the HRU. In defining HRUs, the SWAT model gives the option to have one or multiple HRUs per each sub-basin. For single HRUs per sub-basin, the model uses the dominant land category, soil type and slope class within each watershed for the designation process. For multiple HRUs in a sub-basin the user needs to select a threshold percentage value of land use, soil and slope data that will be used to determine the number and kind of HRUs in each watershed. In this simulation the multiple HRUs per sub-basin was selected. Subsequently, unique HRUs with the following parameter values were created;

- land use percentage (%) over sub-basin area = 5%
- soil class percentage (%) over land use area = 5%
- slope class percentage (%) over soil area = 5%

Table 3.9: Final land use classification of the Black Volta Basin used in the SWAT modelling

Watershed				Area [km^2]	
				135,003.18	
				Area [ha]	%Wat.Area
LANDUSE:	Shrubland	-->	SHRB	1585.91	1.17
	Grassland	-->	GRAS	36542.37	27.07
	Agricultural Land-Generic	-->	AGRL	27273.91	20.2
	Wetlands-Non-Forested	-->	WETN	2396.40	1.78
	Savanna	-->	SAVA	60874.79	45.09
	Water	-->	WATR	2.89	0
	Forest-Evergreen	-->	FRSE	6326.91	4.69

Note: This table is the resulting reclassification of the basin landuse in SWAT after defining the HRUs with a minimum threshold of 5% coverage of landuse class in each sub-basin.

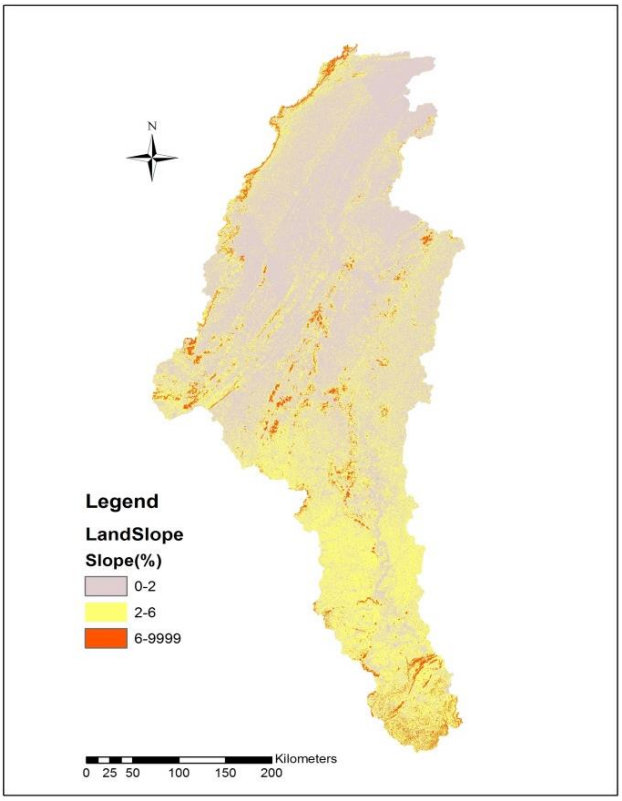

Figure 3.9: SWAT slope classes in the Black Volta River Basin

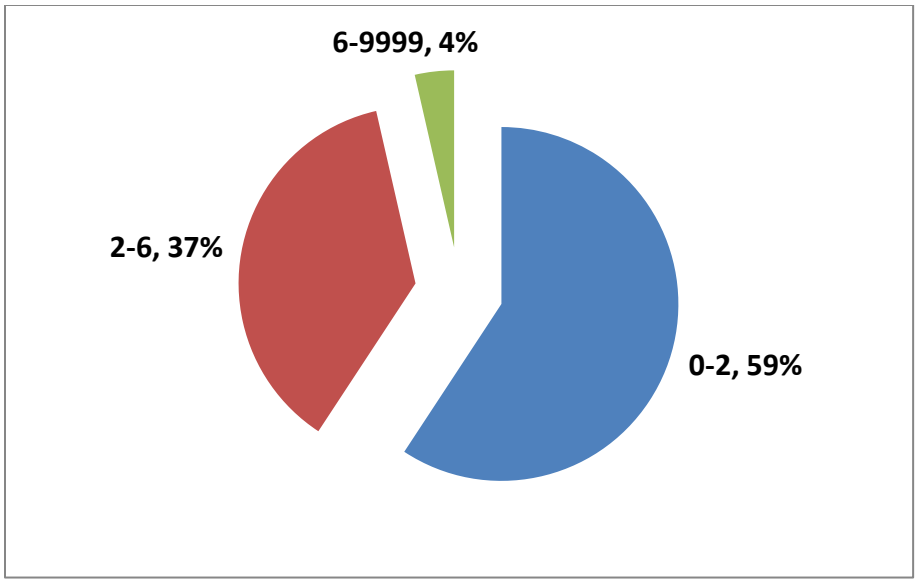

Figure 3.10: Land slope categories in the Black Volta River Basin, in percentage watershed area

3.3.9. Model calibration and validation using SUFI-2 in SWAT-CUP

Model calibration involves the adjustment of sensitive parameters of the model so as to mimic the hydrologic and other processes in a basin. The SWAT model has lots of parameters (physical and process) that needed to be adjusted through calibration. During the calibration process, model parameter values are selected and adjusted within recommended ranges and output variables compared with observed data (Arnold et al., 2012b). After model calibration it is important to verify that the model can make accurate simulations in different time period from the period of calibration without further adjustment in the values of the model parameters (Refsgaard, 1997). This verification process is termed validation. Prior to calibration and validation, sensitivity analysis was done to identify the most sensitive model parameters. Model uncertainty analysis was also undertaken to quantify the uncertainties in the modelling process. The aforementioned processes were achieved using SWAT-CUP (SWAT Calibration Uncertainty Programs: Abbaspour, 2007), which is a program developed at the Swiss Federal

Institute of Aquatic Science and Technology (EAWAG) for the calibration of SWAT. Sensitivity analysis, calibration, validation, and uncertainty analysis can be achieved using any of the five algorithms present in the SWAT-CUP program (Abbaspour, 2015). The procedures are the Particle Swarm Optimization-PSO (Eberhart and Kennedy 1995); the Sequential Uncertainty Fitting-SUFI-2 (Abbaspour et al., 2007); the Generalized Likelihood Uncertainty Estimation-GLUE (Beven and Binley, 1992); the Markov Chain Monte Carlo-MCMC (Vrugt et al., 2003) and the Parameter Solution-ParaSol (van Griensven and Meixner, 2006) to SWAT. In this study the SUFI-2 optimization algorithm for model calibration and validation was used since it represents all the sources of uncertainties (Yang et al., 2008). The details of each of the processes are described below. Further details of SWAT model calibration using the SWAT-CUP program can be found in Abbaspour (2015).

3.3.10. Model parameter sensitivity analysis

Before model calibration, sensitivity analysis needs to be carried out to determine how model outputs change when model input parameters are changed (Arnold et al., 2012b). Since the SWAT model has a lot of parameters, it is necessary to carry out sensitivity analysis to identify and select the most sensitive parameters for the calibration process. In addition to reducing computation time, sensitivity analysis makes calibration much easier since one is left to deal with a relatively small number of parameters. After pre-selection of parameters sensitive to flow based on literature search and expert knowledge, the "global sensitivity analysis" of the SUFI-2 program was used in identifying the most sensitive parameters and the relative significance of each of the parameters to flow output. A t-test which provides a t-stat summary and p-value helped in ranking the model parameters after the sensitivity analysis. Larger t-stats indicate more sensitivity while smaller P-values indicate higher significance of the parameter to the system and

vice-versa. For this study eighteen parameters (shown in Table 3.10) were taken through sensitivity analysis and the 13 most sensitive parameters to flow output used in model calibration.

Table 3.10: Parameters selected for sensitivity analysis with respect to streamflow

No.	Parameter Name	Description
1	R__CH_S2.rte	Average slope of main channel along the channel length (m/m)
2	R__CN2.mgt	SCS runoff curve number
3	R__SHALLST.gw	Initial depth of water in the shallow aquifer (mm)
4	R__SLSUBBSN.hru	Average slope length (m)
5	R__SOL_AWC(..).sol	Available water content of soil layer (mmH_20/mm soil)
6	R__SOL_K(..).sol	Saturated hydraulic conductivity (mm/hr)
7	V__ALPHA_BF.gw	Baseflow alpha factor (days)
8	V__ALPHA_BNK.rte	Baseflow alpha factor for bank storage (days)
9	V__CANMX.hru	Canopy storage (mm)
10	V__CH_K2.rte	Effective hydraulic conductivity in the main channel (mm/hr)
11	V__CH_N2.rte	Manning's "n" value for the main channel
12	V__ESCO.hru	Soil evaporation compensation factor
13	V__GW_DELAY.gw	Groundwater delay (days)
14	V__GW_REVAP.gw	Groundwater revaporation coefficient
15	V__GWQMN.gw	Threshold depth of water in the shallow aquifer required for return flow to occur (mm)
16	V__RCHRG_DP.gw	Deep aquifer percolation fraction
17	V__REVAPMN.gw	Threshold depth of water in the shallow aquifer for "revap" to occur (mm)
18	V_SURLAG.bsn	Surface runoff lag time

Note: 'r__' – indicates relative change in the parameter value which implies multiplying the existing parameter value by 1 plus a given value; 'v__' – indicates replacement by a new value which implies substitution of a parameter by a value from the given range.

3.3.11. Calibration and validation of flow and sediment

The model was calibrated on a monthly basis first for discharge and thereafter for sediment (also on a monthly time step) as recommended by Abbaspour (2015). The model calibration for flow

was carried out using six years (1995-2000) observed monthly discharge data at Bui, close to the outlet of the modeled basin. A warm-up period of three years (1992-1994) prior to the calibration period was allowed to stabilize the initial soil moisture content. The SUFI-2 program is iterative, with around 200 to 500 simulations recommended per iteration. Parameter ranges were used in achieving the calibration instead of single parameters. These parameter ranges were implemented in two different ways: (i) multiplying the existing parameter value by 1 plus a given value (represented by r_) and (ii) replacing the existing parameter value by the given value (represented by v_). The calibration process was ended when satisfactory values of the objective function (Nash-Sutcliffe efficiency-NSE), other goodness-of-fit parameters (coefficient of determination – R^2, percent bias – PBIAS, and RMSR observations standard deviation ratio - RSR) and uncertainty parameters (P-factor and R-factor) used in this study were achieved.

After calibrating for streamflow, the model was calibrated for sediment by selecting (based on literature and expert knowledge) and adding 2 parameters that affect only sediment: SPEXP (Channel re-entrained exponent parameter) and SPCON (channel re-entrained linear parameter) to the 13 calibrated runoff parameters. The sediment data also spanned a period of five years (2000 to 2004). A total of 350 simulations resulted in a successful calibration of flow and total sediment yield.

Thereafter the model was validated for flow and sediment yield by using the calibrated model to simulate streamflow and sediment for periods other than those used for the calibration and without any further changes to the model streamflow and sediment parameters. The streamflow was validated with five years (2002-2006) monthly observed discharge data and the sediment yield, three years (2005 to 2007) monthly sediment yield data.

3.3.12. Model performance evaluation

Four (4) quantitative statistics were used in evaluating the performance of the SWAT model with respect to streamflow and sediment yields in the calibration and validation periods. These were the NSE (eqn. 3.7), R^2 (eqn. 3.8), PBIAS (eqn. 3.9), and RSR (eqn. 3.10). The four statistics are widely used for the assessment of the performance of the SWAT model and have been recommended by Singh et al. (2004), Moriasi et al. (2007) and Duan et al. (2009), among others. The NSE is said to be one of the best fit estimators and evaluation methods for monthly comparison in SWAT hydrological studies (Coffey et al., 2004). Moriasi et al. (2007) describes it as a statistic which "indicates how well the plot of observed versus simulated values fits the 1:1 line". It ranges between $-\infty$ and 1.0 with 1 being the optimal NSE value. The R^2 describes the strength between observed and simulated values and range from 0 to 1, with 1 being the optimal value. PBIAS measures the average tendency of simulated data to be either on the higher or lower side of the corresponding observed data (Gupta et al., 1999). Positive PBIAS values represent model underestimation while negative values show overestimation. As such PBIAS values of 0.0 are desired (Gupta et al., 1999). The RSR is computed as the ratio of RMSE and the standard deviation of the observation data (STDEV), with values ranging from zero (zero RMSE means perfect model) to large values (large RMSE means unsatisfactory model).

A summary of the general performance ratings of the quantitative statistics for flow and sediment load on a monthly time step are shown in Table 3.11.

$$\mathrm{NSE} = 1 - \frac{\sum_{i=1}^{N}(O_i - P_i)^2}{\sum_{i=1}^{N}(O_i - \overline{O})^2} \tag{3.7}$$

$$R^2 = \frac{\sum_{i=1}^{N}\left[(O_i - \overline{O})(O_i - \overline{O})\right]^2}{\sum_{i=1}^{N}(O_i - \overline{O})^2 \sum_{i=1}^{N}(O_i - \overline{O})^2} \tag{3.8}$$

$$\mathrm{PBIAS} = \frac{\sum_{i=1}^{N}(O_i - P_i) * (100)}{\sum_{i=1}^{N}(O_i)} \tag{3.9}$$

$$RSR = \frac{RMSE}{STDEV} = \frac{\sqrt{\sum_{i=1}^{N}(O_i - P_i)^2}}{\sqrt{\sum_{i=1}^{N}(O_i - \overline{O})^2}} \tag{3.10}$$

where O_i is the measured data; P_i is the simulated data; $\overline{O}$ is the mean of the measured data; $\overline{P}$ is the mean of the simulated data; and N is the number of compared values.

Table 3.11: General Performance ratings for recommended statistics for flow and sediment load on a monthly time step (Moriasi et al., 2007; Santhi et al., 2001).

Performance rating	RSR	NSE	R^2	PBIAS (%)	
				Streamflow	Sediment
Very good	$0.00 \leq RSR \leq 0.50$	$0.75 < NSE \leq 1.00$		PBIAS < ±10	PBIAS < ±15
Good	$0.50 < RSR \leq 0.60$	$0.65 < NSE \leq 0.75$		±10 ≤ PBIAS < ±15	±15 ≤ PBIAS < ±30
Satisfactory	$0.60 < RSR \leq 0.70$	$0.50 < NSE \leq 0.65$	>0.6	±15 ≤ PBIAS < ±25	±30 ≤ PBIAS < ±55
Unsatisfactory	RSR > 0.70	NSE ≤ 0.50	<0.6	PBIAS ≥ ±25	PBIAS ≥ ±55

3.3.13. Uncertainty analysis

Quantification of model uncertainty is highly necessary in hydrological modelling studies. Experience from modelling studies has shown that proper model calibration and validation reduce errors in model simulations, but does not necessarily guarantee error-free simulations (Moriasi et al., 2007). For this reason, it was necessary to include uncertainty analysis in the model evaluation of this study. The parameter uncertainty in the SUFI-2 program accounts for all sources of uncertainties including that in the conceptual model, measured data, parameters and in the driving variables. Two important factors, the P- and R-factors (Abbaspour et al., 2004, 2007) were used in measuring uncertainties in the Black Volta SWAT model. The P-factor denotes the percentage of measured data enveloped by a 95% prediction uncertainty (or 95PPU) and measures the ability of a model to capture uncertainties. A P-factor of 1, means 100% bracketing of measured data by the 95PPU which means that all the correct processes have been accounted for. The R-factor gives the thickness of the 95PPU and is a measure of the quality of calibration. It is the average width of the 95PPU divided by the standard deviation of the observed data (Abbaspour, 2015). Ideally, R-factor value should be close to zero (matching with measured data). A simulation which corresponds exactly to measured data will therefore have a P-factor of

1 and an R-factor of 0. Based on how close or far away the P- and R-factors are to the ideal corresponding values, one can judge the goodness of prediction uncertainty and calibration. During calibration attention was paid to the P- and R- factors to ensure a good balance between the two.

3.3.14. Impact of climate change on flow and sediment yield and the sensitivity of streamflow to land use/land cover changes in the Black Volta Basin

The impacts of climate change on the flow and sediment yield of the BVRB was assessed by driving the calibrated and validated SWAT model with the 16 sets of future climate scenarios developed under section 3.3.4 and comparing the seasonal trend and annual magnitude of the resulting stream flow and sediment yield with those of the baseline (1984-2010) period. Three years of warm up (1981-1983) was allowed during the model runs.

Sensitivity analysis of changes in LULC on the flow of the BVRB was conducted through further simulations using the 1990 LULC map. This was done using the calibrated SWAT model after running the model with the 2000 LULC map. For this sensitivity analysis, all the input variables (e.g. rainfall, temperature, soil data) with the exception of the LULC data set remained unchanged. The 1990 LULC dataset was used instead of the 2000 dataset. Flow output at Bamboi was compared with that from the 2000 LULC data, with the period of analysis spanning from 1984 to 2010.

Prior to the sensitivity test, change detection of LULC of the BVRB was carried out based on the 1990 and 2000 LULC change maps obtained. Using the overlay function in ArcGIS 10.2.2 and Microsoft Excel 2010, the percentage changes in land use/ land cover was calculated for the ten (10) year period.

3.4. **Partial Conclusion**

The chapter described in detail the research methodology including the data and software used in this research. The use of the scientific methodology ensures that the results obtained are reliable and also for reproducibility.

CHAPTER 4: EXTREME EVENT ANALYSIS IN THE BVRB (1981-2010)

4.1. Introduction

In the last few decades, the tropics and subtropics have recorded surges in the number of heavy rainfall events and a common occurrence of droughts. These extreme conditions constitute significant threats to water resource, agriculture and public health management (Parry et al., 2007). Understanding the current trends of changes in temperature and rainfall extremes in the BVRB is of key importance to assessing the potential impacts of climate change on human and natural systems. This section presents and discusses the results of the extreme events analysis for the basin during the 1981-2010 period.

4.2. Temperature-based indices [SU25, TR20, GSL, WSDI, DTR]

The temporal patterns (Figure 4.1 and Table 4.1) of present day temperature-related indices show warming in the Black Volta Basin. Generally, all the 5 temperature-based indices show positive (increasing) trends in the basin. However, this trend is insignificant for the growing season length (GSL) and warm spell duration indicator (WSDI) indices. The night time temperature (TR20) depicts a coherent pattern of significantly positive trends at four (Dedougou, Boromo, Bobo-Dioulaso and Wa) of the six climate stations used in the study. Increasing trend in summer day counts (SU25) is significant at Dedougou and Wa. For the Diurnal temperature range (DTR), the increasing trend is significant at Dedougou and Gaoua. The results show that the BVRB experienced warming during the period 1981-2010. These findings of warming trends in the region are consistent with the results from the study of New et al. (2006) which showed increases in both daytime and nighttime hot extremes in the West African region over the period 1961–2000. Mouhamed et al. (2013) also suggests a general warming trend throughout the West African Sahel region from 1960 to 2010.

Figure 4.1(a)

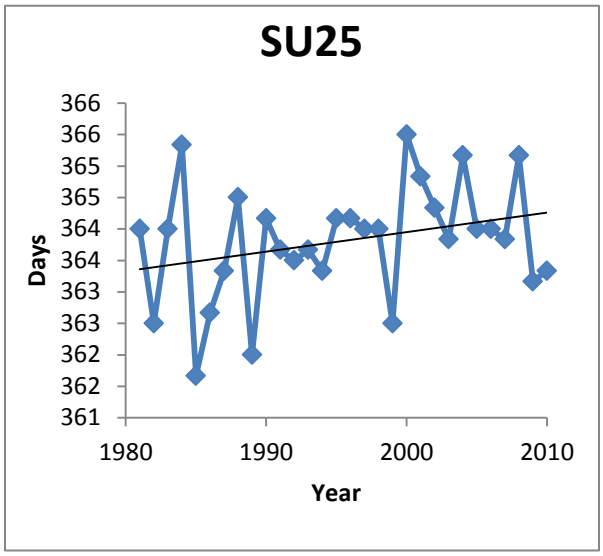

Figure 4.1(b)

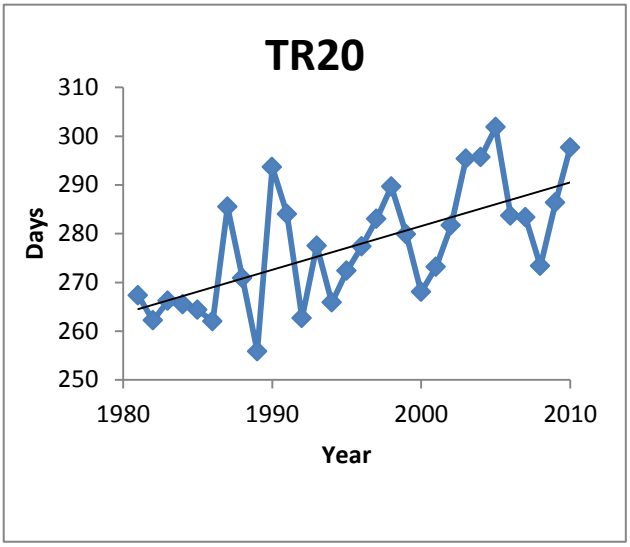

Figure 4.1(c)

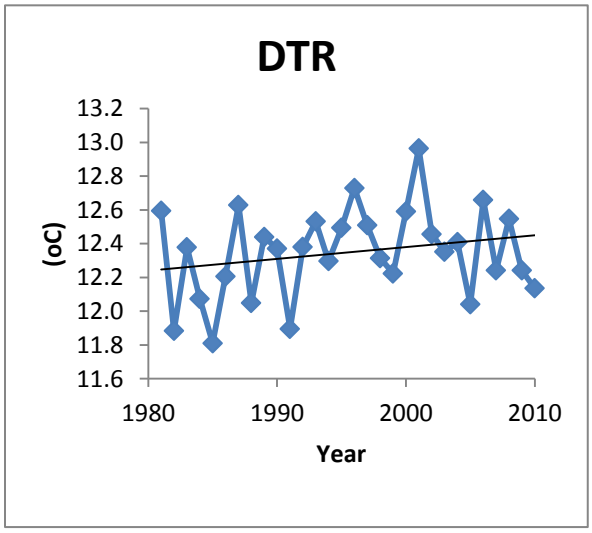

Figure 4.1(d)

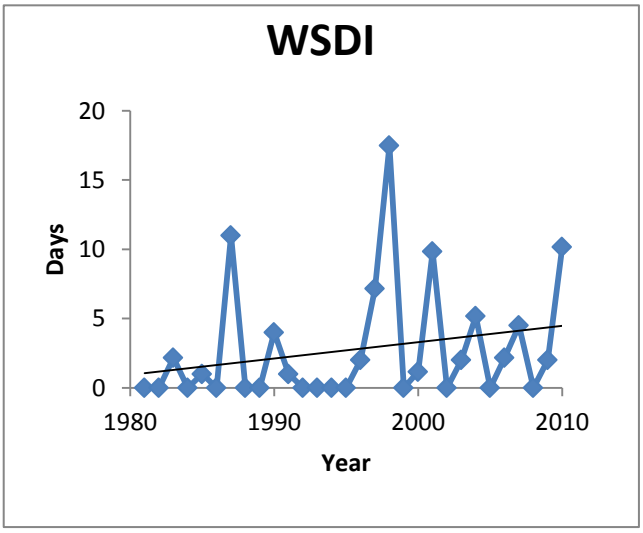

Figure 4.1 Averaged regional time series for temperature related indices: (a) SU25 (summer days), (b) TR20 (tropical nights), (c) DTR (diurnal temperature range) and (d) WSDI (warm spell duration indicator) for the period 1981-2010. The solid line shows the trend

Table 4.1: Slopes of trends of present day temperature-based indices. Bold numbers represent slopes of trends which are statistically significant at 95% level ($p<0.05$)

Station Name	SU25	TR20	GSL	WSDI	DTR
Dedougou	**0.056**	**0.604**	0.066	0.242	**0.030**
Boromo	-0.001	**1.053**	0.002	0.129	-0.009
Bobo-Dioulasso	0.041	**1.352**	0.002	0.184	0.013
Gaoua	0.037	-0.479	0.002	-0.148	**0.028**
Wa	**0.056**	**1.715**	0.000	0.111	-0.004
Bole	0.008	0.677	0.004	0.088	0.004
Number of stations with positive trend	5	5	6	5	4
Number of stations with negative trend	1	1	0	1	2

4.3. **Rainfall-based indices [PRCPTOT, R95, RX5DAY, CWD, SDII, CDD]**

Time series analyses of extreme rainfall indices depicts overall positive (increasing) trend in the basin for the 1981-2010 period (Figures 4.2 and 4.3). All the stations show increasing trends in total annual rainfall (PRCPTOT), consecutive dry day (CDD), and maximum 5-day rainfall (RX5Day) as depicted in Table 4.2. However, the increases are significant at the Dedougou (in the north) climate station alone. Five of the 6 stations show increases in trends of very wet days (R95P) and simple daily intensity index (SDII). The remaining station, Bobo-Dioulaso, located north of the basin, shows an insignificant decreasing trend. The increasing trend in R95P is significant at Dedougou (in the north) and Wa (in the south) while the increasing trend in SDII is insignificant at all the stations. For the consecutive wet days (CWD) index, half of the stations show increasing trend (two in the north and one in the south) whiles the other half (one in the north and two in the south) show decreasing trend, all of which are insignificant at the 95% level (Table 4.2). In general, the analysis showed increases in total rainfall amounts and intensity across the BVRB region during 1981 to 2010. Alexander et al. (2006) found that averaged across the globe, extreme rainfall events have been increasing during the 1951-2003 period. Although findings of Mouhamed et al. (2013) showed a general tendency of decreased annual total rainfall for the West African Sahel and for Burkina Faso in particular during 1961-2010, increasing trends of cumulated rainfall of extremely wet days and maximum number of consecutive wet days were observed in their study for the late 1980s, compared to the 1961-1990 period. The increase in maximum number of wet days observed in this study is in line with the findings by Sarr (2011), which also showed that extreme rainfall events became more frequent in the West African Sahel during the last decade, compared to the 1961-1990 period. In contrast to the largely significant trends noticed in the extreme temperature events for the present day, most of the trends in the extreme rainfall events were statistically insignificant at the 95% level.

Figure 4.2(a)

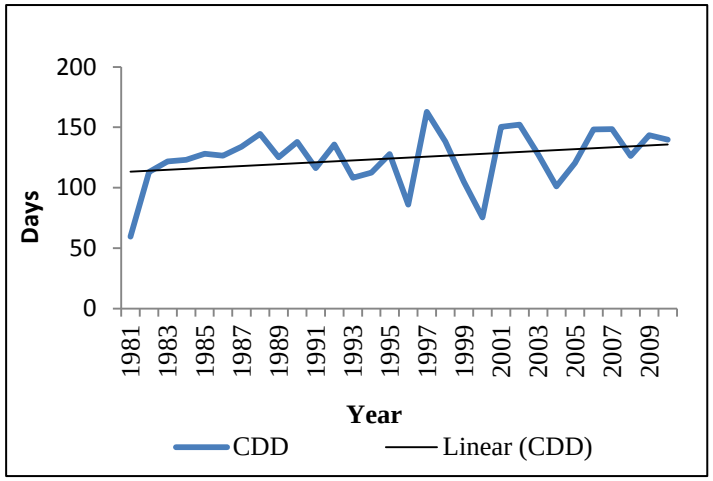

Figure 4.2(b)

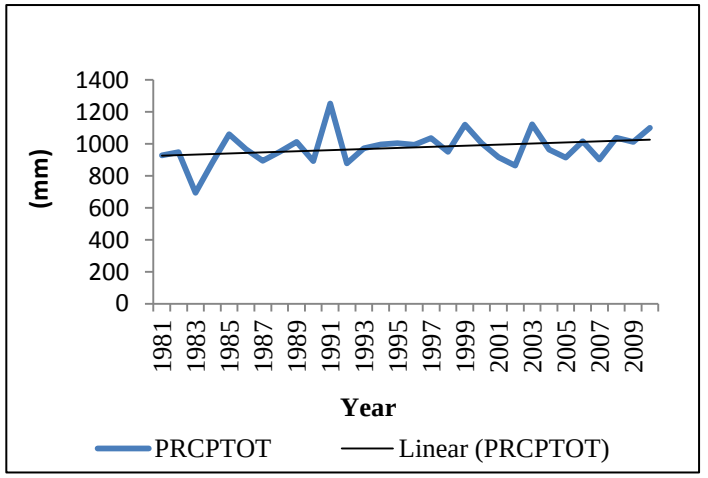

Figure 4.2(c)

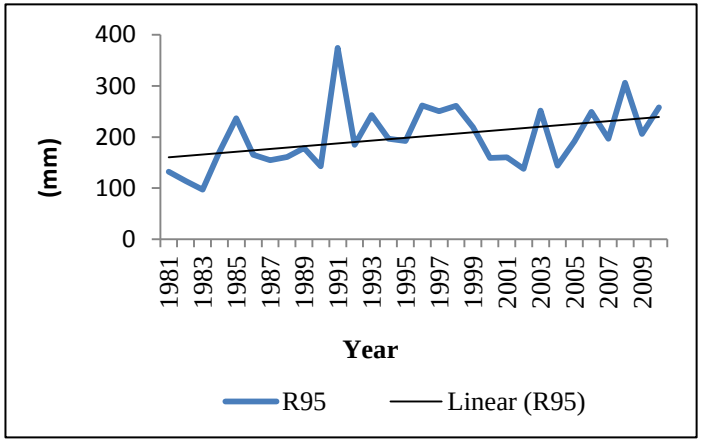

Figure 4.2(d)

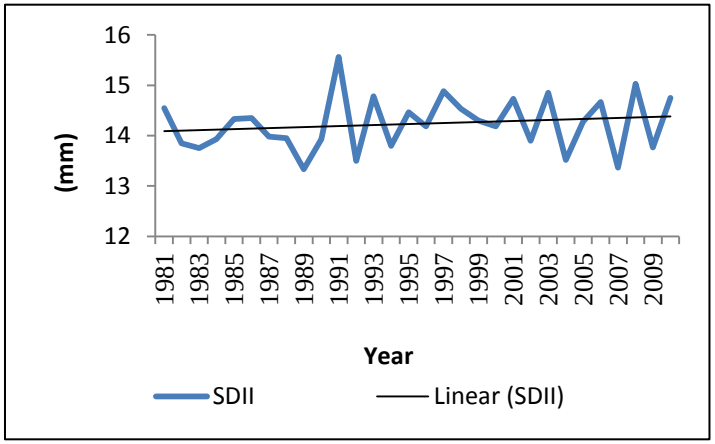

Figure 4. 2 Averaged regional time series for rainfall related indices: (a) CDD (consecutive dry days), (b) PRCPTOT (total annual rainfall), (c) R95 (very wet days) and (d) SDII (simple daily intensity index). The solid line shows the trend

Figure 4.3(a)

Figure 4.3(b)

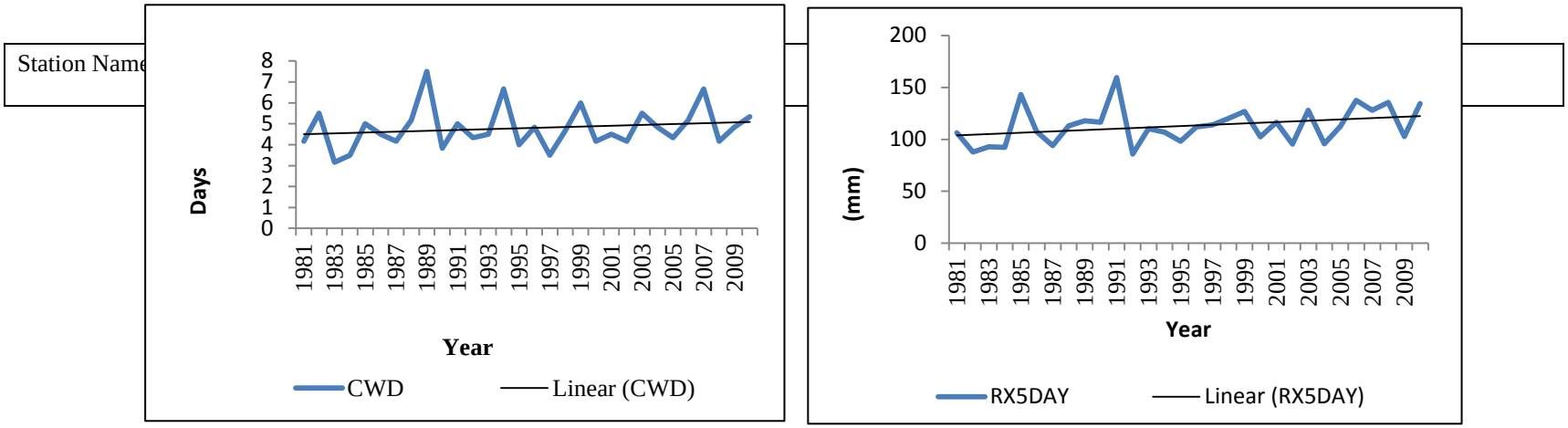

Figure 4. 3 Averaged regional time series for rainfall related indices: (a) CWD (consecutive wet days) and (b) RX5DAY (maximum 5-day rainfall), for the period 1981-2010. The solid line shows the trend

Dedougou	**1.290**	0.000	**1.089**	0.071	**4.204**	**7.172**
Boromo	1.093	0.030	0.598	0.052	1.692	4.478
Bobo-Dioulasso	0.275	-0.016	0.973	-0.021	-0.344	0.790
Gaoua	0.029	0.007	0.605	-0.005	2.796	4.680
Wa	2.271	0.054	0.693	0.042	**7.262**	8.993
Bole	0.094	0.015	0.145	-0.001	3.424	0.663
Number of stations with positive trend	6	5	6	3	5	6
Number of stations with negative trend	0	1	0	3	1	0

Table 4.2: Slopes of trends of present day rainfall-based indices. Bold numbers represent slopes of trends which are statistically significant at 95% level ($p<0.05$)

4.4. **Partial Conclusion**

The extreme event analysis showed mostly increasing trends in the temperature based indices (SU25, TR20, GSL, WSDI and DTR) at almost all the stations considered in the analysis. This indicates that the basin experienced warming between the 1981 – 2010 period in line with reports from other studies in the region. The extreme rainfall indices (PRCPTOT, CDD, RX5Day, R95P and SDII) also showed increasing trends at majority of the stations. Fifty (50%) of the stations showed increasing trends in the CWD index, with the remaining 50% showing a decrease. The results indicate that although the consecutive dry days increased during the period, the amount and intensities of rainfall events increased.

CHAPTER 5: PROJECTED CHANGES IN PRECIPITATION AND TEMPERATURE OVER THE BVRB

5.1. Introduction

The results of projected changes in rainfall and temperature over the basin for the late (2051-2075) and end (2076-2100) of the 21st century are presented and discussed in this chapter. Prior to that the downscaling and bias correction of the future datasets used in the study are presented and discussed.

5.2. Assessment of model-simulated uncorrected and bias-corrected historical climate of the BVRB

To establish the importance of bias-correction of RCM data for use in impact studies, plots of mean monthly rainfall and temperature of the model-simulated uncorrected, model-simulated bias-corrected and observed data were made for four of the 11 climate stations used in this study (depicted in Figures 5.1 and 5.2) and analyzed to determine which of the two model simulated dataset fits more closely to the observed. The analysis included the computation of annual mean and standard deviation (Table 5.1) as well as probability of exceedence of rainfall thresholds (Figure 5.3). It can be observed that the trend and monthly values of rainfall and temperature computed with the bias-corrected projections fit much better to the observed data than those computed with the uncorrected model output. The use of the uncorrected RCM projection data resulted in an overall overestimation of peak rainfall at Bole. For BoBo-Dioulasso the uncorrected model data underestimated rainfall. The uncorrected output from RACMO22T/ EC-EARTH resulted in an underestimation of maximum temperature at Bui (Figure 5.2). The results of the computed mean, standard deviation and probability of exceedence of rainfall thresholds for the selected stations proved further that the corrected data was much closer to the observed data than the uncorrected data was. The use of uncorrected modeled data for impact assessment

may lead to wrong climate change projections. As shown in Figure 5.3b for example, the probability of exceedence of rainfall events between 11mm and 50mm was underestimated by the uncorrected modeled data for station Bole. The use of such data my lead to the missing of flash floods.

(a) (b)

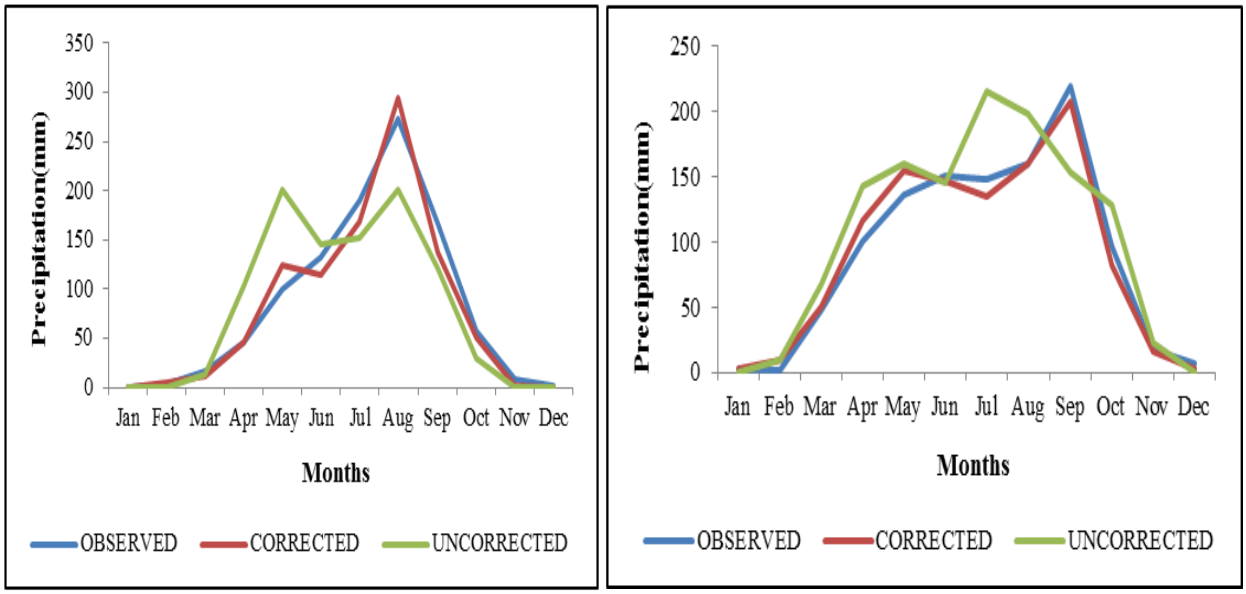

Figure 5.1: Uncorrected and bias-corrected RCM model simulations of historical (1981-2005) rainfall of (a) BoBo-Dioulasso, RCA4/ CanESM2 (b) Bole, RACMO22T/ EC-EARTH

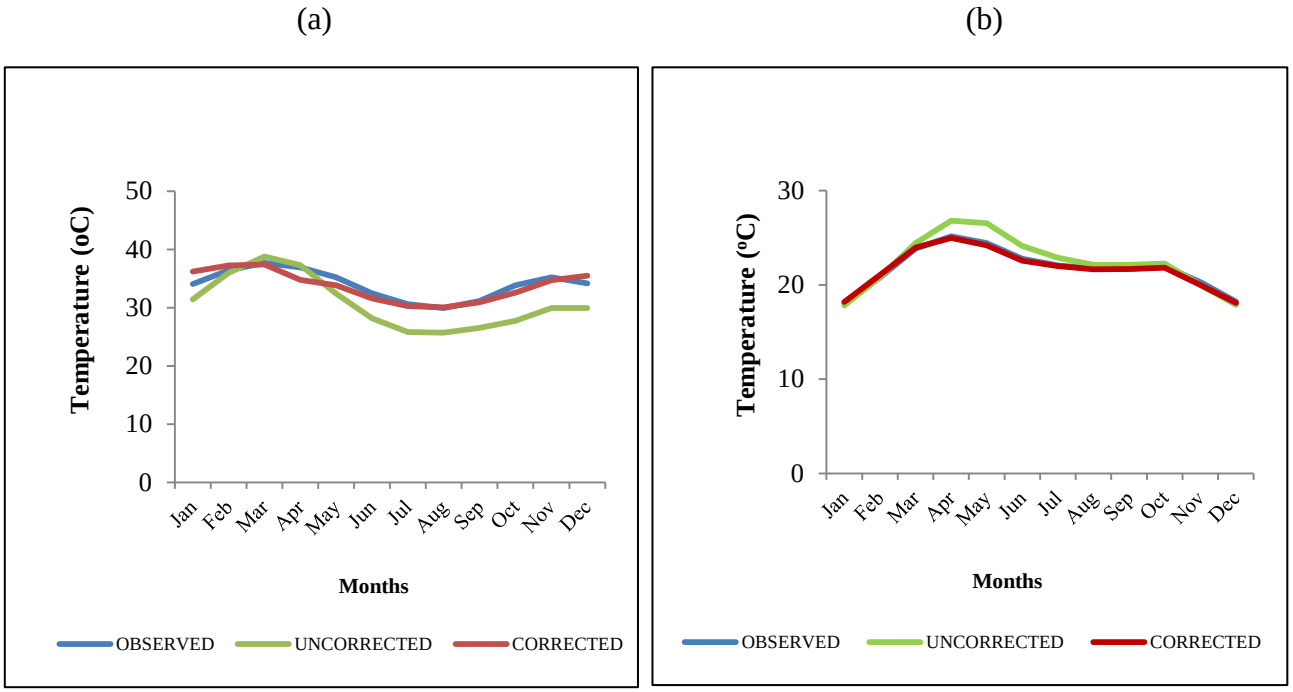

Figure 5.2: Uncorrected and bias-corrected RCM model simulations of historical (1981-2005) maximum and minimum temperature of (a) Bui, RACMO22T/ EC-EARTH (b) Dedougou, RCA4/ CanESM2

Table 5.1: Analysis of uncorrected and bias-corrected RCM model simulations of historical (1981-2005) temperature and rainfall of the Black Volta Basin

Variables	**Climate stations**	**Mean**			**Standard Deviation**		
		Observed	Corrected	Uncorrected	Observed	Corrected	Uncorrected
Temperature	Bui	33.97	33.75	30.81	2.51	2.64	4.49
	Dedougou	21.76	21.68	22.32	2.20	2.17	2.92
Rainfall	Bobo-Dioulasso	2075.73	1985.02	2009.56	2256.24	2278.57	2039.16
	Bole	2267.48	2252.74	2593.02	1853.43	1811.85	1988.75

(a) (b)

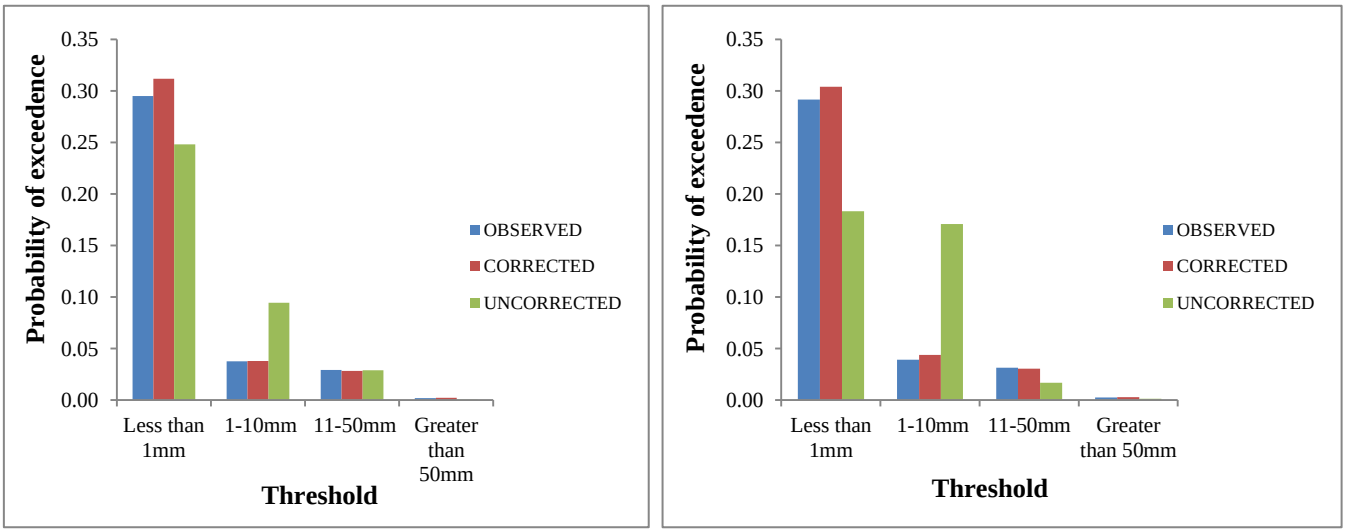

Figure 5.3: Probability of exceedence of rainfall thresholds for the bias-corrected and uncorrected RCM model simulations of historical (1981-2005) rainfall of (a) BoBo-Dioulasso, RCA4/ CanESM2 (b) Bole, RACMO22T/ EC-EARTH

5.3. **Evaluation of RCM performance in simulating of historical climate of the BVRB**

Results of the historical simulation of rainfall over the BVRB by the three RCM/GCM pairs and their ensemble mean are presented in Figure 5.4. The intra-annual rainfall plots show that the RCMs RCA4/MPI-ESM-LR and RACMO22T/ ICHEC-EC-EARTH replicated quite well the rainfall pattern of the basin, capturing the beginning of the rainfall months (April-June; AMJ) as well as the wet season (July-September; JAS). Unlike the other 2 models, RCA4/CanESM2 did not capture the period May-July very well, and overestimated the rainfall amount for most parts of the wet period (May-September; MJJAS). In mid-September and during the wet-dry transition (October-December; OND) the model underestimated rainfall amounts. Since simulations by the RCA4/MPI-ESM-LR performed quite well, the biases shown by RCA4/CanESM2 can be linked to biases inherited through the lateral boundary conditions of the driving GCM (Hong and Kanamitsu 2014) CanESM2.The simulated rainfall by the mean of the RCMs fitted much better

to the observed than that by the individual models. This good performance may be attributed to the counterbalancing of opposite-signed biases in the individual models (Nikulin et. al., 2012). Several studies (e.g. Diallo et. al., 2012; Nikulin et. al., 2012; Paeth et. al., 2011) have reported similar results of best performance by multi-model ensemble means. Historical temperature simulations by the RCMs are displayed in Figure 6.5. Unlike the biases exhibited during rainfall simulation, the RCMs simulated the historical tmax and tmin of the basin very well, capturing the trends and peaks. The RCM RACMO22T/ICHEC-EC-EARTH slightly overestimated the average maximum temperature for the months of February and August-September (Figure 5.5).

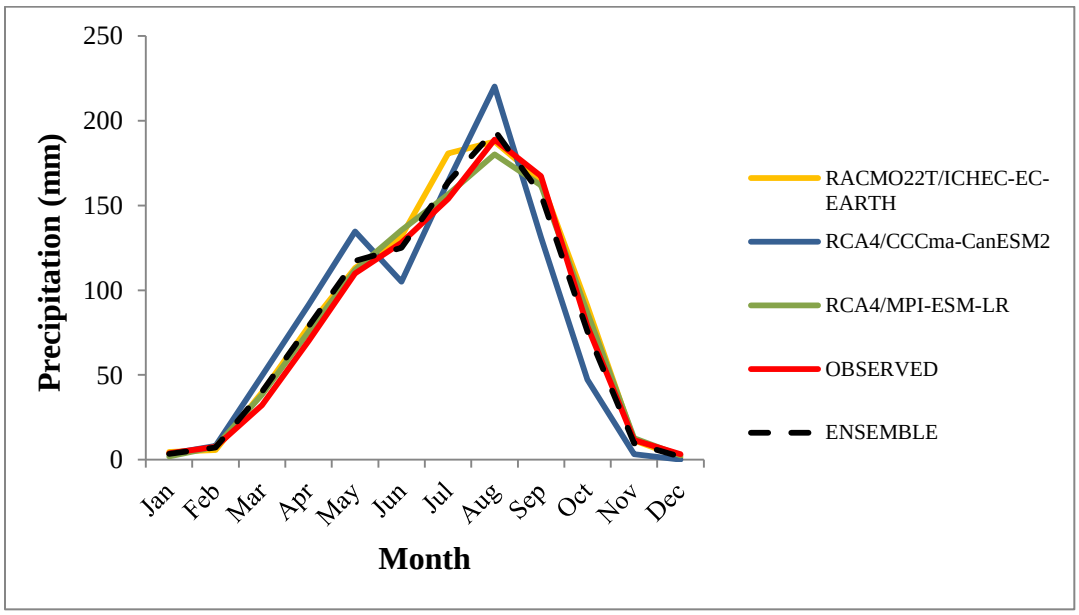

Figure 5.4: Observed and simulated intra-annual rainfall over the Black Volta River Basin from 1981 to 2005

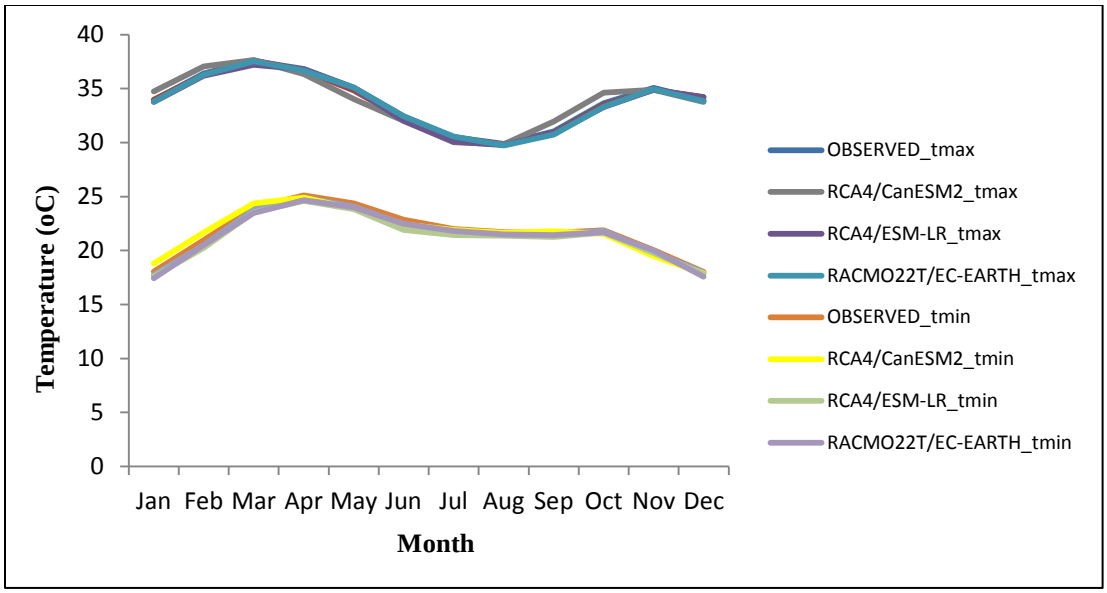

Figure 5.5: Observed and simulated intra-annual maximum and minimum temperature (tmax and tmin respectively) over the Black Volta River Basin from 1981–2005

5.4. **Projected changes in rainfall over the BVRB**

The analysis of average annual rainfall over the basin for the late- and end of the 21st century showed high level of uncertainties, with mixed signals of increases and decreases in rainfall amounts across the models (Table 5.2). Relative to the baseline, mean annual rainfall for the late 21st century ranged between -16% and +6%, with a mean of -2% under the RCP4.5 scenario and between -27% and +14%, with a mean of -1% under the RCP8.5 scenario. The end of the 21st century projection showed rainfall changes of between -23% and +2%, with a mean of -7% under the RCP4.5 scenario. The high emission RCP8.5 scenario projects changes ranging between -33% and +13%, with a mean of -4%. From the results, it is established that the uncertainty in the projections increases with increasing RCP forcing and increasing time frames. Similar observations were made by Sylla *et al*. (2016).

Figure 5.6 and 5.7 show the projected changes in intra-annual rainfall over the BVRB for the late and end of 21st century, respectively. As shown in both graphs (5.6a and 5.6b), future rainfall

projections by the models show high variability consistent with findings for the West African region reported in the IPCC 5th Assessment report (IPCC, 2013). The variability is mostly pronounced during the wet season. Rainfall amount for the month of July for example is projected to range between +51mm and -16mm under the RCP 4.5 scenario and between +81mm and -30mm under the RCP8.5 scenario in the 2060s. From the months of October through December however, the variability is highly reduced, especially under the RCP4.5 scenario. The end of the 21st century rainfall projections also shows substantial variability, in this case especially in the months of February through September, which reduces from October through December. Changes in rainfall for the dry (January-March) and wet (August-October) seasons are presented in Figures 5.8 and 5.9. In the late 21st century, the ensemble runs project a change in the range of +6% to -35% in the dry season rainfall, with a mean change of 11% for the RCP4.5 scenario. The change in wet season rainfall is projected to range from +4% to -10%, with a mean of -3%. Under the RCP8.5 scenario, the change in dry and wet season rainfalls are projected to range from +22% to -67%, with a mean of -26%, and +9% to -16%, with a mean of -1%. Similarly, the dry and wet season rainfalls over the basin for the end of the 21st century are projected to range between +20% and -48%, with a mean of -11% and from -2% to -16%, with a mean of -8% for the RCP4.5 scenario. The high emission RCP8.5 scenario projections show a rate of change in dry season rainfall ranging from +48% and -68%, with a mean of -18% while for the wet season the projected changes are between +16% and -23%. The high variability in the projections across the models and the opposing change in signals are indications of uncertainty surrounding rainfall projections in the basin. Whereas a decrease in rainfall over the region may cause droughts, affect agriculture development and cause a decline in hydropower generation, increases in rainfall may cause floods in the basin.

Table 5.2: Projected changes in rainfall for the late and end of 21st century in the Black Volta River Basin under RCPs 4.5 and 8.5

RCMs	Baseline (1981-2010) observed mean value (mm)	Late-Century (2051-2075)				End-of-Century (2076-2100)			
		RCP4.5		RCP8.5		RCP4.5		RCP8.5	
		Ave (mm)	% change	Ave (mm)	% change	Ave (mm)	% change	Ave (mm)	% change
RACMO22T/ ICHEC-EC-EARTH	999.48	1064.12	6.47	1091.52	9.21	999.37	-0.01	1126.88	12.75
RCA4/MPI-ESM-LR		1050.77	5. 13	1136.19	13.68	1021.95	2.25	1094.23	9.48
RCA4/ CCCma-CanESM2		836.55	-16.30	728.64	-27. 10	767.69	-23.19	665.25	-33.44
ENSEMBLE		983.81	-1.57	985.45	-1.40	929.67	-6.98	926.12	-3.74

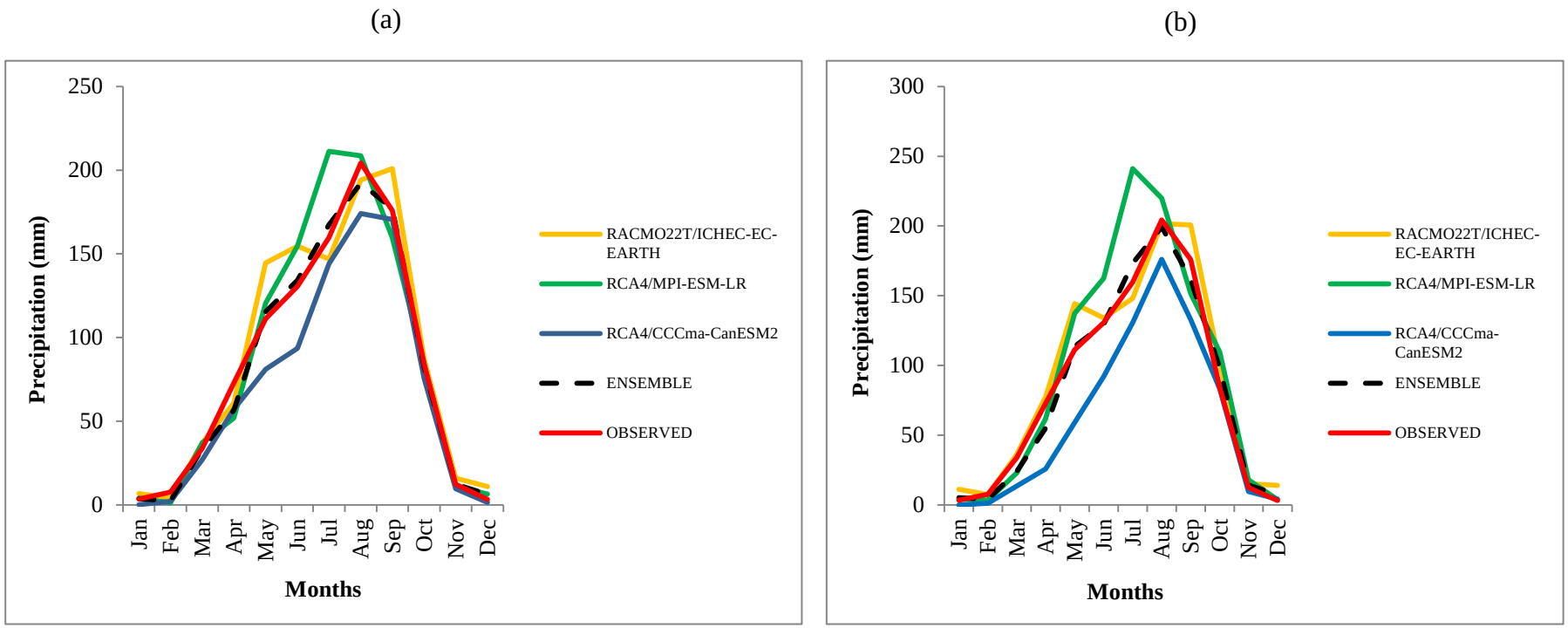

Figure 5.6: Observed and projected intra-annual rainfall under (a) RCP4.5 and (b) RCP8.5 for the 2060s (2051-2075)

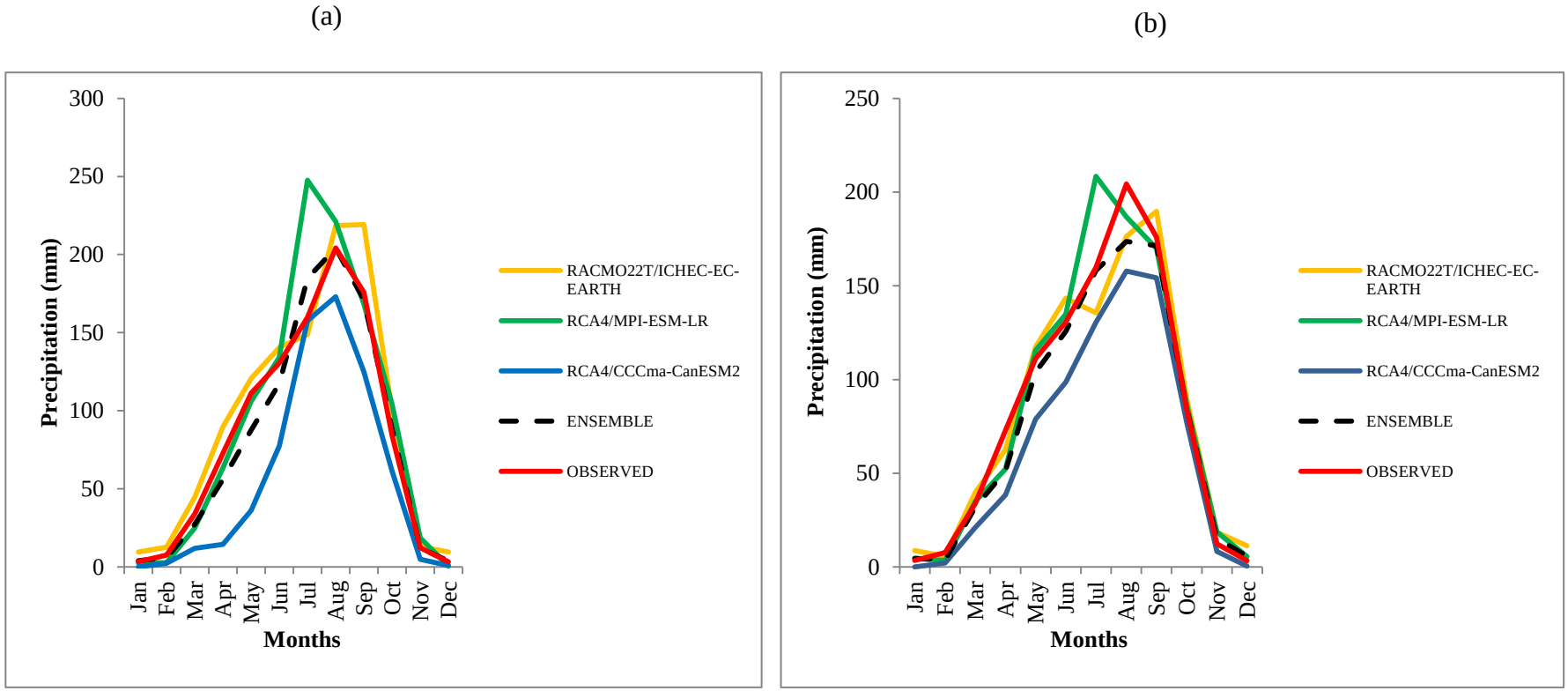

Figure 5.7: Observed and projected intra-annual rainfall under (a) RCP4.5 and (b) RCP8.5 for the 2080s (2076-2100)

(a)

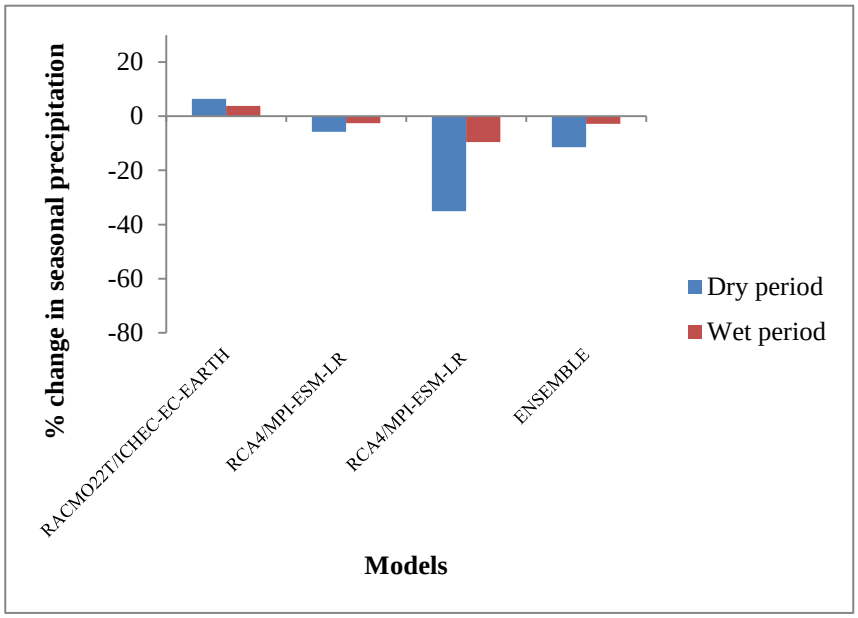

(b)

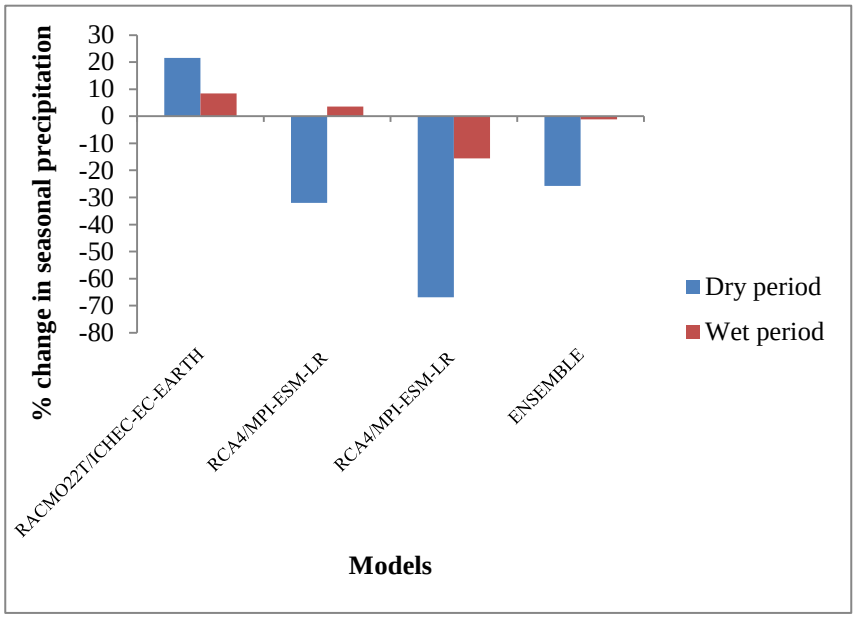

Figure 5.8: Changes in mean seasonal rainfall for the 2060s (2051-2071) under (a) RCP4.5 and (b) RCP8.5 scenarios, relative to the baseline (1981-2010).

(a)

(b)

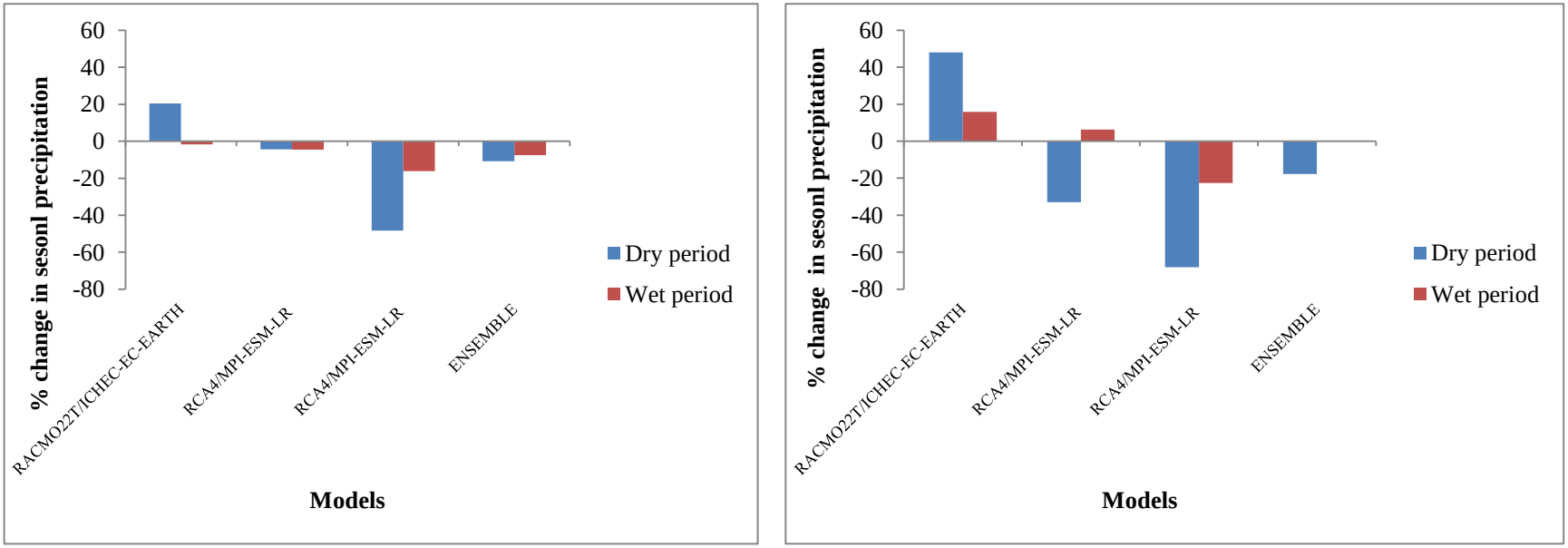

Figure 5.9: Changes in mean seasonal rainfall for the 2080s under (a) RCP4.5 and (b) RCP8.5 scenarios, relative to the baseline (1981-2010).

5.5. Projected changes in temperature over the BVRB

Consistent with the latest IPCC (2013) report, results of the temperature projections for the BVRB (Table 5.3) indicate a warmer climate in the late- and end of the 21st century under both RCP scenarios, relative to the baseline. The projected increase in temperature by all the ensemble models as well as from the mean of the ensemble is statistically significant at the 5% confidence level. As Table 5.3 shows, the magnitude of projected increase in mean temperature over the basin is greater in the 2080s compared to the 2060s. As expected, the increase in temperature is higher in the RCP8.5 scenario than in the RCP4.5 scenario. Possible rise in mean temperature for the late and end of the 21st century under the two RCP scenarios ranges between 2.0 ^{o}C (RCP4.5) and 3.7 ^{o}C (RCP8.5), in line with the projected range for West Africa (Sylla et al., 2016).

5.6. Trends in projected annual rainfall and mean temperature

The Man-Kendall trend test showed increases and decreases in future rainfall over the basin (Table 5.4) with majority of the trends (about 67%) being in the positive direction. The projected trend ranges from a decrease of 5.5 mm/year to an increase of 3.6 mm/year for the RCP4.5 scenario in the late century period. For the RCP8.5 scenario, the trend ranges from a decrease of 2.7 mm/year to an increase of 8.6 mm/year. The end of the century projected trend ranges from a decline of 3 mm/year to an increase of 4.9 mm/year under the RCP4.5 and from a decline of 2.7 mm/year to an increase of 8.6 mm/year under the RCP8.5 scenario. All the trends were however statistically insignificant at the 5% level of significance. Unlike temperature, rainfall projection in the West African Region is in general associated with higher uncertainties (Rowell 2012; Orlowsky and Seneviratne 2012). Trend analysis of temperature, revealed statistically significant (5% level of significance) increases in agreement with the IPCC (2013) report. For the late century increase in trends up to 0.03 ^{o}C/year is projected by both RCP4.5 and RCP8.5 scenarios.

The projected trend for the end of the century ranges from a decrease 0f 0.0 1 ^{o}C/year to an increase of 0.02 ^{o}C/year for the RCP4.5 scenario and from 0.02 ^{o}C/year to 0.06 ^{o}C/year for the RCP8.5 scenario. The decreasing trends are however not significant at the 5% level as shown in Table 5.5.

Table 5.3: Projected changes in temperature (°C) for the late and end of 21st century in the Black Volta River Basin under RCPs 4.5 and 8.5

RCMs	Baseline (1981-2010) Observed mean values	2051-2075				2076-2100			
		RCP4.5		RCP8.5		RCP4.5		RCP8.5	
	Tmean (°C)	Tmean (°C)		Tmean (°C)		Tmean (°C)		Tmean (°C)	
		Ave	Change	Ave	Change	Ave	Change	Ave	Change
RACMO22T/ICHEC-EC-EARTH	27.9	30.0	2.1	30.7	2.8	30.2	2.3	31.4	3.5
RCA4/MPI-ESM-LR		29.9	2.0	30.6	2.7	30.1	2.2	31.4	3.5
RCA4/CCCma-CanESM2		30.2	2.3	30.9	3.0	30.5	2.6	31.6	3.7
ENSEMBLE		30.0	2.1	30.7	2.8	30.2	2.3	31.4	3.5

Table 5.4 Results of the Mann-Kendall test for annual rainfall (mm) for the late and end of 21st century in the Black Volta River Basin under RCPs 4.5 and 8.5

Model runs	Mann-Kendall Statistic (S)	Sen's slope	p-value	Trend
RACMO22T/ICHEC-EC-EARTH (RCP4.5/2060s)	-50.00	-5.53	0.26	Not significant
RACMO22T/ICHEC-EC-EARTH (RCP4.5/2080s)	-46.00	-2.96	0.30	Not significant
RACMO22T/ICHEC-EC-EARTH (RCP8.5/2060s)	18.00	2.53	0.70	Not significant
RACMO22T/ICHEC-EC-EARTH (RCP8.5/2080s)	18.00	2.54	0.70	Not significant
RCA4/CanESM2 (RCP4.5/2060s)	18.00	1.54	0.70	Not significant
RCA4/CanESM2 (RCP4.5/2080s)	42.00	4.90	0.34	Not significant
RCA4/CanESM2 (RCP8.5/2060s)	74.00	8.56	0.09	Not significant
RCA4/CanESM2 (RCP8.5/2080s)	74.00	8.56	0.09	Not significant
RCA4/MPI-ESM-LR (RCP4.5/2060s)	28.00	3.55	0.53	Not significant
RCA4/MPI-ESM-LR (RCP4.5/2080s)	12.00	1.86	0.80	Not significant
RCA4/MPI-ESM-LR (RCP8.5/2060s)	-28.00	-2.67	0.53	Not significant
RCA4/MPI-ESM-LR (RCP8.5/2080s)	-26.00	-2.67	0.56	Not significant

Table 5.5 Results of the Mann-Kendall test for mean annual temperature (°C) for the late and end of 21st century in the Black Volta River Basin under RCPs 4.5 and 8.5

Model runs	Mann-Kendall Statistic (S)	Sen's slope	P-value	Trend
RACMO22T/ICHEC-EC-EARTH (RCP4.5/2060s)	104.00	0.03	0.02	Significant increase
RACMO22T/ICHEC-EC-EARTH (RCP4.5/2080s)	108.00	0.02	0.01	Significant increase
RACMO22T/ICHEC-EC-EARTH (RCP8.5/2060s)	152.00	0.03	0.00	Significant increase
RACMO22T/ICHEC-EC-EARTH (RCP8.5/2080s)	190.00	0.06	< 0.00	Significant increase
RCA4/CanESM2 (RCP4.5/2060s)	-4.00	-0.00	0.94	Not significant
RCA4/CanESM2 (RCP4.5/2080s)	-44.00	-0.01	0.32	Not significant
RCA4/CanESM2 (RCP8.5/2060s)	130.00	0.02	0.00	Significant increase
RCA4/CanESM2 (RCP8.5/2080s)	132.00	0.02	0.00	Significant increase
RCA4/MPI-ESM-LR (RCP4.5/2060s)	26.00	0.00	0.56	Not significant
RCA4/MPI-ESM-LR (RCP4.5/2080s)	-28.00	-0.01	0.53	Not significant
RCA4/MPI-ESM-LR (RCP8.5/2060s)	164.00	0.02	0.00	Significant increase
RCA4/MPI-ESM-LR (RCP8.5/2080s)	148.00	0.03	0.00	Significant increase

5.7. **Partial Conclusion**

The quantile-quantile transformation method for bias correction of the rainfall and temperature data proved useful in reducing the biases in the RCMs. In all the analysis, the corrected data fitted much closer to the observed data than the uncorrected ones. The RCMs exhibited some biases in reproducing the historical rainfall pattern of the BVRB. The historical temperature of the studied basin was however well simulated.

The model projections of rainfall over the basin for the late- and end of the 21st century under the low and high emission scenarios showed both positive and negative signals. These mixed signals were statistically insignificant at the 5% level of significance. Unlike rainfall, the temperature projections by the model runs showed mostly statistically significant increases. Warming of the basin ranges between 2.0 ^{o}C (late 21st century under RCP4.5) and 3.7 ^{o}C (end of the 21st century under RCP8.5).

CHAPTER 6: HYDROLOGICAL MODELLING WITH SWAT

6.1. Introduction

This section presents and discusses the results of the hydrological modelling with the Soil and Water Assessment Tool model. The model sensitivity analysis result is presented first, followed by calibration and validation, then finally, the uncertainty analysis.

6.2. Model sensitivity analysis

Results of the model sensitivity analysis show that the most sensitive parameter to streamflow in BVRB is the curve number (CN2), followed by threshold depth of water in the shallow aquifer required for return flow to occur (GWQMN), and baseflow alpha factor for bank storage (ALPHA_BNK) (Table 6.1). Canopy storage (CANMX) was the least sensitive of the eighteen (18) model parameters analyzed.

Table 6.1: Global sensitivity analysis of flow parameters of SWAT for the Black Volta Basin

Rank	Parameter Name	t-Stat[1]	P-Value[2]
1	r_CN2.mgt	-13.57	0.05
2	v_GWQMN.gw	13.01	0.05
3	v_ALPHA_BNK.rte	-11.44	0.06
4	v_ REVAPMN.gw	10.68	0.06
5	v_GW_DELAY.gw	8.89	0.07
6	v _RCHRG_DP.gw	-7.22	0.09
7	v_CH_N2.rte	-6.85	0.09
8	v_ESCO.hru	-6.33	0.10
9	r __SHALLST.gw	-5.77	0.11
10	r__SLSUBBSN.hru	5.71	0.11
11	r __SOL_AWC.sol	5.00	0.13
12	r_SOL_K.sol	-4.58	0.14
13	v_ALPHA_BF.gw	3.98	0.16
14	r__CH_S2.rte	3.80	0.16
15	v__ CH_K2.rte	3.11	0.20
16	v__GW_REVAP.gw	1.87	0.31
17	v__SURLAG.hru	-1.60	0.35
18	v__CANMX.hru	-0.29	0.82

[1] t-stat provides the sensitivity measure. The larger the absolute value the more sensitive the parameter.
[2] p-value determines a sensitivity's significance. A value closer to zero indicates more significance.

6.3. Calibration and validation results for streamflow and sediment yield

The final parameter value ranges used in SUFI-2 for the calibration and subsequently for validation are presented in Table 6.2. Figure 6.1 presents results of the simulated monthly streamflow with observed data for the calibration and validation periods. Performance assessment via quantitative statistics during the calibration period resulted in R^2 of 0.86, RSR of 0.38 and NSE of 0.85 (Table 6.3), indicating that the model simulated the streamflow with reasonable accuracy. The model was able to replicate the low flow fairly well and captured most of the peak flows. In comparison with the general statistical performance ratings given by Moriasi et al. (2007) and Santhi et al. (2001) and provided in Table 3.11, the overall discharge calibration results indicate "very good" model performance. The flow validation results were generally "satisfactory" (NSE; 0.60, R^2; 0.62, RSR; 0.64, PBIAS; 20.1%). The trend of the simulation during both calibration and validation periods basically followed that of the measured data, except for the discrepancies in some of the years. During the calibration period the model underestimated the flows for September 1996, 1997, 1999 and 2000 and overestimated the flow for September 1998. For the validation period, the discrepancies existed from September 2002 to October 2002 and from July 2003 to October 2003. The differences in the model simulated and observed flows basically existed during/after peak rainfall periods during both calibration and validation periods, demonstrating that the SWAT model had problems simulating peak flows. A number of studies worldwide have demonstrated the inability of the SWAT model to simulate peak runoffs very accurately (e.g. Chu et al., 2004; Wang et al., 2015; Himanshu et al., 2017). The PBIAS value of 8.1% and 20.1% obtained during the calibration and validation periods, respectively, indicates that the model has the tendency to under-predict flows. According to Phomcha et al. (2011), a possible reason for underestimation of surface runoff by the SWAT model is the non-consideration of rainfall intensity and duration by the soil conservation services

(SCS) curve number (CN) method (SCS, 1972). According to Wang et al. (2015) these effects may be stronger during heavy rainfall events. Based on the results of their study, Borah et al. (1999) indicated that SWAT had a limitation in evaluating peak monthly runoffs (mostly under-estimations) recommending that the model be improved in storm event simulations to enhance its peak and high runoff predictions.

The calibration and validation plots of total sediment yield are presented in Figure 6.2. In general, the model simulated sediment yield matched the trends of the observed in both calibration and validation periods. During the calibration period, the peaks were under-estimated in September 2000 and June 2003 while in September 2001, September 2002 and August 2004, the peaks were over-estimated. The PBIAS value of 27.5% obtained during the calibration period shows a general under-prediction of sediment yield by the model. Overall, the evaluation results (NSE; 0.68, R^2; 0.76 and RSR; 0.57) indicates "good" model performance. For the validation period, the pattern of the sediment yield with the observed was maintained. However, the model overestimated the sediment loads during September - November 2005. In September - November 2006 and in September-October 2007, the sediment simulation was under estimated. The validation results obtained (NSE; 0.65, R^2; 0.74, RSR; 0.59 and PBIAS; 39.1) were satisfactory. The results show that like the peak runoff, the SWAT model couldn't simulate well the peak sediment loads. A similar result has been reported by Wang et al. (2015). The overestimation of sediment loads for some of the high-flow events might be because the SWAT model fails to consider sediment deposition remaining on surface catchment, allowing all the soil that is eroded by runoff to reach the river directly (Wang et al., 2015). On the other hand, the underestimation of sediment load during some peak events may be a result of the very simple sediment routing algorithm used in the model (ibid). According to Qiu et al. (2012), the SWAT model does not

evaluate specific sediment load and peak flows very accurately because of its dependence on different empirical and semi empirical models (for example SCS-CN and MUSLE). Among other things, a possible reason for achieving satisfactory results during flow and sediment load validation may be from the relatively short period of data used during these periods. A much longer period of data would probably have led to better comparison between the observed and simulated flow and sediment loads since a longer record will not be affected much by few high or low values as will be evident in short records.

Table 6.2. Final parameter value ranges at calibration of discharge and total sediment in the Black Volta River Basin via SUFI-2 of SWAT-CUP

Variable	Parameter name	Parameter value		
		Fitted	Min	Max
FLOW	r_CN2.mgt	-0.120	-0.168	-0.107
	v_GWQMN.gw	1344.085	1261.467	1393.655
	v_ALPHA_BNK.rte	0.6705	0.649	0.683
	v_ REVAPMN.gw	459.941	455.758	462.451
	v_GW_DELAY.gw	483.756	482.813	484.798
	v _RCHRG_DP.gw	0.041	0.040	0.100
	v_CH_N2.rte	0.238	0.202	0.243
	v_ESCO.hru	0.643	0.642	0.653
	r __SHALLST.gw	0.265	0.261	0.267
	r__SLSUBBSN.hru	-0.506	-0.543	-0.506
	r __SOL_AWC.sol	0.542	0.534	0.556
	r_SOL_K.sol	-0.660	-0.685	-0.650
	v_ALPHA_BF.gw	0.373	0.366	0.385
SEDIMENT	v __SPEXP.bsn	1.194	1.192	1.199
	v __SPCON.bsn	0.007	0.007	0.007

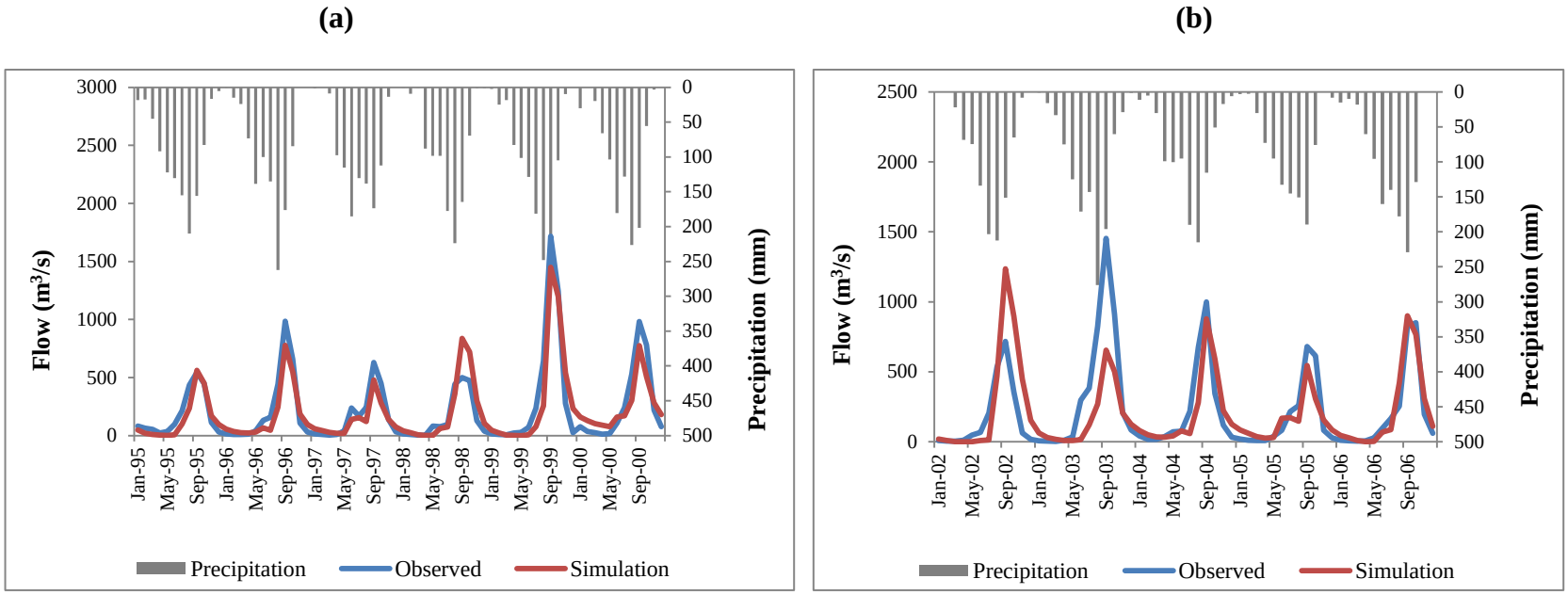

Figure 6.1: Plots of rainfall and comparison of observed and simulated discharges during (a) calibration and (b) validation of SWAT for the Black Volta River Basin

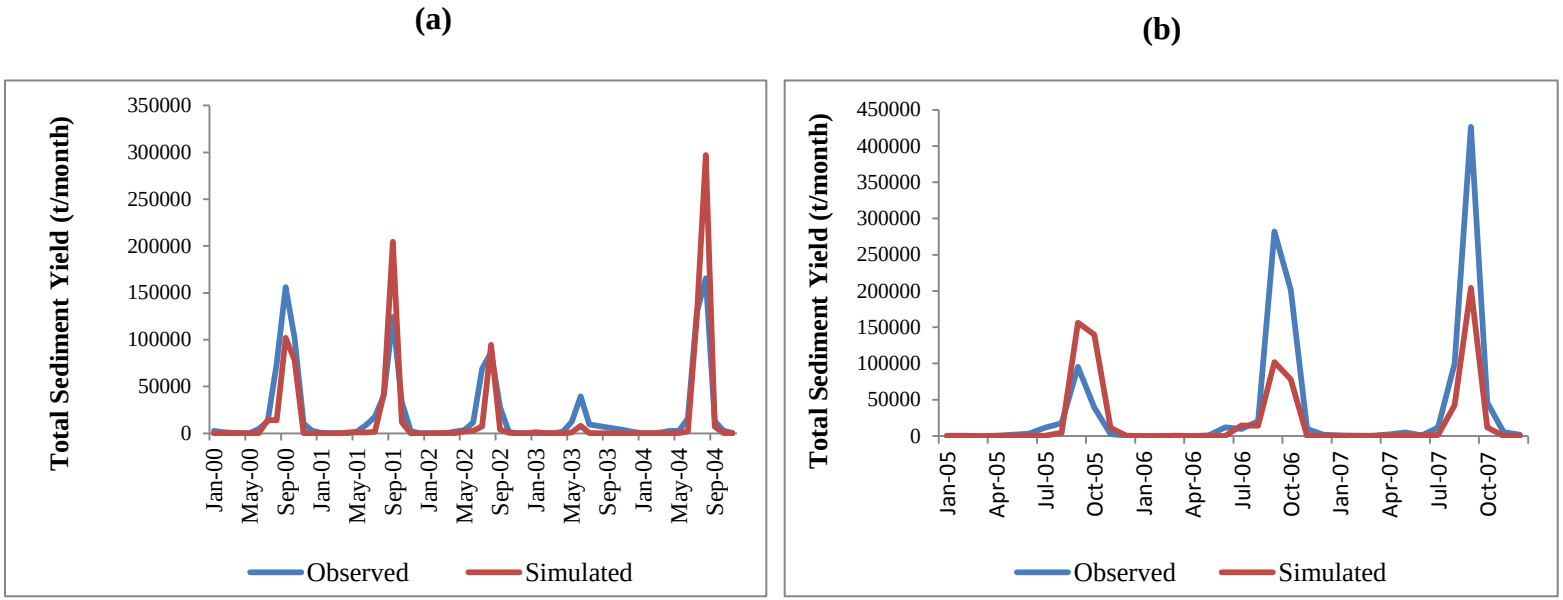

Figure 6.2: Plots of observed and simulated total sediment yield during (a) calibration and (b) validation of SWAT for the Black Volta River Basin

Table 6.3: Results of SWAT calibration and validation for streamflow and sediment yield for the Black Volta River Basin

Component	Simulated period	R^2	RSR	NSE	PBIAS
Runoff	Calibration	0.86	0.38	0.85	8.1
	Validation	0.62	0.64	0.60	20.1
Total Sediment yield	Calibration	0.76	0.57	0.68	27.5
	Validation	0.74	0.59	0.65	39.1

6.4. **Uncertainty analysis**

The uncertainty analysis results for monthly discharge and sediment yield of the study basin indicated that some levels of uncertainty existed in the model simulations. As shown in the discharge and sediment yield calibration results (Figure 6.3), a very low proportion of the observed discharge and sediment data were captured by the 95PPU band. The p-factor values were 0.21 and 0.11 for discharge and sediment yield respectively. Desirable r-factor values (0.21 for discharge and 0.22 for sediment) were however achieved.

For validation, 25% of the observed discharge was captured by the 95PPU band while 14% of the observed sediment was captured. Like the calibration results, these values are also low. However, the r- factor values were good (0.19 for discharge and 0.10 for sediment). The uncertainties existing in the discharge and sediment simulations may have resulted from errors in the input driving variables such as rainfall, temperature and the streamflow data used in generating the sediment rating curve. Uncertainties in SWAT modelling caused by poor accuracy of input data have been reported in several studies (e.g Narsimlu, et al., 2015; Tanveer

Abbas et al., 2016). Some levels of the uncertainties may also have stemmed from the SWAT model itself.

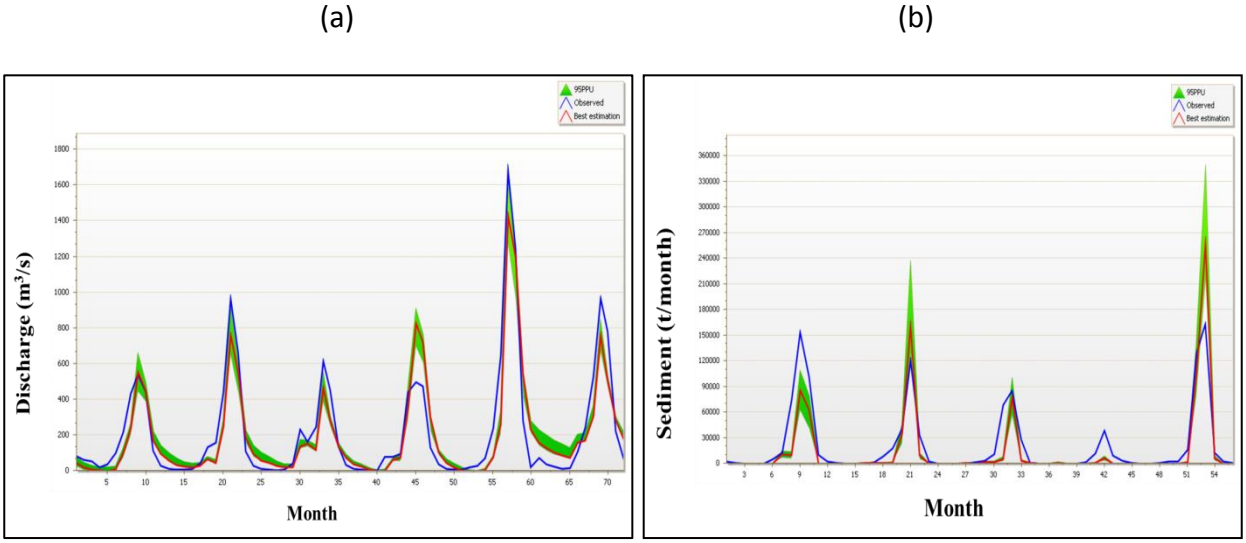

Figure 6.3: Plot of 95PPU for (a) discharge and (b) total sediment yield at calibration in SWAT-CUP

6.5. **Partial Conclusion**

The results of the quantitative statistics (NSE, R^2, RSR and PBIAS) through which the performance of the SWAT model was assessed indicated that the model simulated streamflow and sediment yield of the BVRB quite well. For flow calibration an R^2 of 0.86; NSE of 0.85; RSR of 0.38; and PBIAS of 8.1 was obtained. Sediment yield analysis yielded an R^2 of 0.76; NSE of 0.68; RSR of 0.57, and PBIAS of 27.5. The validation results for streamflow were R^2 of 0.62; NSE of 0.60; RSR of 0.64 and PBIAS of 20.1% while that for sediment yield were R^2 of 0.74; NSE, 0.65; RSR of 0.59, and PBIAS of 39.1%. The P- and R-factor values obtained during the model calibration indicated the existence of low levels of uncertainties in the model.

CHAPTER 7: IMPACT OF CLIMATE CHANGE ON STREAMFLOW AND SEDIMENT YIELD AND THE SENSITIVITY OF FLOW TO LANDUSE/LANDCOVER CHANGES IN THE BVRB

7.1. Introduction

This chapter discusses the projected changes in flow and sediment yield in the basin due to the impact of climate change. The results of the LULC change analysis of the BVB and the sensitivity of the basin's flow to the changes in land use considered in the study are also discussed.

7.2. Impact of climate change on flow and sediment yield

The results of the seasonal change in streamflow and total sediment yield in the Black Volta Basin during the late- and end of the 21st century are presented in Figures 7.1 - 7.4. Relative to the baseline, the model scenarios projected an increase in flow and sediment yield during the dry period for the 2060s under RCP45 scenario as shown in Figure 7.a. The increase in flow ranged between +35% and +45% with a mean of +39% while that of sediment ranged between +51% and +120% with a mean of +85%. For the wet period, the same pattern of general increase in flow and sediment yield was recorded (Figure 7.1b). The range of change in flow was between +28% and +37% with a mean of +35% while that for sediment yield ranged between +113% and +195% with a mean of 143%. Under the high emission RCP8.5 scenario, all the models again projected increases in flow (up to +163%) and sediment yield (+704%) for both dry and wet period. The increase dry period flow ranged between +64% and +163% with a mean of +113% and that of sediment between +169% and +704% with a mean of +473%. For the wet period, the flow increase ranged between +35% and +146% with a mean of +80% while the sediment increase ranged between +179% and +365% with a mean of 279%. The end of the 21st century projection of streamflow and sediment yield for the RCP 4.5 and RCP 8.5 scenarios also showed

increases (Figure 7.3a and b). The only exception to this pattern was a projected decrease in wet period flow with increasing sediment yield by the RACMO22T/ICHEC-EC-EARTH. This results of decrease in flow with increase in sediment yields is similar to the findings of Phan et al. (2011) and Shrestha et al. (2013). Decrease in flows with corresponding increase in sediment yield in river basins can sometimes occur with rainfall decrease and temperature increase (Shrestha et al. 2013). According to Zhu et al. (2008) and Li et al. (2011), increase in temperature with decreasing rainfall reduces plant growth, exposes the soil surface and results in increasing erosion rates and sediment yields. Under RCP8.5 scenario, all the models projected increases in both flow and sediment during the dry and wet periods. The increase in flow across the models was projected to reach +309% (RCA4/CCCma/CanESM2) and 229% (RCA4/CCCma/CanESM2) compared to the historical value, for the dry and wet periods respectively. The projected increase in sediment was between approximately 112% and 750% (Figure 7.4 a and b). High sediment yields following increases in streamflow in river basins can occur from intense rainfall events, erosion and scouring at river banks. The banks of the BVB are mostly sandy and might have contributed to the high sediment yields values obtained. In general, the seasonal cycle of the sediment yield followed that of flow, with increasing flows resulting in increasing sediment yield.

The results of the impact of climate change on the mean annual flow and sediment yield are shown in Table 7.1. Relative to the baseline period, the change is projected to range between +40% and +42% with a mean +41% of for flow and between +100% and +143% with a mean of +139% for sediment yield during the late 21st century under the RCP4.5 scenario. By the end of the 21st century, the change in flow is projected to range between -6% and +78% with a mean of +22% while sediment yield will range from approximately 100% up to about 216% with a mean

of +182%. Under the high emission RCP8.5 scenario, the projections showed that the change in flow during the late century period will range between +48% and up to +148% with a mean of +95% across the models. For sediment yield the projected change was from +249% to +335% with a mean of +285. The end of century projections of flow ranged between +69% and up to +243% with a mean of +130% while that of total sediment ranged between +358% and 412% with a mean of +368% across models under this high scenario. In general, the trend analysis results of streamflow and sediment yield (Table 7.2) indicated statistically significant increase ($p<0.05$) in both streamflow and sediment yield under both emission scenarios during the late - and end of the - 21st century. Increase in streamflow may result in floods in the basin region and thereby affect livelihoods and food security. Sediment load increase in the basin may increase the turbidity of the river and cause loss of reservoir storage (Walling, 2008).

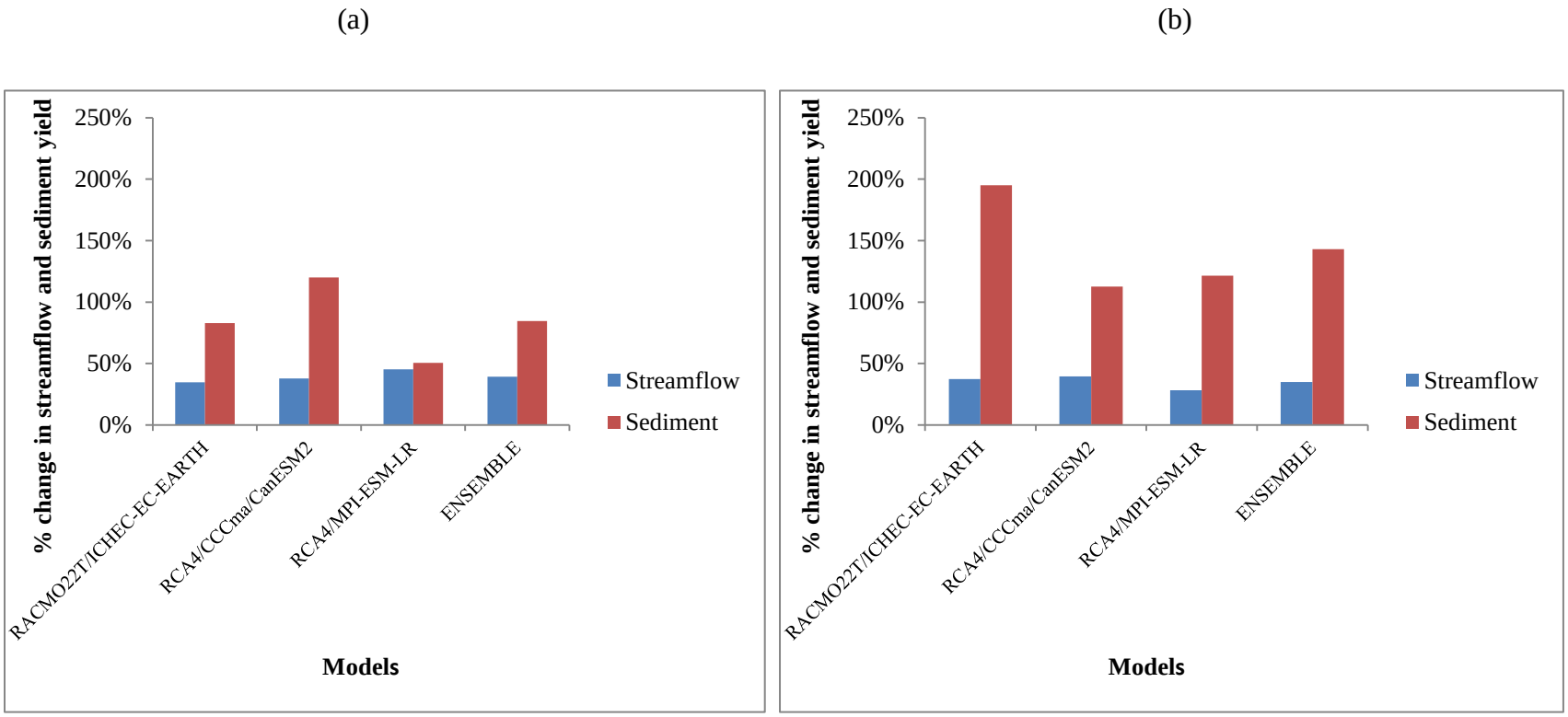

Figure 7.1: Changes in mean seasonal streamflow and sediment yield for the late 21st century (2060s) under RCP4.5 scenario compared to the baseline period. (a) Dry period (January-March) and (b) Wet period (August-October).

(a) (b)

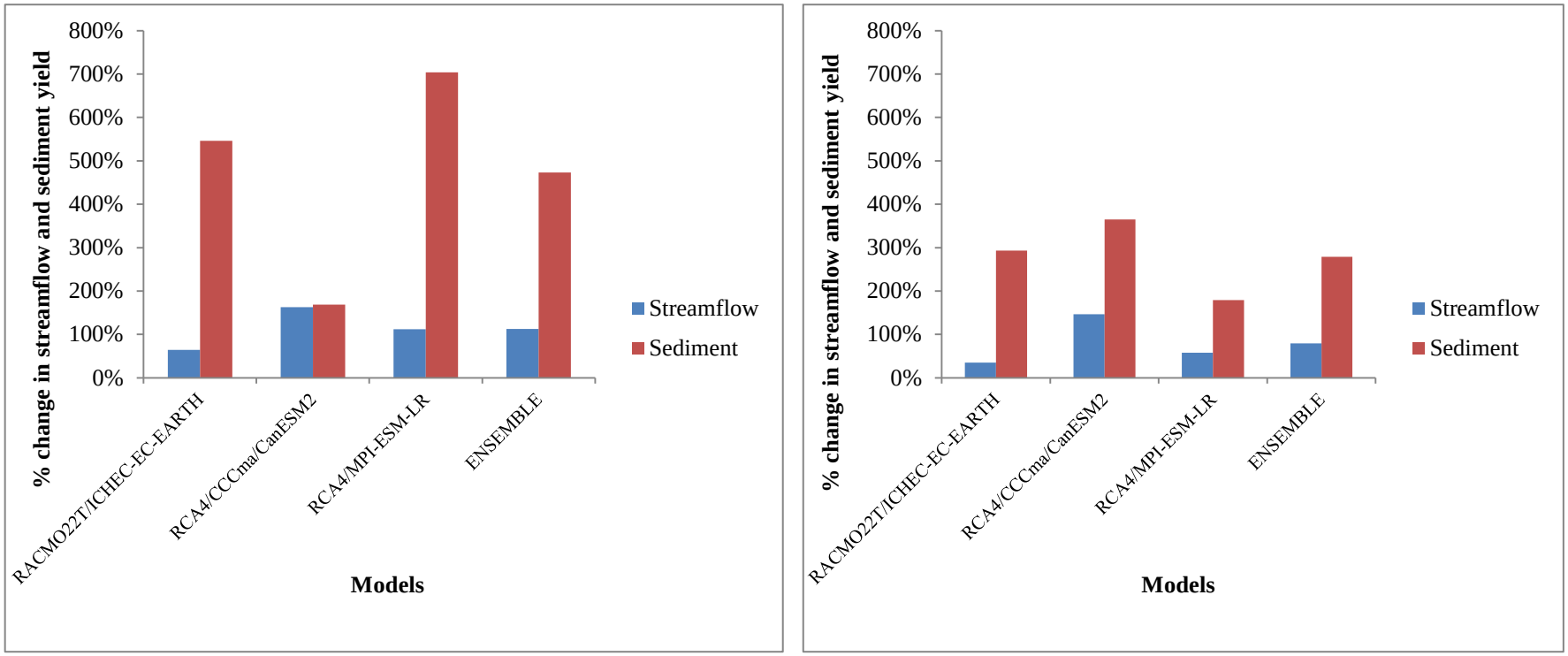

Figure 7.2: Changes in mean seasonal streamflow and sediment yield for the late 21st century (2060s) under RCP8.5 scenario compared to the baseline period. (a) Dry period (January-March) and (b) Wet period (August-October).

(a)

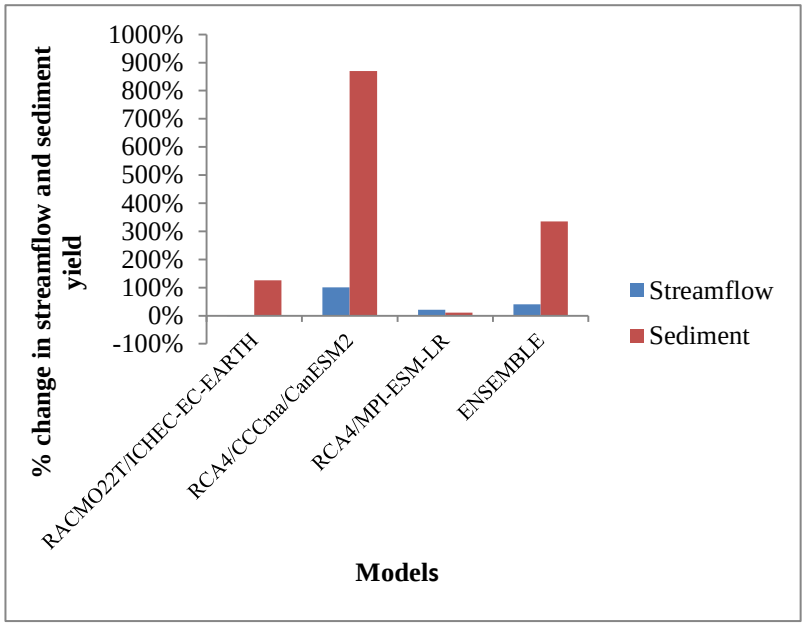

(b)

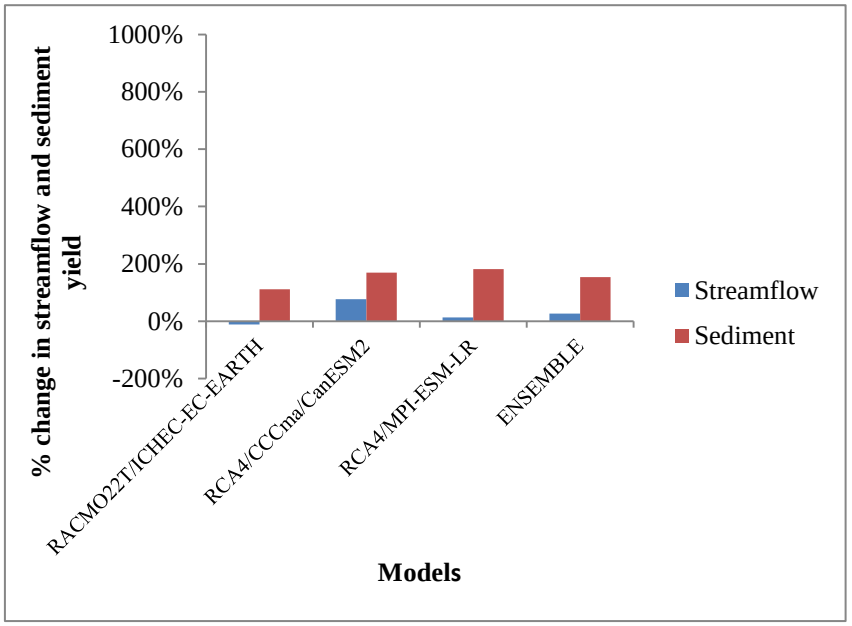

Figure 7.3: Changes in mean seasonal streamflow and sediment yield for the end of the 21st century (2080s) under RCP4.5 scenario compared to the baseline period. (a) Dry period (January-March) and (b) Wet period (August-October).

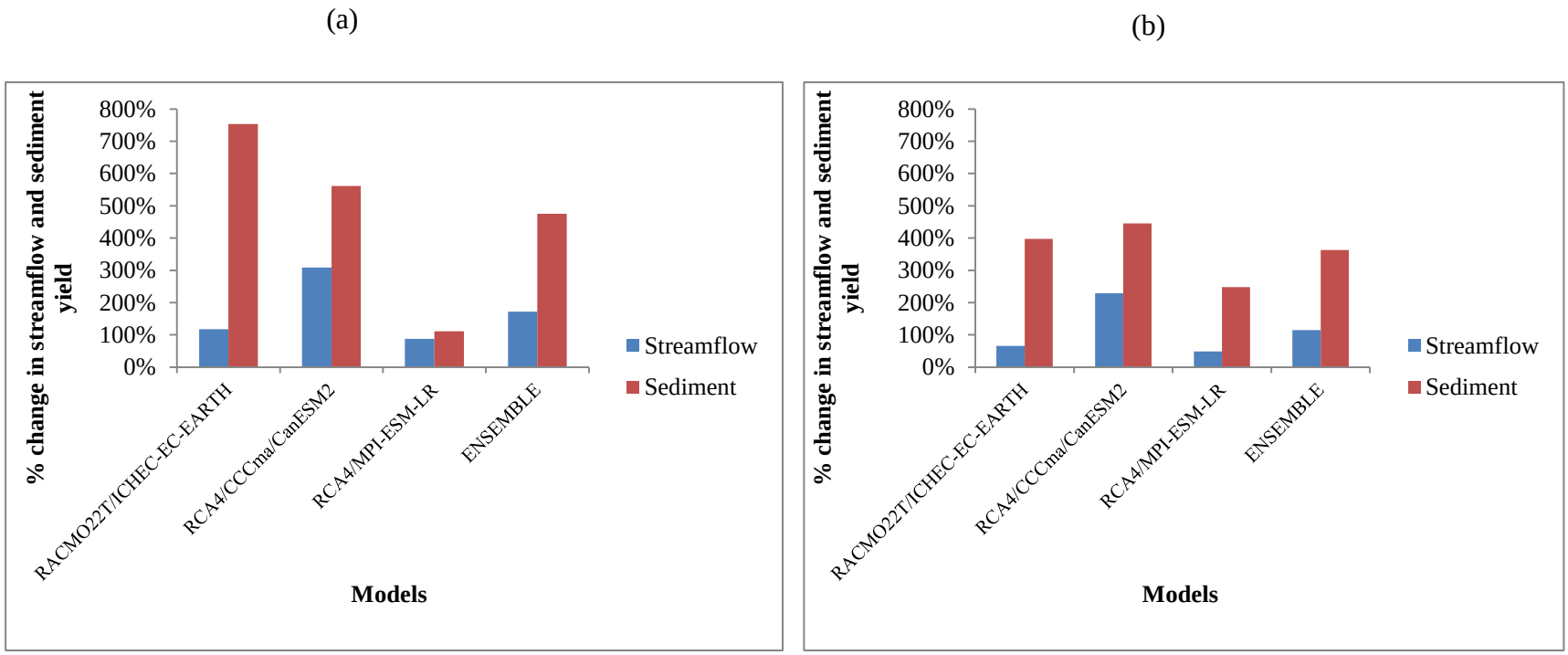

Figure 7.4: Changes in mean seasonal streamflow and sediment yield for the end of the 21st century (2080s) under RCP8.5 scenario compared to the baseline period. (a) Dry period (January-March) and (b) Wet period (August-October).

Table 7.1: Projected changes in mean annual stream flow and total sediment yield, relative to the 1984-2010 period

RCMs	Scenarios	Streamflow (m^3/s)	% Change in streamflow	Total Sediment yield (t/month)	% Change in Total Sediment yield
	Historical	309	0	155542	0
RCA4/CCCma-CanESM2	Late-Century RCP4.5	432	40	311288	100
	Late-Century RCP8.5	769	149	676733	335
	End-of-Century RCP4.5	551	78	424965	173
	End-of-Century RCP8.5	1062	243	797398	413
RACMO22T/ICHEC-EC-EARTH	Late-Century RCP4.5	434	40	311288	100
	Late-Century RCP8.5	460	49	578270	272
	End-of-Century RCP4.5	289	-6	310308	100
	End-of-Century RCP8.5	549	77	705923	354
RCA4/MPI-ESM-LR	Late-Century RCP4.5	440	42	379010	144
	Late-Century RCP8.5	578	87	542214	249
	End-of-Century RCP4.5	382	24	492050	216
	End-of-Century RCP8.5	523	69	682351	339
MULTIMODEL ENSEMBLE MEAN	Late-Century RCP4.5	435	41	371349	139
	Late-Century RCP8.5	602	95	599072	285
	End-of-Century RCP4.5	377	22	437976	182
	End-of-Century RCP8.5	711	130	728557	368

Table 7.2: Results of Mann-Kendall trend test for average annual streamflow and total sediment yield in the BVB for the 2060s and 2080s under RCP 4.5 and RCP 8.5 emission scenarios.

Model Scenarios		Mann-Kendall's test			
		Kendall's Tau	p-value (two tiled test)	alpha	Trend
FLOW	RACMO22T/ ICHEC-EC-EARTH (RCP4.5/2060s)	0.276	0.004	0.05	Significant increase
	RACMO22T/ ICHEC-EC-EARTH (RCP4.5/2080s)	-0.051	0.597	0.05	Not significant
	RACMO22T/ ICHEC-EC-EARTH (RCP8.5/2060s)	0.389	< 0.0001	0.05	Significant increase
	RACMO22T/ ICHEC-EC-EARTH (RCP8.5/2080s)	0.474	< 0.0001	0.05	Significant increase
	RCA4/CanESM2 (RCP4.5/2060s)	-0.176	0.066	0.05	Not significant
	RCA4/CanESM2 (RCP4.5/2080s)	-0.336	0.000	0.05	Significant decrease
	RCA4/CanESM2 (RCP8.5/2060s)	0.683	< 0.0001	0.05	Significant increase
	RCA4/CanESM2 (RCP8.5/2080s)	0.624	< 0.0001	0.05	Significant increase
	RCA4/MPI-ESM-LR (RCP4.5/2060s)	0.385	< 0.0001	0.05	Significant increase
	RCA4/MPI-ESM-LR (RCP4.5/2080s)	0.210	0.029	0.05	Significant increase
	RCA4/MPI-ESM-LR (RCP8.5/2060s)	0.440	< 0.0001	0.05	Significant increase
	RCA4/MPI-ESM-LR (RCP8.5/2080s)	0.394	< 0.0001	0.05	Significant increase
SEDIMENT	RACMO22T/ ICHEC-EC-EARTH (RCP4.5/2060s)	0.275	0.004	0.05	Significant increase
	RACMO22T/ ICHEC-EC-EARTH	0.273	0.004	0.05	Significant

	(RCP4.5/2080s)				increase
	RACMO22T/ ICHEC-EC-EARTH (RCP8.5/2060s)	0.425	< 0.0001	0.05	Significant increase
	RACMO22T/ ICHEC-EC-EARTH (RCP8.5/2080s)	0.608	< 0.0001	0.05	Significant increase
	RCA4/CanESM2 (RCP4.5/2060s)	0.290	0.003	0.05	Significant increase
	RCA4/CanESM2 (RCP4.5/2080s)	0.121	0.210	0.05	Not significant
	RCA4/CanESM2 (RCP8.5/2060s)	0.552	< 0.0001	0.05	Significant increase
	RCA4/CanESM2 (RCP8.5/2080s)	0.531	< 0.0001	0.05	Significant increase
	RCA4/MPI-ESM-LR (RCP4.5/2060s)	0.356	0.000	0.05	Significant increase
	RCA4/MPI-ESM-LR (RCP4.5/2080s)	0.410	< 0.0001	0.05	Significant increase
	RCA4/MPI-ESM-LR (RCP8.5/2060s)	0.495	< 0.0001	0.05	Significant increase
	RCA4/MPI-ESM-LR (RCP8.5/2080s)	0.475	< 0.0001	0.05	Significant increase

7.3. **Land use land cover change analysis**

The most visible change in LULC of the basin during the 10-year period (1990 to 2000) was an increase in cropland and grassland and a decrease in savanna (Figures 7.5 and 7.6). Croplands increased by 13,710 km^2, representing a basin-wide coverage of 10% and grasslands by 8,633 km^2, representing an increase of 6% in basin coverage. Savanna woodland decreased by 19,442 km^2, a reduction from coverage of 57.0% to 42.6% (Table 7.3).

From 1990 to 2000, the average population growth rate in the Basin area occupied by Burkina Faso and Ghana was 2.38% and 2.5% respectively (Barry *et al*., 2005). In Burkina Faso about 78% of the total population lived in the Volta Basin in the year 2000 and the cropped area represented 82.5% of the total cropped land in Burkina Faso (ibid). The increase in cropland can thus be attributed to the increase in population in the basin within that period since expanding population demands more cultivation of crops for sustenance. In assessing the population and land use/land cover dynamics in the Volta River Basin of Ghana, Codjoe (2004), found a moderate to strong correlation between population size and agriculture land use, suggesting that population growth might have contributed to the increase in agriculture land use in 1992 and 2000. Agriculture (cultivation of crops and rearing of cattle) is the main land use type in the Volta Basin and plays a primary role in food security and poverty reduction by providing food and household incomes. Livestock (cattle, sheep and goats) production is highly developed in the Burkinabe and Ghanaian (Northern part) sides of the basin, with the animals being kept mostly for prestige and security in times of economic crises (Codjoe, 2004).

Forest areas showed a slight decline (309 km^2) between 1990 and 2000. The decrease can be linked to the cutting down of vegetation for cultivation of grass to feed the livestock. The grazing

method of the livestock in the basin, which is based on free mobility in all open forests, might have also contributed to the decline in vegetation. In addition, agricultural practices such as slash and burn technique which is widespread in the basin might have contributed to this decline.

Fuel wood is a cheap source of energy, and with rural population forming the dominant population (64-88%) of the Volta Basin (WDI, 2003 in Barry *et al*., 2005) as at the year 2000, dependence on savanna and forests for energy was commonplace. In big cities such as Ouagadougou (Burkina Faso) woodlands are the primary source of firewood and charcoal (Ouedraogo, 2006; Krämer, 2002). In Ghana, about 90% of households use charcoal or firewood for cooking (Derkyi *et al*, 2011). Therefore, in addition to clearing woodlands for cropping, the decline in savanna was most likely due to woodcutting for charcoal and firewood by the habitats of the basin. According to FAO (2001), the ascendency in cutting down trees for fuelwood and charcoal among others are responsible for deforestation in Africa.

Compared to all other land use/land cover types, shrublands showed the least changes (decrease of 19 km^2). Figure 7.7 shows the absolute difference in the different LULC classed during the 10 years. Despite all the changes however, savanna woodlands remained the dominant LULC during the 10 years (Figure 7.8). This was followed by grasslands and croplands in decreasing order of importance. As shown in Table 7.3, other minor changes included decreases in coverage of barren land and herbaceous wetlands by 1,450 km^2 and 1,455 km^2 respectively. Infrastructure development led to an increase in area (101 km^2) of urban development. Shrublands, urban areas, barren land, herbaceous wetland and water body covered less than 2% of the total watershed area in both years.

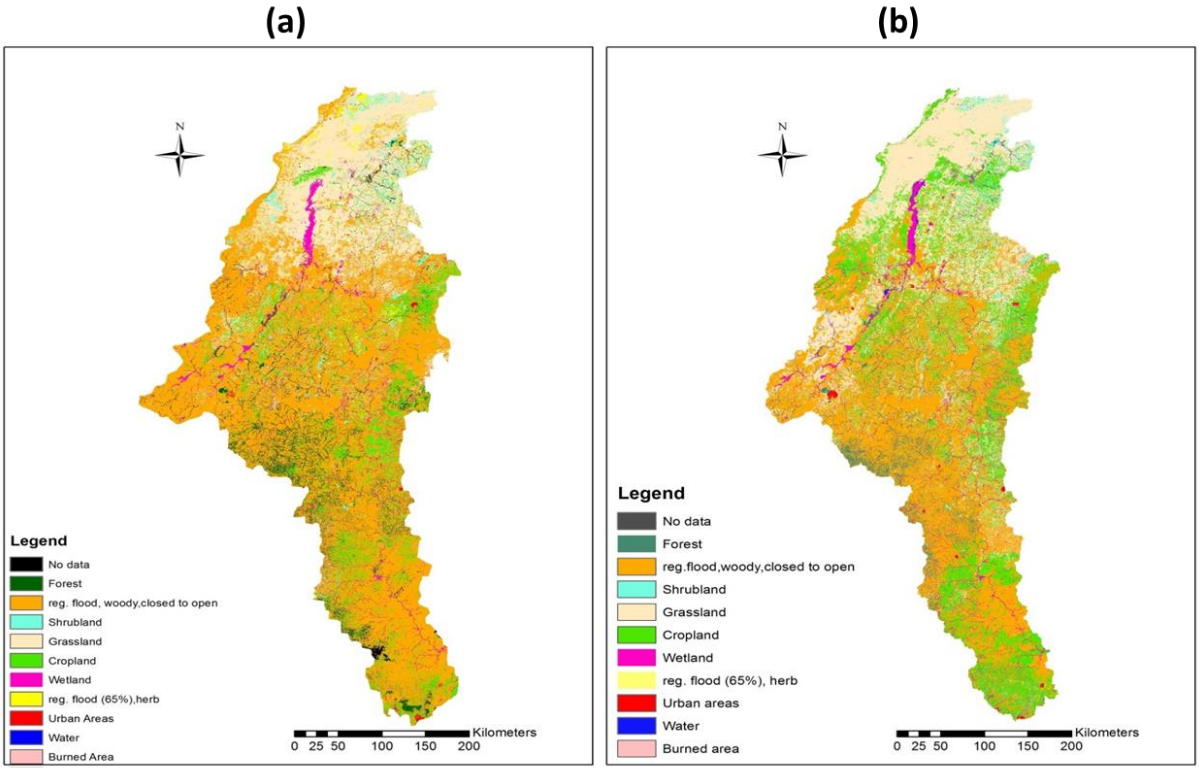

Note: reg. flood, woody, closed to open = savanna; reg. flood (65%), herb = herbaceous wetland

Figure 7.5: LULC maps for the Black Volta River Basin for the years (a) 1990 and (b) 2000 (source: Glowa Volta Portal)

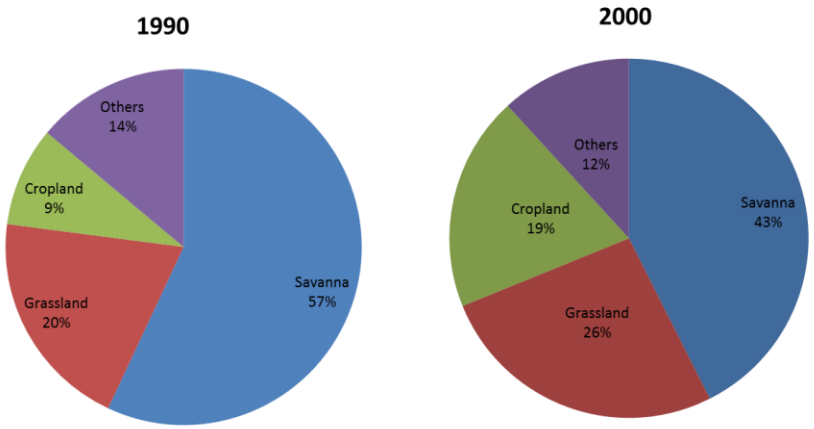

Figure 7.6: Most visible LULC changes in the Black Volta River Basin from 1990 to 2000

Table 7.3: Changes in land use/land cover types in the Black Volta River Basin between 1990 and 2000

Land use types	1990		2000		Absolute Difference	
	Area (km^2)	% Watershed Area	Area (km^2)	% Watershed Area	Area (km^2)	% Watershed Area
Savanna	76950	57.00	57508	42.60	19442	14.40
Forest-Evergreen	7417	5.49	7107	5.26	309	0.23
Shrubland	2302	1.71	2283	1.69	19	0.02
Grassland	26773	19.83	35406	26.23	8633	6.40
Agricultural Land-Generic	12440	9.21	26150	19.37	13710	10.16
Wetlands-Non-Forested	5286	3.92	5356	3.97	71	0.05
Herbaceous Wetland	1583	1.17	129	0.10	1455	1.07
Urban-Medium Density	154	0.11	255	0.19	101	0.08
Water	41	0.03	201	0.15	160	0.12
Barren	2057	1.52	608	0.45	1450	1.07

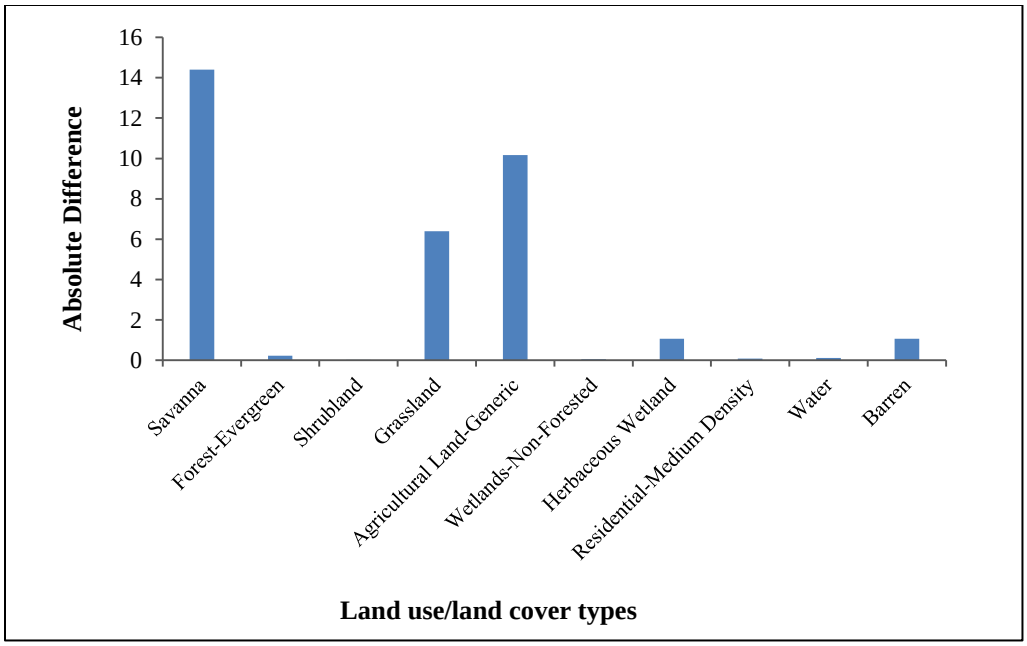

Figure 7.7: Absolute difference in LULC class in the Black Volta River Basin between 1990 and 2000

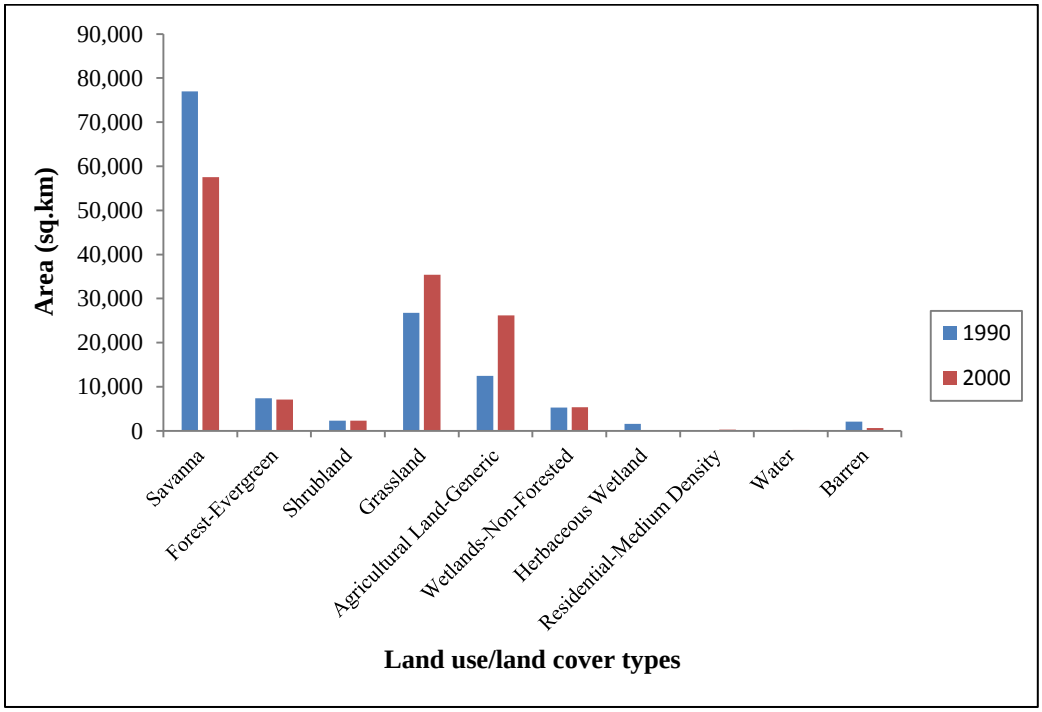

Figure 7.8: Land use/land cover coverage in the Black Volta River Basin from 1990 to 2000

7.4. Sensitivity of streamflow to land use/land cover change

The results of the annual and seasonal variability of streamflow in relation to changes in LULC in the BVRB are depicted in Figure7.9 and Table 7.4 respectively. The total annual flows based on the 1984-2010 simulation showed slight decreases in streamflow following the change in land use from 1990 to 2000. The decrease ranged between 0.5% in 1992 and 5.7% in 1984. For the seasonal analysis, whereas the change in land use resulted in a 1% increase in flow during the dry season (Jan-Mar), a decrease of 4% flow was recorded for the wet season (Jul-Sep). The analysis revealed no change in flow during the beginning of the rainfall season (Apr-Jun). The mean annual streamflow for the period of simulation using the LULC of the year 1990 was 319.12 m^3/s while that for the LULC of the year 2000 was 309.53 m^3/s, representing a slight reduction of -2% over the year 1990.This reduction is statistically insignificant. The coefficients of variation were 1.20 and 1.18 for the 1990- and 2000-LULC simulations, respectively (Table 7.5)

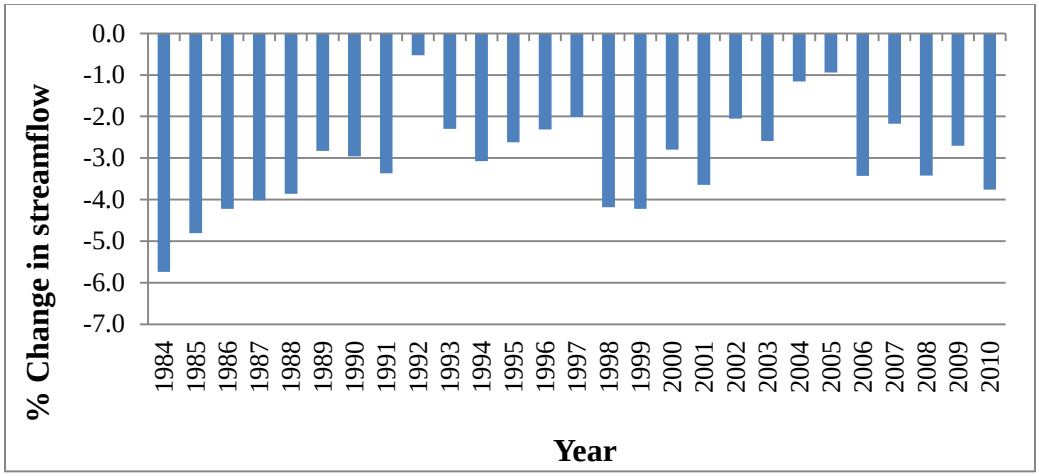

Figure 7.9: Simulated changes in total annual streamflow of the Black Volta River Basin using year 2000 land use map, relative to year 1990 land use map

Table 7.4: Change in seasonal streamflow of the Black Volta River Basin due to LULC change from 1990 to 2000

Seasons	LULC1990 (m^3/s)	LULC2000 (m^3/s)	% Change
Dry season (Jan-Mar)	2,324.535	2,337.934	+1
Beginning rainfall season (Apr-Jun)	2,314.123	2,312.178	0
Wet season (Jul-Sep)	3,758.848	3,619.221	-4
Wet dry season (Oct-Dec)	3,391.906	3,445.026	+2

Table 7.5: Statistics of streamflow simulation (1984-2010) for the Black Volta River Basin based on the LULC maps of the years 1990 and 2000

Statistical Parameter	**LULC1990**	**LULC2000**
Mean (m^3/s)	319.12	309.53
Maximum (m^3/s)	2,173.00	2,137.00
Minimum (m^3/s)	8.69	8.15
Standard Deviation (m^3/s)	383.10	363.96
Coefficient of Variation	1.20	1.18

7.5. **Partial Conclusion**

Seasonal analysis of streamflow and sediment yield for the BVRB showed increases in both flow and sediment for the dry and wet periods for the 2060s and 2080s under both RCP 4.5 and RCP 8.5 scenarios. Projected mean annual flow and sediment yield also showed mostly increases, statistically significant at the 5% level of significance. The land use/land cover change analysis

of the BVRB revealed that some changes occurred during the 1990/2000 period. Notable among the changes were an increase in cropland and a decrease in savanna. Analysis of annual streamflow for the years (1990 and 2000) showed decreases. With regards to seasonal flows an increase of 1% was observed for the dry season while the wet season flow decreased by 4%. The wet-dry season saw a slight increment. The statistics of the flow simulation however showed that the observed changes were statistically not significant.

CHAPTER 8: GENERAL CONCLUSIONS AND PERSPECTIVES

8.1. Conclusions

The extreme event analysis showed that the BVB got warmer and wetter (revealed through increases in the amount and intensities of rainfall) during the 1981-2010 period.

The performance of the SWAT model in simulating the historical flow and sediment yield of the BVB, assessed through the quantitative statistics NSE, R^2, RSR and PBIAS, during monthly calibration and validation shows that the model reasonably simulates the two variables. The calibration results for flow were R^2 of 0.86; NSE of 0.85; RSR of 0.38; and PBIAS of 8.1. For sediment yield, the results were R^2 of 0.76; NSE of 0.68; RSR of 0.57, and PBIAS of 27.5. Both results show "good" model performance. The validation results were "satisfactory" for both flow and sediment yield, with R^2 of 0.62; NSE of 0.60; RSR of 0.64 and PBIAS of 20.1% for streamflow and R^2 of 0.74; NSE, 0.65; RSR of 0.59, and PBIAS of 39.1% for sediment yield. The PBIAS values show that the model has the tendency of underestimating flow and sediment yield in the basin. Results of the sensitivity analysis show that the most sensitive parameter to streamflow in basin is the curve number (CN2). The P-factor and R-factor values obtained during the model calibration shows that the uncertainties which exist in the model should not be ignored and must be taken into account when using the results for impact assessment.

The plots of mean monthly rainfall and temperature of the model-simulated uncorrected, model-simulated bias-corrected and observed data showed that the quantile-quantile downscaling and quantile-quantile transformation method performed well in reducing the RCM biases. The analysis of the data further showed that the corrected data fit much better to the observed data than the uncorrected data. The individual RCMs exhibited some biases in the simulation of

historical rainfall of the basin. With regards to temperature, all the models simulations fit well to the historical temperature of the basin.

Relative to the baseline, annual rainfall amounts showed positive and negative signals across the models. Similar to the annual rainfall, the intra-annual and seasonal rainfall analysis also showed high uncertainty in the future rainfall amounts, with higher variability in the wet season compared to the dry season. Temperature projections by the models unanimously suggested warming of the basin during the 2060s and 2080s with increases ranging between 2.0 ^{o}C (late 21st century under RCP4.5) and 3.7 ^{o}C (end of the 21st century under RCP8.5). Trend analysis of annual future rainfall pointed in both positive and negative directions. The trends were however statistically insignificant at the 5% level of significance. Trends in the annual mean temperature however, showed mostly statistically significant (5% level of significance) increases in future temperature over the basin. A few of the model runs showed statistically insignificant decreasing trends. High temperatures may affect water availability and use in the basin. Since majority of the basin's population depend on agriculture for their livelihood, problems related to water scarcity in the basin may worsen the poverty situation in the basin. Measures to cope with the increasing temperature over the basin should therefore be explored and developed well ahead of time.

Seasonal analysis of streamflow and sediment yield showed increases in flow and sediment during the dry and wet periods for the late- and end of the 21st century under both RCP 4.5 and RCP 8.5 scenarios. Analysis of the mean annual flow and sediment yield also showed mostly statistically significant increases.

The land use/land cover change analysis of the Black Volta Basin showed that between the period 1990 and 2000, the coverage of cropland and grassland increased drastically, with corresponding reduction in savanna. These changes could be linked to population growth and the dependence on savanna for fuelwood in the basin. The sensitivity analysis of streamflow over the basin with respect to the 10 year change in land use also showed only slight changes. The statistics of the flow simulation showed, however, that the changes were not significant. Considering the role of land-use/cover in flow, sensitivity analysis using different "extreme" hypothetical scenarios can prove useful in concluding more robustly on the sensitivity or not of the flow of the Black Volta to changes in land use.

8.2. **Perspectives**

Extreme events in the BVRB during the 1980 - 2010 period have been analyzed, and projections of precipitation and temperature in the basin during the late- and end-of-the 21st century made. In addition, the impact of climate change on flow and sediment yield of the BVRB has been evaluated, and the sensitivity of the basin's flow to changes in LULC changes assessed. Given the high level of uncertainty in the precipitation projections for the basin, the use of more models is recommended to increase the level of confidence in the projections. To enable better simulation of sediment loads in the basin, future study should consider sampling sediments over a longer period of time, other than the one (1) year period employed in this study. Finally, future studies should consider developing hypothetical land use/land cover scenarios to allow for better assessment of the sensitivity of LULC change on both flow and sediment loads in the basin.

8.3. **Recommendations**

To reduce the vulnerability of the BVRB and indeed the entire VRB to the projected impacts of climate change, the following recommendations are proposed:

1. A comprehensive flood management plan should be developed for the entire VRB. This plan should include among other things the enhancement of existing reservoirs to take up extra water and the development of flood early warning systems;
2. Development of flood early warning systems;
3. A drought management plan which includes having irrigation facilities for supplemental irrigation in rainfed agriculture to offset the negative effect of drought on agriculture and food security should be developed;
4. Integrated watershed management approaches, aimed at reducing erosion and sedimentation in the basin should be explored and implemented;
5. Establishment of a regulatory framework on sediment loads in the basin;
6. The use of alternative sources of energy such as solar and biogas should be explored.

REFERENCES

Abbas, I.I., Muazu, K.M. and Ukoje, J.A. (2010). Mapping Land Use-Land Cover and Change Detection in Kafur Local Government, Katsina, Nigeria (1995–2008) Using Remote Sensing and GIS. Res. J. Environ. Earth Sci., 2 (1), 6–12.

Abbaspour (2015). SWAT-CUP: SWAT Calibration and Uncertainty Programs - A User Manual. Department of Systems Analysis, Integrated Assessment and Modelling (SIAM), Eawag, Swiss Federal Institute of Aquatic Science and Technology, Duebendorf, Switzerland, 100pp.

Abbaspour, K.C., Johnson, A., van Genuchten, M.Th. (2004). Estimating uncertain flow and transport parameters using a sequential uncertainty fitting procedure. Vadose Zone Journal 3(4), 1340-1352.

Abbaspour, K.C., Yang, J., Maximov, I., Siber, R. Bogner, K. K., Mieleitner, J., Zobrist, J. and Srinivasan, R. (2007). Modelling hydrology and water quality in the pre- alpine/alpine Thur watershed using SWAT. Journal of Hydrology, 333:413- 430.

Abiodun, B.J., Abba, Omar. S., Lennard, C. and Jack, C. (2015). Using regional climate models to simulate extreme rainfall events in the Western Cape, South Africa. International Journal of Climatology. DOI: 10.1002/joc.4376.

Akrasi, S.A. (2011). West African Journal of Applied Ecology, volume 18.

Alexander, L.V., X, Zhang., Peterson, T., Caesar, J., Gleason, B., Klein Tank, A.M.G., Haylock, M., Collins, D., Trewin, B., Rahimzadeh, F., Tagipour, A., Kumar Kolli, R., Revadekar, J, V., Griffiths, G., Vincent, L., Stephenson, D, B., Burn, J., Aguilar, E., Brunet, M., Taylor, M., New, M., Zhai, P., Rusticucci, M. and Vazquez Aguirre, J.L. (2006). Global observed changes in daily climate extremes of temperature and precipitation. Journal of Geophysical Research-Atmospheres, 111, D05109.

Allwaters Consult (2012). Diagnostic Study of the Black Volta Basin in Ghana; Final Report; ALLWATERS Consult Limited: Kumasi, Ghana.

Amadou, A., Abdouramane, G., Seidou, O. and Seidou Sanda, I. (2015). Changes to flow regime on the Niger River at Koulikoro under a changing climate. Hydrological Sciences Journal, doi 10.1080/02626667.2014.916407.

Amisigo, B.A. (2005). Modelling riverflow in the Volta Basin of West Africa: A data-driven framework. PhD Thesis. Ecology and Development Series No. 34. ZEF Bonn. Cuvillier Verlag, Göttingen, http://www.glowa-golta.de/fileadmin/template/Glowa/downloads/Amisigo_doc_thesis_2006 .pdf.

Andah, W., van de Giesen, N., Huber-Lee, A. and Biney, C. (2004). Can we maintain food security without losing hydropower? The Volta Basin. Climate Change in Contrasting River Basins: Adaptation Strategies for Water, Food and Environment, J. Cayford, Ed., CABI Publishing,Wallingford, 181-194.

Annor, F. O. (2012). Diagnostic Study of the Black Volta Basin in Ghana. In-Service Training Centre, Upper West Region- Ghana.

Armah, F.A., Yawson, D.O., Yengoh, G.T., Odoi, J.O. and Afrifa. E.K.A. (2010). Impact of Floods on Livelihoods and Vulnerability of Natural Resource Dependent Communities in Northern Ghana. Water, 2, 120–139.

Arnold, J. G., Moriasi, D. N., Gassman, P. W., Abbaspour, K. C.,White, M. J., Srinivasan, R., Santhi, C., Harmel, R. D., van Griensven, A., Van Liew, M. W., Kannan, N., Jha, M. K. (2012b).

Arnold, J. G., Srinivasan, R., Muttiah, S., and Williams, J. R. (1998). "Large area hydrologic modelling and assessment: Part I. Model development." Journal of American Water Resource Association, 34(1), 73-89.

Arnold, J.G., Allen P.M. and Bernhardt, G. (1993). A comprehensive surface-groundwater flow model. Journal of Hydrology 142, p. 47-69.

Arnold, J.G., Kiniry, J.R., Srinivasan, R., Williams, J.R., Haney, E.B., Neitsch, S.L. (2012a). Soil and Water Assessment Tool. Input/Output Documentation, Version 2012. Texas Water Resources Institute. TR-439. Available at http://swat.tamu.edu/documentation/2012-io/. Accessed on 7/23/2015.

Awotwi, A., Yeboah, F. and Kumi M. (2015). Assessing the impact of land cover changes on water balance components of White Volta Basin in West Africa Water and Environment Journal 29, 259-267.

Babiński, Z. (2005) The relationship between suspended and bed load transport in river channels. In: Sediment Budgets 1 (Proc. Foz do Iguazu Symo., April 2005) (ed. by D. E. Walling & A. J. Horowitz), 182–188. IAHS Publ. 291. IAHS Press,Wallingford, UK.

Barry B, Obuobie E, Andreini M, Andah W and Pluquet, M. (2005). The Volta river basin. Comprehensive assessment of water management in agriculture. Comparative study of river basin development and management.

Beven, K. and Binley, A. (1992). The Future of Distributed Models - Model Calibration and Uncertainty Prediction. Hydrological Processes, 6(3): 279-298.

Biney, C.A. (2010). Connectivities and linkages within the Volta Basin. Paper presented at the Conference of the Global Catchment Initiative (GCI), December 6-8, 2010, University Club, Bonn, Germany.

Boko, M., Niang, I., Nyong, A., Vogel, C., Githeko A, Medany, M., Osman-Elasha, B., Tabo, R., & Yanda, P. (2007). Africa Climate Change 2007: impacts, adaptation and vulnerability. In M. L. Parry, O. F. Canziani, J. P. Palutikof, P. J. van der Linden, & C. E. Hanson (Eds.), Contribution of Working Group II to the Fourth Assessment Report of the Intergovernmental Panel on Climate Change (pp. 433–467). Cambridge, UK: Cambridge University Press.

Borah, D.K., Bera, M., Shaw, S. and Keefer, L. (1999). Dynamic modeling and monitoring of water, sediment, nutrients, and pesticides in agricultural watersheds during storm events. Contract Report 655, Illinois State Water Survey Watershed Science Section Champaign, IL.

Braimoh, A.K. and Vlek, P.L.G. (2005). Land Cover Change Trajectories in Northern Ghana. Environ. Manage., 36 (3), 356–373.

Brath, A., Montanari, A., Moretti, G. (2006). Assessing the effect on flood frequency of land use change via hydrological simulation (with uncertainty). Journal of Hydrology 324 (1–4), 141–153.

Burkina Faso Post-Disaster Needs Assessment (2010). Inondations de 1erSeptembre 2009 au Burkina Faso, Evaluation des dommages, pertes et besoins de construction, de reconstruction et de relèvement.

Butt, B., and Olson, J. M. (2002). An approach to dual land use and land cover interpretation of 2001 satellite imagery of the eastern slopes of Mt. Kenya. Land use Change Impacts and Dynamics (LUCID) Project Working Paper 16. International Livestock Research Institute (ILRI), Nairobi, Kenya.

CDKN (Climate and Development Knowledge Network) (2014). The IPCC's Fifth Assessment Report: What's in it for Africa? Available from http://cdkn.org/resource/highlights-africa-ar5/ [Accessed 14 August, 2015].

Chevallier, P. and Planchon, O. (1993). Hydrological processes in a small humid savanna basin (Ivory Coast); Journal of Hydrology; Vol. 151: pp. 173–191.

Chinowsky, Paul., Schweikert, Amy., Strzepek, Niko., Manahan, Kyle., Strzepek, Kenneth. and Schlosser, C. Adam (2011). "Adaptation Advantage to Climate Change Impacts on Road. Infrastructure in Africa through 2100," Working Paper 25, UNU-WIDER.

Chu, T.W., Shirmohammadi, A., Montas H. and Sadeghi, A. (2004). Evaluation of the SWAT model's sediment and nutrient components in the Piedmont physiographic region of Maryland. Transactions of the ASAE, 47, 1523–1538.

Chylek, P., Li, J., Dubey, M.K., Wang, M., and Lesins, G. (2011). Observed and model simulated 20th century Arctic temperature variability: Canadian Earth System Model CanESM2 22893–22907. doi:10.5194/acpd-11-22893-2011.

Codjoe, S.N.A. (2004). Population and Land use/land cover dynamics in the Volta River Basin of Ghana, 1960-2010. Ecology and Development Series, No.15. Gottingen: Cuvillier Verlag. 184 pages.

Coffey, A.E., Workman, S.R., Taraba, J.L., Fogle, A.W. (2004). Statistical procedures for evaluating daily and monthly hydro- logic model predictions. Trans. ASAE 47 (1), 59–68.

Costa, M.H., Botta, A., Cardille, J.A. (2003). Effects of large-scale changes in land cover on the discharge of the Tocantins River, Southeastern Amazonia. Journal of Hydrology 283, 206–217.

Crooks, S., Davies, H. (2001). Assessment of land use change in the Thames catchment and its effect on the flood regime of the river. Physics and Chemistry of the Earth, Part B 26 (7–8), 583–591.

Derkyi, N.S.A., Sekyere, D., Okyere, P.Y., Darkwa, N.A. and Nketiah, S.K. (2011). Development of bioenergy conversion alternatives for climate change mitigation.International Journal of Energy and Environment, 2(3), pp 525-532.

Di Gregorio, A. and Jansen, L.J.M. (1998). Land cover classification system. Proceedings of the 1st Earth Observation and Environment Information 1997 Conference (EOET97), 13-16 October, 1997, Alexandria, Egypt.

Diallo, I., Sylla, M.B., Giorgi, F., Gaye, A.T., Camara, M. (2012). Multimodel GCM-RCM Ensemble-Based Projections of Temperature and Precipitation over West Africa for the Early 21st Century 2012. doi:10.1155/2012/972896.

Dosio, A., Panitz, H.-J., Schubert-Frisius, M., and Lüthi, D. (2015). Dynamical downscaling of CMIP5 global circulation models over CORDEX-Africa with COSMO-CLM: evaluation over the present climate and analysis of the added value. Climate Dynamics, 44:2637–2661.

Duan, Z., Xianfeng, S. and Liu, J. (2009). Application of SWAT for sediment yield estimation in a mountainous agricultural basin. International Conference on Geoinformatics, Fairfax, 2009, pp. 1-5. Forkuo, E.K. (2011). Flood Hazard Mapping using Aster Image data with GIS. International Journal of Geomatics and Geosciences, 1, 932–950.

Duru, U. (2015). Modelling Sediment Yield and Deposition Using the Swat Model: A Case Study of Cubuk I and Cubuk II Reservoirs, Turkey. PhD. Thesis. Colorado State University, Fort Collins.

Dwarakish, G.S. and Ganasri, B.P. (2015). Impact of land use change on hydrological systems:A review of current modelling approaches. Cogent Geoscience, 1: 1115691. http://dx.doi.org/10.1080/23312041.2015.1115691.

Eberhart, R. C. and Kennedy, J. (1995). A new optimizer using particle swarm theory. Proceedings of the sixth international symposium on micro machine and human science pp. 39- 43. IEEE service center, Piscataway, NJ, Nagoya, Japan.

Edwards, K. (1993). Soil erosion and conservation in Australia. In: Pimentel, D. (Ed.). World Soil Erosion and Conservation, Cambridge, pp. 147–169.

Elfert, S., Bormann, H. (2010). Simulated impact of past and possible future land use changes on the hydrological response of the Northern German lowland 'Hunte' catchment. J HYDROL 383, 245 – 255, 2010.

Endris, H.S., Lennard, C., Hewitson, B., Dosio, A., Nikulin, G., Panitz, H. (2015). Teleconnection responses in multi-GCM driven CORDEX RCMs over Eastern Africa. Climate Dynamics. DOI 10.1007/s00382-015-2734-7.

Environmental Resources Management (2007). Environmental and social impact assessment of the Bui Hydropower Project. Prepared by Environmental Resources Management, in association with SGS Environment for the Ministry of Energy/Bui Development Committee, Ghana. http://library.mampam.com/Final%20ESIA%20-%20Bui%20HEP.pdf.

FAO (1997a). Africover land cover classification. Rome, Italy.

FAO (1997b). Irrigation potential in Africa: A basin approach. FAO Land and Water Bulletin 4

FAO (2001). Global forest resource assessment. Main report. (FAO Forest Paper 140. Food and Agriculture Organization of the United Nations,Rome, Italy.

FAO. 1995. Digital soil map of the World. Rome, Italy.

Fleming, M. and Neary, V. (2004). Continuous Hydrologic Modelling Study with the Hydrologic Modelling System, Journal of Hydrological Engineering, 9, 175–183.

Foley, J.A., DeFries, R., Asner, G.P., Barford, C., Bonan, G., Carpenter, S.R., Chapin, F.S., Coe, M.T., Daily, G.C., Gibbs, H.K., Helkowski, J.H., Holloway, T., Howard, E.A., Kucharik, C.J., Monfreda, C., Patz, J.A., Prentice, I.C., Ramankutty, N., Snyder, P.K. (2005). Global Consequences of Land Use. Science 309(5734), 570-574.

Gassman P.W, Reyes M, Green, C.H. and Arnold, J.G. (2007). The Soil and Water Assessment Tool: Historical development, applications, and future directions. Trans. ASABE 50(4):1211-1250.

Gassman, P.W. (2015). The Soil and Water Assessment Tool (SWAT) Ecohydrological Model Circa 2015: Global Application Trends, Insights and Issues. Abstract H11k-01 presented at 2015 Fall meeting, AGU, San Francisco, California, 14-18 Dec.

Ghaffari, G., Keesstra, S., Ghodousi, J., Ahmadi, H. (2010). SWAT-simulated hydrological impact of land-use 10 change in the Zanjanrood Basin, Northwest Iran. Hydrological Processes 24(7), 892-903.

Ghana Energy Commission (2015). 2015 Energy (Supply and Demand) Outlook for Ghana. 50pp.

Giertz, S. (2004). Analyse der hydrologischen Prozesse in den sub-humiden Tropen Westafrikas unter besonderer Ber¨ucksichtigung der Landnutzung am Beispiel des AguimaEinzugsgebietes in Benin; PhD thesis; University Bonn.

Gilbert, R.O. (1987). Statistical Methods for Environmental Pollution Monitoring, Wiley, NY.

Giorgi, F., Jones, C., Asrar, G. (2009). Addressing climate information needs at the regional level: the CORDEX framework. World Meteorology Organ Bulletin Available online at http://wcrp.ipsl.jussieu.fr/RCD_Projects/CORDEX/CORDEX_giorgi_WMO.pdf., 58, 175-183.

Gordon, C. and Amatekpor, J. K. (1999). The Sustainable Integrated Development of the Volta Basin in Ghana. VBRP, University of Ghana-Legon 159 p.

Green Cross International (2001). Trans-boundary Basin Sub-Projects: The Volta River Basin. Website: www.gci.ch/Green- crossPrograms/ waterres/pdf/WFP_Volta.

Green, W. and Ampt, G. (1911). "Studies on soil physics, 1. The flow of air and water through soils." Journal of Agricultural Sciences 4: 11-24.

Gupta, H. V., Sorooshian, S. and Yapo, P. O. (1999). Status of automatic calibration for hydrologic models: Comparison with multilevel expert calibration. Journal of Hydrologic Engineering, 4(2): 135-143.

Guy, H.P. and Normann, V.W. (1970). Field Methods for Measurements of Fluvial Sediment. - Techniques of Water- Resources Investigations of the United States Geological Survey, Book 3, Chapter C2, 59 p.

Gyau-Boakye, P. and Tumbulto, J.W. (2006). Comparison of rainfall and runoff in the humid south-western and the semiarid northern savannah zone in Ghana. African Journal of Science and Technology. Science and Engineering Series Vol. 7, No.1, pp. 64-72.

Hargreaves, G. L., Hargreaves, G. H. and Riley, J. P. (1985). Agricultural benefits for Senegal River basin. Journal of Irrigation and Drainage Engineering. 108(3): 225-230.

Hazeleger, W., Severijns, C., Semmler, T., Stefanescu, S., Yang, S., Wang, X., Wyser, K., Dutra, E., Baldasano, J.M., Bintanja, R., Bougeault, P., Caballero, R., Ekman, A.M.L., Christensen, J.H., van den Hurk, B., Jimenez, P., Jones, C., Kallberg, P., Koenigk, T., McGrath, R., Miranda, P., van Noije, T., Parodi, J.A., Schmith, T., Selten, F., Storelvmo, T., Sterl, A., Tapamo, H., Vancoppenolle, M., Viterbo, P. and Willen, U. (2010) EC-earth: a seamless earthsystem prediction approach in action. Bulletin of American Meteorological Society, 91:1357–1363.

Hewitson, B. C. and Crane, R.G. (2006). Consensus between GCM climate change projections with empirical downscaling: Precipitation downscaling over South Africa, International Journal of Climatology 26: 1315–1337.

Himanshu, S.K., Pandey, A. and Shrestha, P. (2017). Application of SWAT in an Indian river basin for modeling runoff, sediment and water balance, Environmental Earth Sciences, 76:3. https://doi.org/10.1007/s12665-016-6316-8.

Hong, S.Y. and Kanamitsu, M. (2014). Dynamical downscaling: fundamental issues from an NWP point of view and recommendations. Asia Pacific Journal of Atmospheric Science 50(1):83–104. doi:10.1007/ s13143-014-0029-2.

Intergovernmental Panel on Climate Change: IPCC (2007b) Climate Change 2007, Synthesis Report (AR4).

Intergovernmental Panel on Climate Change: IPCC Expert Meeting Report, (2007a). Towards New Scenarios for Analysis of Emissions, Climate Change, Impacts, And Response Strategies, IPCC 2007.

IPCC - AR4 (2005). Available (https://esg.llnl.gov:8443/home/publicHomePage.do).

IPCC (2007). IPCC 4th Assessment Report - Climate Change 2007. Working Group II on "Impacts, Adaptation and Vulnerability". http://www.ipcc-wg2.org.

IPCC (2013). Climate Change 2013. The Physical Science Basis. Headline Statements from the Summary for Policymakers, 2pp.

IPCC (2014a). Climate Change 2014. Impacts, Adaptation, and Vulnerability. Chapter 12, Human Security (p2).

IPCC (2014b). Climate Change 2014. Impacts, Adaptation, and Vulnerability. Technical Summary (pp7, 27).

IPCC AR4 (2005). Available (https://esg.llnl.gov:8443/home/publicHomePage.do).

IPCC, Special Report of the IPCC (2012). Managing the risks of extreme events and disasters to advance climate Advance Climate Change Adaptation (SREX). Pp 115-117.

IPCC. (2013). Climate Change 2013: The Physical Science Basis. In T. F. Stocker, D. Qin, G. - K. Plattner, M. Tignor, S. K. Allen, J. Boschung, A. Nauels, Y. Xia, V. Bex & P. M. Midgley (Eds.), Contribution of Working Group I to the Fifth Assessment Report of the Intergovernmental Panel on Climate Change (p. 1535). Cambridge, United Kingdom and New York, NY, USA: Cambridge University Press. doi:10.1017/CBO9781107415324.

Jain, M. K. and Das, D. (2010). Estimation of sediment yield and areas of soil erosion and deposition for watershed prioritization using GIS and remote sensing. Water Resource Management, 24: 2091–2112.

Jansen, L.J.M. and Di Gregorio, A. (1998). The problem of current land cover classifications: Development of a new approach. Proceedings of the Eurostat Seminar on Land Cover and Land Use information Systems for European Union Policy Needs, 21-23 January, Luxembourg, Luxembourg.

Jones, C. G., Ullerstig, A., Willén, U. and Hansson, U. (2004). The Rossby Centre regional atmospheric climate model (RCA). Part I: model climatology and performance characteristics for present climate over Europe, AMBIO, 33, 199–210.

Jones, C., Giorgi, F. and Asrar, G. (2011). The Coordinated Regional Downscaling Experiment: CORDEX, An international downscaling link to CMIP5: CLIVAR Exchanges, No. 56, Vol 16, No.2 pages 34-40. Available from www.clivar.org/sites/default/files/imported/publications/exchanges/Exchanges_56.pdf (also see http://www.cordex.org/).

Julien, P.Y. (2010). Erosion and Sedimentation. 2nd ed. Cambridge University Press, Cambridge.

Jung, G. (2006). Regional Climate Change and the Impact on Hydrology in the Volta Basin of West Africa. PhD. Thesis Institut fur Meteorologie und Klimaforschung, Germany.

Kankam-Yeboah, K., Obuobie, E., Amisigo, B., and Opoku-Ankomah, Y. (2013). Impact of climate change on streamflow in selected river basins in Ghana. Hydrological Sciences Journal, 58(4), 773–788. doi:10.1080/02626667.2013.782101.

Kasei, R. A. (2009). Modelling impacts of climate change on water resources in the Volta Basin, West Africa. PhD. Thesis Rheinischen Friedrich-Wilhelms-Universität Bonn. http://hss.ulb.uni-bonn.de/diss_online elektronisch publiziert.

Kendall, M.G. (1975). Rank Correlation Methods, 4th edition, Charles Griffin, London.

Kjellström, E., Bärring, L., Gollvik, S., Hansson, U., Jones, C., Samuelsson, P., Rummukainen, M., Ullerstig, A., Willén, U. and Wyser, K. (2005). A 140-year simulation of European climate with the new version of the Rossby Centre regional atmospheric climate model (RCA3). In: Reports Meteorology and Climatology.Volume 108, SMHI, SE-60176 Norrköping, Sweden, 54.

Klutse, N.A.B., Sylla, M.B., Diallo, I., Sarr, A., Dosio, A., Diedhiou, A., Kamga, A., Lamptey, B., Ali, A., Gbobaniyi, E.O., Owusu, K., Lennard, C., Hewitson, B., Nikulin, G., Panitz, H-J., Bucher, M. (2014). Daily characteristics of West African summer monsoon precipitation in CORDEX simulations. Theoretical and Applied Climatology DOI 10.1007/s00704-014-1352-3.

Knisel, W. G. (1980). CREAMS, a field-scale model for chemicals, runoff, and erosion from agricultural management systems. USDA Conservation Research Report No. 26. Washington, D.C.: USDA.

Krämer, P. (2002). The fuel wood crisis in Burkina Faso, solar cooker as an alternative. Solar cooker archive. Ouagadougou, Burkina Faso.

Kupiainen, M., Samuelsson, P., Jones, C., Jansson, C., Willen, U., Hansson, U., Ullerstig, A., Wang, S. and Doscher, R. (2011). Rossby Centre regional atmospheric model, RCA4. Rossby Centre Newsletter, June.

Lahmer, W., Pfutzner, B., Becker, A. (2001). Assessment of land use and climate change impacts on the mesoscale. Physics and Chemistry of the Earth Part B 26 (7–8), 565–575.

Lambin, F. E. and Geist, J. (2006). Land-use and land-cover Change, local processes and Global impacts.

Lane, L. J. (1982). Distributed model for small semi-arid watersheds. Journal of Hydraulic Engineering, ASCE, 108(HY10): 1114-1131.

Lane, L.J. (1983). Chapter 19: Transmission Losses. p.19-1–19-21. In Soil Conservation Service. National engineering handbook, section 4: hydrology. U.S. Government Printing Office, Washington, D.C.

Lenderink, G., van den Hurk, B.J.J.M., van Meijgaard, E., van Ulden, A.P. and Cuijpers, H. (2003). Simulation of present-day climate in RACMO2: first results and model developments. KNMI Technical Report 252, 24 p.

Leonard, R. A., W. G. Knisel, and D. A. Still. 1987. GLEAMS: Groundwater loading effects of agricultural management systems. Trans. ASAE 30(5): 1403-1418.

Li, Y., Chen, B.-M., Wang, Z.-G., and Peng, S.-L. (2011). Effects of temperature change on water discharge, and sediment and nutrient loading in the lower Pearl River basin based on SWAT modeling, Hydrological Science Journal., 56, 68–83.

Li, Z., Liu, W., Zhang, X., and Zheng, F. (2009). Impacts of land use change and climate variability on hydrology in an agricultural catchment on the Loess Plateau of China, J. Hydrol., 377, 35–42,2009.

Liang, X., Lettenmaier, D. P., Wood, E. F. and Burges, S. J. (1994). A Simple hydrologically Based Model of Land Surface Water and Energy Fluxes for GSMs, Journal of Geophys. Research., 99(D7), 14,415-14,428.

Liebe, J., Arntz, C., and Vlek P.L.G. (2010). GLOWA Volta Phase 111 completion report. Available at https://www.zef.de/fileadmin/template/Glowa/Downloads/GLOWA_Volta_Completion_Report_Phase_III.pdf (assessed on March 13, 2018).

Lin, Y.P., Hong, N.M., Wu, P.J., Wu, C.F. and Verburg, P.H. (2007). Impacts of land use change scenarios on hydrology and land use patterns in the Wu-Tu watershed in Northern Taiwan. Landscape and Urban Planning, 80 (1–2), 111–126.

Lumor, M. (2017). Estimation of streamflow and sediment loads in the White Volta Basin under future climate projections. PhD Thesis. Available at file:///C:/Users/Fati/Desktop/Thesis%20Defense/Aftre%20defense_Thesis_final%20revision/MawuliLUMOR.pdf (assessed on March 12, 2018).

Maddock, T. (1975). Table 3.2 in Sediment Engineering, V.A. Vanoni (ed.). ASCE, New York.

Mann, H.B. (1945). Non-parametric tests against trend, Econometrica 13:163-171.

Maraun, D, Wetterhall F, Ireson AM., Chandler RE, Kendon EJ, Widmann M, Brienen S, Rust, HW, Sauter T, Themeßl M, Venema VKC, Chun KP, Goodess CM, Jones RG, Onof C, Vrac M and Thiele-Eich I (2010). Precipitation downscaling under climate change: Recent developments to bridge the gap between dynamical models and the end user. Reviews of Geophysics, 48, RG3003.

Martin, N. (2006). Development of a water balance for the Atankwidi catchment, West Africa – A case study of groundwater recharge in a semi-arid climate. Ecology and Development Series, No. 41. Goettingen, Germany: Cuvillier Verlag. 168p.

McMahon, T.A., Brian, L.F., and Christopher, J.G. (2004). Stream Hydrology: An Introduction for Ecologists. John Wiley and Sons.

Meyer, W.B. and Turner, B.L. II (eds.) (1994). Changes in Land Use and Land Cover: A Global Perspective, 537pp. Cambridge: Cambridge University Press.

Monteith, J.L. (1965). Evaporation and the environment. p. 205-234. In The state and movement of water in living organisms, XIXth Symposium. Soc. For Exp. Biol., Swansea, Cambridge University Press.

Moriasi, D. N., Arnold, J. G., Van Liew, M. W., Bingner, R. L., Harmel, R.D. and Veith, T. L. (2007). Model evaluation guidelines for systematic quantification of accuracy in watershed simulations. Trans. ASABE 50(3): 885-900.

Moss, R. H., Babiker, M., Brinkman, S., Calvo, E., Carter, T., Edmonds, J., Elgizouli, I., Emori, S., Erda, L., Hibbard, K., Jones, R., Kainuma, M., Kelleher, J., Lamarque, J. F., Matthews, M. M. B., Meehl, J., Meyer, L., Mitchell, J., Nakicenovic, N., O'Neill, B., Pichs, R., Riahi, K., Rose, S., Runci, P., Stou_er, R., van Vuuren, D., Weyant, J., Wilbanks, T., van Ypersele, J. P. and Zurek, M. (2008). Towards New Scenarios for Analysis of Emissions, Climate Change, Impacts, and Response Strategies. IPCC

Technical Summary, Geneva, Switzerland. Technical Summary, Intergovernmental Panel on Climate Change, WMO, Geneva, Switzerland.

Moss, R. H., Edmonds, J. A., Hibbard, K. A., Manning, M. R., Rose, S. K., van Vuuren, D. P., Carter, T. R., Emori, S., Kainuma, M., Kram, T., Meehl, G. A., Mitchell, J. F. B., Nakicenovic, N., Riahi, K., Smith, S. J., Stou_er, R. J., Thomson, A. M., Weyant, J. P. and Wilbanks, T. J. (2010). The next generation of scenarios for climate change research and assessment. Nature, 463, 747-756, doi:10.1038/nature08823.

Mouhamed, L., Traore, S.B., Alhassane, A. and Sarr, B. (2013). Evolution of some observed climate extremes in the West African Sahel. Weather and Climate Extremes, 1, 19–25.

Mul, M., Obuobie, E., Appoh, R., Kankam-Yeboah, K., Bekoe-Obeng, E., Amisigo, B., Logah, F.Y., Ghansah, B. and McCartney, M. (2015). Water resources assessment of the Volta River Basin. Colombo, Sri Lanka: International Water Management Institute (IWMI). 78p. (IWMI Working Paper 166). doi: 10.5337/2015.220.

Mutchler, C. K., Murphree, C.E. and McGregor, K. C. (1988). Laboratory and field plots for soil erosion studies. In Soil erosion research methods, ed. R. Lal, 9-36. Soil and Water Conservation Society, Ia.

Nagle, G. (2000). Advanced Geography. Oxford University Press, Oxford, UK.

Narsimlu, B., Gosain, A.K., Chahar, B.R, Singh, S.K and Srivastava, P.K. (2015). SWAT model calibration and uncertainty analysis for streamflow prediction in the Kunwari River Baisn, India, using Sequential Uncertainty Fitting. Environmental Processes 2, 79-95. https://doi.org/10.1007/s40710-015-0064-8.

Neitsch, S. L., Arnold, J. G. Kiniry, J. R. and Williams, J. R. (2005). Soil and Water Assessment Tool Theoretical Documentation, Version 2005. Temple, Tex.: USDA-ARS Grassland, Soil and Water Research Laboratory. Available at: www.brc.tamus.edu/swat/doc.html. Accessed 10/04/2015.

New, M., Hewitson, B., Stephenson, D.B., Tsiga, A., Kruger, A., Manhique, A., Gomez, B., Coelho, C.A.S., Masisi, D.N., Kululanga, E., Mbambalala, E., Adesina, F., Saleh, H., Kanyanga, J., Adosi, J., Bulane, L., Fortunata, L., Mdoka, M.L. and Lajoie, R. (2006). Evidence of trends in daily climate extremes over southern and west Africa. Evidence of trends in daily climate extremes over southern and West Africa. Journal of Geophysical Research, 111, D14102.

Nikulin, G., Jones, C., Giorgi, F., Asrar, G., Büchner,M., Cerezo-Mota, R., Christensen, O. B., Déqué,M., Fernandez, J., Hänsler, A., et al. (2012). Precipitation climatology in an ensemble of CORDEX-Africa regional climate simulations. Journal of Climate, 25(18):6057–6078. doi:10.1175/JCLI-D-11-00375.1.

Obuobie E, Asante-Sasu, C. (2013). River flow under changing climate in Onchocerciasis-endemic Pru and Black Volta River Basins, West Africa. CSIR-Water Research Institute Technical Report No.367.

Obuobie, E. (2008). Estimation of groundwater recharge in the context of future climate change in the White Volta River Basin. Doctoral thesis, Rheinische Friedrich Wilhelms Universität, Bonn/ Germany.

Obuobie, E. and Barry, B. (2012). Burkina Faso. In: Chapter 2 of Groundwater availability and use in Sub-Saharan Africa:A review of 15 countries, eds., Pavelic, P.; Giordano, M.;

Keraita, B.; Rao, T.; Ramesh, V. Colombo, Sri Lanka: International Water Management Institute (IWMI). Pp. 7-23p.

Obuobie, E., Barry, B. and Agyekum, W. (2016). Groundwater Resources of the Volta Basin. In: Timothy O. Williams, Marloes L. Mul , Charles A. Biney and Vladimir Smakhtin (eds). The Volta River Basin: Water for Food, Economic Growth and Environment, Routledge, September 2016.

Obuobie, E., Diekkrueger, B. and Reichert, B. (2010). Use of chloride mass balance method for estimating the groundwater recharge in northeastern Ghana, International Journal of River Basin Management, 8:3-4, 245-253, DOI:10.1080/15715124.2010.505895.

Obuobie, E., Kankam-Yeboah, K., Amisigo, B., Opoku-Ankomah, Y., Ofori, D. (2012). Assessment of vulnerability of river basins in Ghana to water stress conditions under climate change. Journal of Water and Climate Change (03.4), pp 276-286, doi: 10.2166/wcc.2012.030.

OCHA, (2007). "Special update on floods in West Africa". Available from http://reliefweb.int/report/ghana/special-update-floods-west-africa-04-oct-2007 [Accessed 4th October, 2007].

Odada, E.O. (2006). Freshwater resources of Africa: major issues and priorities. Global Water News, No. 3. Available at http://www.gwsp.org/downloads/GWSP_NL3_Internet.pdf.

Oguntunde, P. G. (2004) Evapotranspiration and complimentarity relations in the water balance of the Volta Basin: Field measurements and GIS-based regional estimates;. Ecology and Development Series No. 22 Cuvillier Verlag Göttingen, http://www.zef.de/fileadmin/webfiles/downloads/zefc_ecology_development/ecol_dev_22_text.pdf.

Opoku-Ankomah, Y. (2000). Impacts of Potential Climate Change on River Discharge in Climate Change Vulnerability and Adaptation Assessment on Water Resources of Ghana.Water Research Institute (CSIR), Accra. Ghana.

Orlowsky, B., and Seneviratne, S. (2012). Global changes in extreme events: Regional and seasonal dimension. Climatic Change, 110, 669–696.

OTT Hydromet (2011). 'Operating instructions. Mobile River discharge measurement system OTT Qliner2'. Technical manual.

Ouedraogo, B. (2006). Household energy preferences for cooking in urban Ouagadougou, Burkina Faso. Energy Policy 34(18), 3787-3795.

Ouedraogo, I., Tigabu1, M., Savadogo, P., Compaore, P.C., Ode'N, H. and Ouadba, J.M. (2010). Land Cover Change and its Relation with Population Dynamics in Burkina Faso, West Africa. Land Degrad.Dev., 21 (5), 453–462.

Owusu, K., Klutse, N.A.B. (2013). Simulation of the rainfall regime over Ghana from CORDEX. International Journal of Geosciences, 4,785-791.

Oyebande, L. and Odunuga, S. (2010). Climate Change impact on water resources at the transboundary level in West Africa: The Cases of the Senegal, Niger and Volta Basins. The Open Hydrology Journal, 4,163-172.

Paeth, H., Hall, N.M.J., Gaertner, M.A., Alonso, M.D., Moumouni, S., Polcher, J., Ruti, P.M., Fink, A.H., Gosset, M., Lebel, T., Gaye, A.T., Rowell, D.P., Moufouma-Okia, W., Jacob, D., Rockel, B., Giorgi, F., Rummukainen, M. (2011). Progress in regional downscaling of West African precipitation. Atmospheric Science Letters doi:asl.306., 12, 75-82.

Panitz, H.J., Dosio, A., Büchner, M., Lüthi, D. and Keuler, K. (2014). COSMO-CLM (CCLM) climate simulations over CORDEXAfrica domain: analysis of the ERA-Interim driven simulations at 0.44 and 0.22 resolution. Climate Dynamics. doi:10.1007/ s00382-013-1834-5.

Parry, M.L. et al. (2007). Climate change 2007: Impacts, adaptation and vulnerability. Contribution of Working Group II to the Fourth Assessment Report of the Intergovernmental Panel on Climate Change (IPCC). Cambridge, Cambridge University Press.

Parsons, A.J. and Stromberg, S.G.L. (1998). Experimental analysis of size and distance of travel of unconstrained particles in interrill flow. Water Resources Research, 34, pp. 2377–2381.

Patra, K.C. (2001). Hydrology and water resources engineering. Pangbourne, UK: Alpha Science International.

Phan, D. B.,Wu, C. C., and Hsieh, S. C.(2011). Impact of climate change on stream discharge and sediment yield in Northern Viet Nam, Water Research., 38, 827–836.

Phomcha P., Wirojanagud P., Vangpaisal T. and Thaveevouthti T. (2011). Predicting sediment discharge in an agricultural watershed: a case study of the Lam Sonthi watershed, Thailand. Science Asia, 37, 43–50.

Priestley, C.H.B and Taylor, R.J. (1972). On the assessment of surface heat flux and evaporation using large scale parameters. Mon. Weather Rev. 100, p. 82 – 92.

Prowse, T.D. et al. (2006). Climate change, flow regulation and land-use effects on the hydrology of the Peace-Athabasca-Slave system; findings from the northern rivers ecosystem initiative. Environmental Monitoring and Assessment 113,167–197.

Qiu L.J., Zheng F.L. and Yin R.S. (2012). SWAT-based runoff and sediment simulation in a small watershed, the loessial hilly-gullied region of China: capabilities and challenges. International Journal of Sediment Research, 27, 226–234.

Räisänen, J., Hansson, U., Ullerstig, A., Döscher, R., Graham, L.P., Jones, C., Meier, M., Samuelsson, P. and Willén, U. (2003). GCM driven simulations of recent and future climate with the Rossby Centre coupled atmosphere – Baltic Sea regional climate model RCAO. Reports Meteorology and Climatology 101, SMHI, SE 60176 Norrköping, Sweden, 61 pp.

Räisänen, J., Hansson, U., Ullerstig, A., Döscher, R., Graham, L.P., Jones, C., Meier, H.E.M., Samuelsson, P. and Willén, U. (2004). European climate in the late 21st century: regional simulations with two driving global models and two forcing scenarios. Climate Dynamics, 22, 13-31.

Rantz, S.E., et al. (1982). Measurement and computation of streamflow: Volume 1. Measurement of stage and discharge and Volume 2. Computation of discharge: U.S. Geological Survey Water-Supply Paper 2175, 631 p.

Refsgaard, J. C. (1997). Parameterisation, calibration, andvalidation of distributed hydrological models. J. Hydrol., 198(1),69-97. http://dx.doi.org/10.1016/S0022-1694(96)03329-X.

Riahi, K., Rao, S., Krey, V., Cho, C., Chirkov, V., Fischer, G., Kindermann, G., kicenovic, N. and Rafaj, P. (2011). RCP8.5—A scenario of comparatively high greenhouse gas emissions, Climate Change, 109, 33–57. doi:10.1007/s10584-011-0149-y.

Rodgers, C, van de Giesen N, Laube W, Vlek P.L.G, Youkhana, E. (2007). The GLOWA Volta project: A framework for water resources decision-making and scientific capacity building in a transnational West African Basin. In: E. Craswell, M. Bonell, D. Bossio, S. Demuth, and N. van de Giesen (Editors), Intergrated assessment of water resources and global change (A north-south analysis). Springer, p.295-313.

Rogelji, J., Meinshausen, M., and Knutti, R., (2012). Global Warming Under Old and New Scenarios Using IPCC Climate Sensitivity Range Estimates. Nature Climate Change, 2:248. http://dx.doi.org/10.1038/nclimate1385.

Rosenzweig, C.E., Tubiello, F., Goldberg, R. and Bloomfield, J. (2002). Increased crop damage in the US from excess precipitation under climate change. Global Environmental Change, 12, 197-202.

Rowell, D. (2012). Sources of uncertainty in future changes in local precipitation. Climate Dynamics, 39, 1929–1950.

Rummukainen, M., Räisänen, J., Bringfelt, B., Ullerstig, A., Omstedt, A., Willén, U., Hansson, U. and Jones, C. (2001). A regional climate model for northern Europe: model description and results from the downscaling of two GCM control simulations. Climate Dynamics, 17, 339-359.

Rummukainen, M., Räisänen, J., Ullerstig, A., Bringfelt, B., Hansson, U., Graham, P. and Willén, U. (1998). RCA – Rossby Centre regional Atmospheric climate model: model description and results from the first multi-year simulation, Reports Meteorology and Climatology 83, SMHI, SE-601 76 Norrköping, Sweden, 76 pp.

Samuelsson, P., Jones, C.G., Willen, U., Ullerstig, A., Gollvik, S., Hansson, U., Jansson, C., Kjellstrom, E., Nikulin, G. and Wyser, K. (2011). The Rossby Centre Regional Climate model RCA3: model description and performance. Tellus Series A – Dynamic Meteorology and, 63, 1, 4-23, doi: 10.1111/j.1600-0870.2010.00478.x.

Santhi, C., Arnold, J.G., Williams, J.R., Dugas, W.A., Srinivasan, R. Hauck, L.M. (2001). Validation of the SWAT Model on a Large River Basin with Point and Nonpoint Sources, Journal of the American Water Resources Association, 37(5), pp 1169-1188.

Sarr, A.M., Seidou, O. and Tramblay, Y. (2015). Comparison of downscaling methods for mean and extreme precipitation in Senegal. Journal of Hydrology: Regional Studies (4): 369-385.

Sarr, B. (2011). Return of heavy downpours and floods in a context of changing climate. Climate change in the Sahel. A challenge for sustainable development. AGRHYMET Monthly Bulletin, 9-11. htpp://www.agrhymet.ne/PDF/Bulletin%20mensuel/specialChCang.pdf (assessed on 2 October 2015).

Schoul, J and Abbaspour, K. C. (2006). "Calibration and uncertainty issues of a hydrological model (SWAT) applied to West Africa," Advances in Geosciences,pp. 137-143.

Schulla, J. (1997). Hydrologische Modellierung von Flussgebieten zur Abschatzung der Folgen von Klimaanderungen., Zuricher Geographische Schriften, Zurich.

Sen, P. K. (1968). Estimates of the Regression Coefficient Based on Kendall's Tau. Journal of the American Statistical Association, 63(324), 1379-1389. DOI: 10.1080/01621459.1968.10480934.

Shrestha, B., Babel, M. S., Maskey, S., van Griensven, A., Uhlenbrook, S., Green, A., and Akkharath, I. (2013). Impact of climate change on sediment yield in the Mekong River

basin: a case study of the Nam Ou basin, Lao PDR, Hydrol. Earth Syst. Sci., 17, 1-20, doi:10.5194/hess-17-1-2013.

Singh, J., Knapp, H. V. and Demissie. M. (2004). Hydrologic modeling of the Iroquois River watershed using HSPF and SWAT. ISWS CR 2004-08. Champaign, Ill.: Illinois State Water Survey. Availableat: www.sws.uiuc.edu/pubdoc/CR/ISWSCR2004-08.pdf. Accessed 8 September 2015.

Sloan, P.G. and Moore, I.D. (1984). Modelling subsurface stormflow on steeply sloping forested watersheds. Water Resources Research. 20(12), p. 1815-1822.

Sloan, P.G., Morre, I.D., Coltharp, G.B. and Eigel, J.D. (1983). Modelling surface and subsurface stormflow on steeply-sloping forested watersheds. Water Resources Inst. Report 142. Univ. Kentucky, Lexington.

Soil Conservation Service (1972). Section 4: Hydrology. In: National Engineering Handbook. SCS.

Sood, A., Muthuwatta, L. and McCartney, M. (2013). A SWAT evaluation of the effect of climate change on the hydrology of the Volta River basin, Water International, 38:3, 297-311, DOI: 10.1080/02508060.2013.792404.

Stevens, B., Giorgetta, M., Esch, M., Mauritsen, T., Crueger, T., Rast, S., Salzmann, M., Schmidt, H., Bader, J., Block, K., Brokopf, R., Fast, I., Kinne, S., Kornblueh, L., Lohmann, U., Pincus, R., Reichler, T., and Roeckner, E. (2013). Atmospheric component of the MPI-M Earth System Model: ECHAM6. Journal of Advances in Modelling Earth Systems, 5, 146– 172.

Stonestrom, D. A., Scanlon, B. R., and Zhang, L. (2009). Introduction to special section on Impacts of Land Use Change on Water Resources, Water Resources Research, 45, W00A00, doi:10.1029/2009WR007937.

Strandberg, G., B¨arring, L., Hansson, U., Jansson, C., Jones, C., Kjellstr ¨om, K., Kolax, M., Kupiainen, M., Nikulin, G., Samuelsson, P., Ullerstig, A. and Wang, S. (2014). CORDEX scenarios for Europe from the Rossby Centre regional climate model RCA4. Reports Meteorology and Climatology 999, SMHI, SE-601 76 Norrk¨oping, Sweden.

SWAT: Model use, calibration, and validation. Trans.ASABE, 55(4), 1494-1508. http://dx.doi.org/10.13031/2013.42256.

Sylla, M.B., Nikiema, P.M., Gibba, P., Kebe, I., and Klutse, N.A.B. (2016). Climate Change over West Africa: Recent Trends and Future Projections Climate Change over West Africa: Recent Trends and Future Projections. doi:10.1007/978-3-319-31499-0.

Tanveer, A., Ghulam, N., Boota, M. W., Fiaz, H., Azam, M. I., Jun, J. H., and Faisal, M. (2016). Uncertainty analysis of runoff and sedimentation in a forested watershed using sequential uncertainty fitting method. Science in Cold and Arid Regions., 8, 297–310.

Taylor, K.E., Stouffer, R.J., Meehl, G.A. (2012) An overview of CMIP5 and the experiment design. Bulletin of the American Meteorological Society, 93(4):485–498, DOI 10.1175/BAMS-D-11-00094.1.

The CGIAR-CSI Consortium for Spatial Information Server. http://srtm.csi.cgiar.org/index.asp

The Soil and Water Assessment Tool (SWAT) model website. http://swat.tamu.edu/

Themeßl, M., Gobiet, A. and Leuprecht, A. (2011). Empirical-statistical downscaling and error correction of daily precipitation from regional climate models. *International Journal of Climatology*, 31, 1531–1544.

Tilrem, A.O. (1979). Sediment transport in streams sampling, analysis and computation. Manual on procedures in operational hydrology. Volume 5, 110p.

Tu, T. (2009). Combined impact of climate and land use changes on streamflow and water quality in eastern Massachusetts, USA, Journal of Hydrology., Vol. 379, pp.268-283.

Undèn, P., Rontu, L., Järvinen, H., Lynch, P., Calvo, J., Cats, G., Cuxart, J., Eerola, K., Fortelius, C., Garcia-Moya, J. A., Jones, C., Lenderlink, G., Mcdonald, A., Mcgrath, R., Navascues, B., Nielsen, N. W., Degaard, V., Rodriguez, E., Rummukainen, M., Sattler, K., Sass, B. H., Savijarvi, H., Schreur, B. W., Sigg, R. and The, H. (2002). HIRLAM-5, Scientific Documentation, Technical Report, 2002.

Van Griensven, A. and Meixner, T. (2006). Methods to quantify and identify the sources of uncertainty for river basin water quality models. Water Science and Technology, 53(1): 51-59.

van Meijgaard, E., van Ulft, L. H., van de Berg, W. J., Bosveld, F. C., van den Hurk, B., Lenderink, G. and Siebesma A. P. (2008). The KNMI regional atmospheric climate model RACMO version 2.1, Technical Report 302.

van Vuuren, D. P., et al. (2011b). RCP2.6: Exploring the possibility to keep global mean temperature increase below 2 °C, Climate Change., 109,95–116. Doi:10.1007/s10584-011-0152-3.

van Vuuren, D. P., et al. (2011c): The representative concentration pathways: An overview. Climatic Change, 109, 5-31.

van Vuuren, D.P., Edmonds, J., Kainuma, M., Riahi, K., Thomson, A., Hibbard, K., Hurtt, G.C., Kram, T., Krey, V., Lamarque, J.-F., Masue, T., Meinshausen, M., Nakicenovic, N., Smith, S. and Rose, S.K. (2011a). The Representative Concentration Pathways: An Overview. Climatic Change, 109:1-2:5. http://dx.doi.org/10.1007/s10584-011-0148-z.

VBA Geoportal (2015). 131.220.109.2/geonetwork. Accessed 4th August, 2015.

Vrugt, J. A., Gupta, H. V. Bouten, W. and Sorooshian, S. (2003). A shuffled Complex Evolution Metropolis Algorithm for Estimating Posterior Distribution of Watershed Model Parameters, in Calibration of Watershed Models, ed. Q. Duan, S. Sorooshian, H. V. Gupta, A. N. Rousseau, and R. Turcotte, AGU Washington DC, DOI: 10.1029/006WS07.

Walling, D. E. (1977). Assessing the Accuracy of Suspended Sediment Rating Curves for a Small Basin. Water Resources Research 13 (3): 531–38. doi:10.1029/WR013i003p00531.

Walling, D. E. (1994). Measuring sediment yield from river basins in Lal, R. ed., Soil Erosion Research Methods. Soil and Water Conservation Society, Ankeny, IA.

Walling, D. E. (2008) The changing sediment load of the Mekong River, Ambio, 37, 150–157.

Wang, C., Jiang, R., Mao, X., Sauvage, S., Sanchez-Perez, J.M., Woli, K. P., Kuramochi, K., Hayakawa, A. and Hatano, R. (2015). Estimating sediment and particulate organic nitrogen and particulate organic phosphorous yields from a volcanic watershed characterized by forest and agriculture using SWAT model. International Journal of Limnology. 51(1); 23-35 DOI: 10.1051/limn/2014031.

Wasson, R.J., L.J. Olive, Rosewell, C.J. (1996). Rates of erosion and sediment transport in Australia. D.E. Walling, R. Webb (Eds.), Erosion and Sediment Yield: Global and Regional Perspectives, pp. 139–148 (IAHS Publication No. 236).

Water Resource Commission (2016). Rain Water Harvesting Strategy, Final Report 2011. 45pp. www.wrc-gh.org/dmsdocument/25.

Williams, J. R. (1975). Sediment-Yield Prediction with Universal Equation Using Runoff Energy Factor.In Present and Prospective Technology for Predicting Sediment Yields and Sources, Agricultural Research Service, ARS-S-40, 244-252. Washington, DC: U.S. government Printing Office.

Williams, J.R. (1995). Chapter 25. The EPIC Model. In Computer Models of Watershed Hydrology. Water Resources Publications. Highlands Ranch, CO. p. 909-1000.

Wischmeier, W. H. and Smith, D. D. (1978). Predicting rainfall erosion losses - A guide to conservation planning. Agricultural Handbook 537. USDA. Washington (DC): 58pp.

Wischmeier, W.H. and Smith, D.D. (1965). Predicting rainfall-erosion losses from cropland east of the Rocky Mountains. Agriculture Handbook 282. USDA-ARS.

World Bank (2011). Burkina Faso: Disaster risk management country note. Washington, DC, USA: World Bank. Available at https://openknowledge.worldbank.org/handle/10986/2752 (assessed on March 12, 2018).

Yang, J., Reichert, P., Abbaspour, K.C., Xia, J. and Yang, H. (2008). Comparing uncertainty analysis techniques for a SWAT application to Chaohe Basin in China. Journal of Hydrology., 358: 1-23.

Yves Tramblay, Andre St-Hilaire and Taha B. M. J. Ouarda (2008). Frequency analysis of maximum annual suspended sediment concentrations in North America / Analyse fréquentielle des maximums annuels de concentration en sédiments en suspension en Amérique du Nord, Hydrological Sciences Journal, 53:1, 236-252, DOI: 10.1623/hysj.53.1.236.

Zhang, W., Wei, X., Jinhai, Z. Yuliang, Z. and Zhang, Y. (2012). Estimating Suspended Sediment Loads in the Pearl River Delta Region Using Sediment Rating Curves. Continental Shelf Research 38 (April): 35–46. doi:10.1016/j.csr.2012.02.017.

Zhang, X. and Yang, F. (2004). RClimdex (1.0) user manual. http://cccma.seos.uvic.ca/ETCCDMI/software.shtml. (Assessed on 4 January 2015).

Zhu, Y.-M., Lu, X. X., and Zhou, Y. (2008). Sediment flux sensitivity to climate change: a case study in the Longchuanjiang catchment of the upper Yangtze River, China, Global Planet. Change, 60, 429–442.

ANNEX 1

Table 1A: Weather generated input files for SWAT

STATION	BOLE	DEDOUGOU	BOBO-DIOULASSO
WLATITUDE	9.03	12.46	11.16
WLONGITUDE	-2.48	-3.48	-4.31
WELEV	-	-	-
RAIN_YRS	30	30	30
TMPMX1	35.21	33.35	32.60
TMPMX2	36.92	36.52	35.45
TMPMX3	36.83	38.99	37.18
TMPMX4	34.80	40.07	37.03
TMPMX5	33.11	38.65	35.00
TMPMX6	31.02	35.13	32.12
TMPMX7	29.56	32.47	30.13
TMPMX8	29.11	31.13	29.38
TMPMX9	30.17	32.80	30.61
TMPMX10	32.25	36.45	33.29
TMPMX11	34.13	36.85	34.48
TMPMX12	34.64	34.43	33.05
TMPMN1	17.73	17.47	18.83
TMPMN2	20.83	20.64	21.80
TMPMN3	23.28	24.34	24.49
TMPMN4	23.82	26.86	25.14
TMPMN5	23.07	26.59	24.04
TMPMN6	22.05	24.34	22.35
TMPMN7	21.47	22.87	21.54
TMPMN8	21.31	22.14	21.23
TMPMN9	21.20	22.10	21.19
TMPMN10	21.24	22.45	21.85
TMPMN11	19.18	20.19	20.93
TMPMN12	16.84	17.90	19.15
TMPSTDMX1	1.93	2.88	2.61
TMPSTDMX2	1.75	2.79	2.39
TMPSTDMX3	2.16	2.39	2.15
TMPSTDMX4	2.44	2.31	2.42
TMPSTDMX5	2.08	2.69	2.45
TMPSTDMX6	1.81	2.83	2.31
TMPSTDMX7	1.65	2.35	2.01

TMPSTDMX8	1.61	2.04	1.87
TMPSTDMX9	1.78	2.28	2.06
TMPSTDMX10	1.78	1.93	1.86
TMPSTDMX11	1.27	1.58	1.42
TMPSTDMX12	1.54	2.47	2.15
TMPSTDMN1	2.66	2.50	2.20
TMPSTDMN2	3.41	2.65	2.30
TMPSTDMN3	2.25	2.59	1.86
TMPSTDMN4	1.59	2.08	1.82
TMPSTDMN5	1.38	2.27	1.98
TMPSTDMN6	1.20	2.20	1.76
TMPSTDMN7	1.01	1.60	1.34
TMPSTDMN8	0.94	1.28	1.13
TMPSTDMN9	1.01	1.21	1.20
TMPSTDMN10	0.95	1.34	1.07
TMPSTDMN11	2.35	2.14	1.53
TMPSTDMN12	2.89	2.19	1.82
PCPMM1	2.46	0.05	0.22
PCPMM2	8.40	1.22	2.39
PCPMM3	49.53	6.32	15.08
PCPMM4	104.19	16.48	44.45
PCPMM5	131.18	68.60	99.11
PCPMM6	141.97	98.94	131.18
PCPMM7	143.73	172.30	195.08
PCPMM8	159.17	231.62	271.51
PCPMM9	207.30	134.25	175.35
PCPMM10	95.78	38.65	61.41
PCPMM11	18.07	1.89	7.49
PCPMM12	6.02	0.01	0.98
PCPSTD1	1.37	0.04	0.12
PCPSTD2	2.89	1.07	1.47
PCPSTD3	7.69	2.08	3.00
PCPSTD4	9.98	3.06	5.83
PCPSTD5	10.84	7.74	9.01
PCPSTD6	10.27	8.51	10.01
PCPSTD7	11.43	11.27	11.55
PCPSTD8	12.67	13.38	14.63
PCPSTD9	13.90	9.78	11.12
PCPSTD10	8.38	4.64	5.82
PCPSTD11	4.18	0.93	2.92

PCPSTD12	2.19	0.01	0.62
PCPSKW1	22.99	26.52	18.30
PCPSKW2	14.69	27.87	24.47
PCPSKW3	8.31	13.61	9.27
PCPSKW4	4.14	7.62	6.20
PCPSKW5	3.54	5.35	4.31
PCPSKW6	2.92	3.64	3.19
PCPSKW7	4.10	2.75	2.42
PCPSKW8	3.85	2.59	2.37
PCPSKW9	3.91	3.78	3.12
PCPSKW10	3.97	5.20	4.11
PCPSKW11	10.54	18.47	17.65
PCPSKW12	15.00	30.50	23.00
PR_W1_1	0.01	0.00	0.01
PR_W1_2	0.04	0.00	0.02
PR_W1_3	0.13	0.03	0.06
PR_W1_4	0.28	0.08	0.20
PR_W1_5	0.34	0.21	0.34
PR_W1_6	0.41	0.32	0.42
PR_W1_7	0.38	0.44	0.54
PR_W1_8	0.43	0.55	0.68
PR_W1_9	0.57	0.37	0.53
PR_W1_10	0.27	0.13	0.21
PR_W1_11	0.05	0.01	0.02
PR_W1_12	0.02	0.00	0.00
PR_W2_1	0.00	0.00	0.25
PR_W2_2	0.12	0.33	0.40
PR_W2_3	0.16	0.27	0.31
PR_W2_4	0.21	0.22	0.30
PR_W2_5	0.33	0.25	0.35
PR_W2_6	0.32	0.29	0.37
PR_W2_7	0.45	0.43	0.52
PR_W2_8	0.52	0.49	0.64
PR_W2_9	0.50	0.43	0.55
PR_W2_10	0.34	0.30	0.36
PR_W2_11	0.20	0.23	0.24
PR_W2_12	0.10	0.00	0.00
PCPD1	0.23	0.07	0.27
PCPD2	0.87	0.10	0.67
PCPD3	4.00	1.00	2.60

PCPD4	7.97	2.57	6.63
PCPD5	9.90	6.17	10.40
PCPD6	11.00	9.03	12.07
PCPD7	11.93	13.50	16.23
PCPD8	14.07	15.93	20.30
PCPD9	15.67	11.90	16.27
PCPD10	9.07	5.03	8.03
PCPD11	2.00	0.43	1.10
PCPD12	0.67	0.03	0.10
RAINHHMX1	12.4	0.37	0.83
RAINHHMX2	19.9	10.23	13.37
RAINHHMX3	36.8	12.03	16.5
RAINHHMX4	27.1	12.07	26.87
RAINHHMX5	30.9	29.87	24.83
RAINHHMX6	27.2	26.87	25.67
RAINHHMX7	43.4	26.03	23.7
RAINHHMX8	40.7	31.83	31.43
RAINHHMX9	46.4	37.73	34.67
RAINHHMX10	26.2	13.43	16.67
RAINHHMX11	24.7	6.3	22.1
RAINHHMX12	15.1	0.07	5.57
SOLARAV1	21.75193548	21.11031183	21.88035484
SOLARAV2	21.82035419	23.25414404	23.13768595
SOLARAV3	21.58137634	24.24336559	22.42603226
SOLARAV4	20.91045556	23.52022222	20.33536667
SOLARAV5	20.51666667	22.25516685	20.4888172
SOLARAV6	19.30751111	22.62063404	21.22778889
SOLARAV7	16.93456989	20.98801075	18.80260215
SOLARAV8	17.0021828	19.90676344	18.86547312
SOLARAV9	19.12341111	20.76876667	20.17678889
SOLARAV10	19.72076344	20.30930108	19.29926882
SOLARAV11	19.92984444	21.4456	20.98394444
SOLARAV12	20.96318478	20.50864425	20.85556522
DEWPT1	0.25916129	0.130096774	0.129978495
DEWPT2	0.366257379	0.113801653	0.16231405
DEWPT3	0.452483871	0.14027957	0.257741935
DEWPT4	0.527166667	0.220866667	0.371211111
DEWPT5	0.608741935	0.31467169	0.457096774
DEWPT6	0.675444444	0.37868743	0.516
DEWPT7	0.746075269	0.501354839	0.664010753

DEWPT8	0.792623656	0.622935484	0.74
DEWPT9	0.761444444	0.557188889	0.650033333
DEWPT10	0.642215054	0.381752688	0.476913978
DEWPT11	0.454777778	0.187088889	0.232544444
DEWPT12	0.254537634	0.140629067	0.143608696
WNDAV1	1.976010753	2.699204301	2.66455914
WNDAV2	2.100330579	2.612916175	2.398807556
WNDAV3	2.474645161	2.331677419	2.26983871
WNDAV4	2.8106	2.166355556	2.586944444
WNDAV5	2.764763441	2.531776103	2.855290323
WNDAV6	2.740822222	2.742825362	2.915588889
WNDAV7	2.584043011	2.655784946	2.678645161
WNDAV8	2.26244086	2.372537634	2.313354839
WNDAV9	2.012155556	2.19	2.181944444
WNDAV10	1.96183871	1.918397849	1.934150538
WNDAV11	1.7754	2.097022222	2.008322222
WNDAV12	1.821021739	2.539414317	2.559793478

ANNEX 2

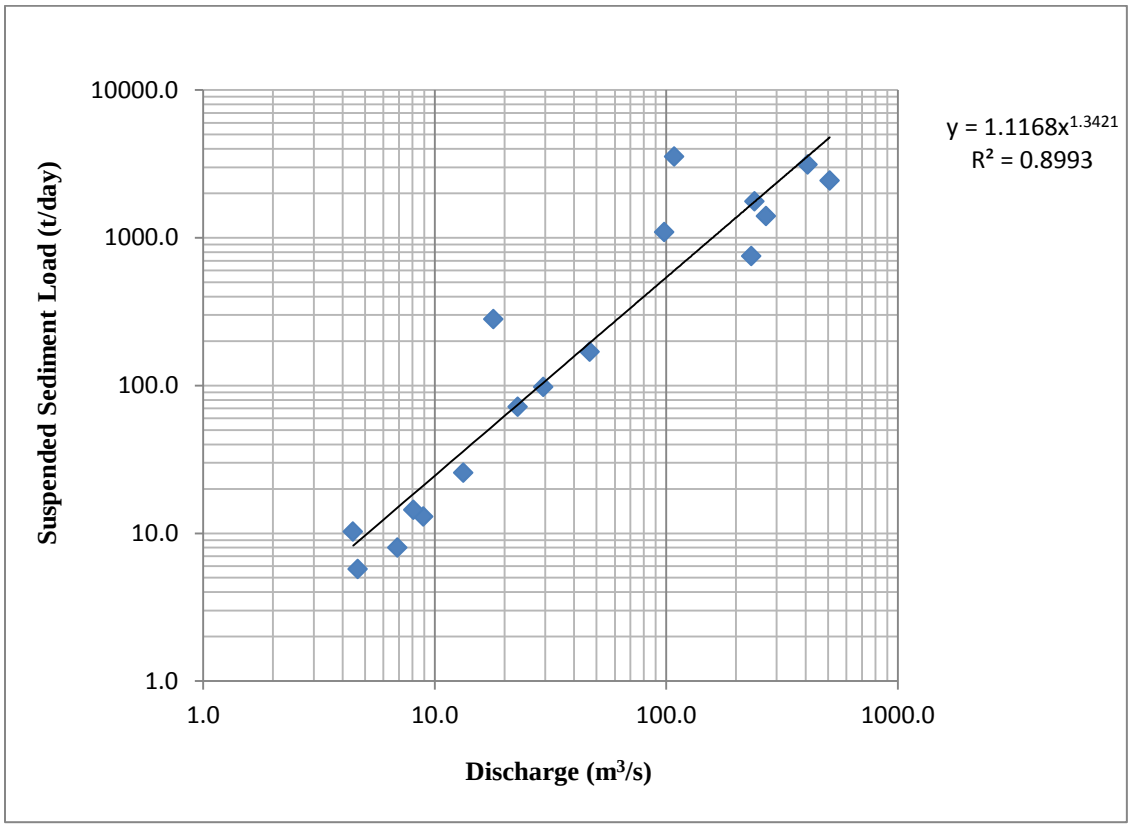

Figure A2: Sediment rating curve for the Black Volta Basin at Chache

ANNEX 3

Table A3: Maddock's classification for estimation of the bedload (Maddock, 1975)

Concentration of Suspended Load (ppm)	Type of Material forming the Stream Channel	Texture of Suspended Material	% of Measured Suspended Load that could be taken as Bed Load
Less than 1000	Sand	Similar to bed material	25 to 150
Less than 1000	Gravel, rock or consolidate clay	Small amount of sand	5 to 12
1000 to 7500	Sand	Similar to bed material	10 to 35
1000 to 7500	Gravel, rock or consolidate clay	25% sand or less	5 to 15
Over 7500	Sand	Similar to bed material	5 to 15
Over 7500	Gravel, rock or consolidate clay	25% sand or less	2 to 8

(Source: http://www.fao.org/docrep/t0848e/t0848e-10.htm)

ANNEX 4

Table A4: Estimated monthly total sediment load for Chache

Date	Mean monthly suspended load (tonnes)	25% of suspended load	Total sediment load (tonnes)
Jan-00	2111.0	527.8	2638.8
Feb-00	876.5	219.1	1095.6
Mar-00	323.1	80.8	403.9
Apr-00	207.9	52.0	259.9
May-00	211.4	52.9	264.3
Jun-00	3816.4	954.1	4770.5
Jul-00	10248.5	2562.1	12810.7
Aug-00	59532.5	14883.1	74415.7
Sep-00	124933.7	31233.4	156167.1
Oct-00	81428.7	20357.2	101785.8
Nov-00	8424.0	2106.0	10530.0
Dec-00	1985.7	496.4	2482.1
Jan-01	405.6	101.4	507.1
Feb-01	75.4	18.8	94.2
Mar-01	47.4	11.8	59.2
Apr-01	98.8	24.7	123.5
May-01	1534.1	383.5	1917.6
Jun-01	6872.2	1718.0	8590.2
Jul-01	13996.9	3499.2	17496.1
Aug-01	32400.7	8100.2	40500.9
Sep-01	99393.9	24848.5	124242.4
Oct-01	26602.3	6650.6	33252.9
Nov-01	1786.1	446.5	2232.6
Dec-01	252.2	63.1	315.3
Jan-02	-99.9	-99.9	-99.9
Feb-02	12.5	3.1	15.6
Mar-02	41.6	10.4	52.0
Apr-02	152.6	38.2	190.8
May-02	1460.6	365.1	1825.7
Jun-02	2569.4	642.4	3211.8
Jul-02	9129.3	2282.3	11411.7
Aug-02	54971.7	13742.9	68714.6
Sep-02	69159.9	17290.0	86449.8
Oct-02	22304.1	5576.0	27880.1

Nov-02	842.9	210.7	1053.7
Dec-02	148.1	37.0	185.2
Jan-03	70.4	17.6	88.1
Feb-03	53.1	13.3	66.4
Mar-03	51.7	12.9	64.6
Apr-03	140.7	35.2	175.8
May-03	1134.7	283.7	1418.4
Jun-03	9670.5	2417.6	12088.1
Jul-03	31521.7	7880.4	39402.2
Aug-03	-99.9	-99.9	-99.9
Sep-03	-99.9	-99.9	-99.9
Oct-03	-99.9	-99.9	-99.9
Nov-03	7396.9	1849.2	9246.2
Dec-03	2499.5	624.9	3124.4
Jan-04	929.7	232.4	1162.2
Feb-04	237.5	59.4	296.9
Mar-04	213.4	53.3	266.7
Apr-04	571.2	142.8	714.1
May-04	1938.0	484.5	2422.5
Jun-04	1978.6	494.6	2473.2
Jul-04	12596.8	3149.2	15746.0
Aug-04	103547.3	25886.8	129434.2
Sep-04	132493.5	33123.4	165616.8
Oct-04	10344.2	2586.1	12930.3
Nov-04	2101.9	525.5	2627.3
Dec-04	395.3	98.8	494.1
Jan-05	206.3	51.6	257.9
Feb-05	114.2	28.6	142.8
Mar-05	62.7	15.7	78.3
Apr-05	186.5	46.6	233.1
May-05	-99.9	-99.9	-99.9
Jun-05	2451.2	612.8	3064.0
Jul-05	8920.5	2230.1	11150.6
Aug-05	13992.1	3498.0	17490.1
Sep-05	76261.8	19065.5	95327.3
Oct-05	31439.6	7859.9	39299.5
Nov-05	2044.4	511.1	2555.5
Dec-05	166.0	41.5	207.5
Jan-06	72.4	18.1	90.5

Feb-06	48.9	12.2	61.1
Mar-06	57.3	14.3	71.6
Apr-06	41.2	10.3	51.5
May-06	495.2	123.8	619.0
Jun-06	9340.6	2335.2	11675.8
Jul-06	7810.6	1952.6	9763.2
Aug-06	15997.8	3999.5	19997.3
Sep-06	225778.5	56444.6	282223.1
Oct-06	161361.3	40340.3	201701.6
Nov-06	7807.3	1951.8	9759.1
Dec-06	1163.3	290.8	1454.1
Jan-07	709.7	177.4	887.2
Feb-07	329.8	82.5	412.3
Mar-07	295.2	73.8	369.1
Apr-07	1799.4	449.8	2249.2
May-07	3628.3	907.1	4535.3
Jun-07	566.4	141.6	708.0
Jul-07	9081.0	2270.2	11351.2
Aug-07	79846.2	19961.5	99807.7
Sep-07	341221.4	85305.3	426526.7
Oct-07	37136.1	9284.0	46420.2
Nov-07	3974.4	993.6	4967.9
Dec-07	1457.4	364.4	1821.8

ANNEX 5

Table A5: List of ETCCDMI core Climate Indices

Indicator ID	Indicator Name	Definition	Units
FD0	Frost days	Annual count when TN(daily minimum)<0ºC	Days
SU25	Summer days	Annual count when TX(daily maximum)>25ºC	Days
ID0	Ice days	Annual count when TX(daily maximum)<0ºC	Days
TR20	Tropical nights	Annual count when TN(daily minimum)>20ºC	Days
GSL	Growing season Length	Annual (1st Jan to 31st Dec in NH, 1st July to 30th June in SH) count between first span of at least 6 days with TG>5ºC and first span after July 1 (January 1 in SH) of 6 days with TG<5ºC	Days
TXx	Max Tmax	Monthly maximum value of daily maximum temp	ºC
TNx	Max Tmin	Monthly maximum value of daily minimum temp	ºC
TXn	Min Tmax	Monthly minimum value of daily maximum temp	ºC
TNn	Min Tmin	Monthly minimum value of daily minimum temp	ºC
TN10p	Cool nights	Percentage of days when TN<10th percentile	Days
TX10p	Cool days	Percentage of days when TX<10th percentile	Days
TN90p	Warm nights	Percentage of days when TN>90th percentile	Days
TX90p	Warm days	Percentage of days when TX>90th percentile	Days
WSDI	Warm spell duration indicator	Annual count of days with at least 6 consecutive days when TX>90th percentile	Days
CSDI	Cold spell duration indicator	Annual count of days with at least 6 consecutive days when TN<10th percentile	Days
DTR	Diurnal temperature range	Monthly mean difference between TX and TN	ºC
RX1day	Max 1-day rainfall amount	Monthly maximum 1-day rainfall	Mm
Rx5day	Max 5-day rainfall amount	Monthly maximum consecutive 5-day rainfall	Mm
SDII	Simple daily intensity index	Annual total rainfall divided by the number of wet days (defined as PRCP>=1.0mm) in the year	Mm/day
R10	Number of heavy rainfall days	Annual count of days when PRCP>=10mm	Days
R20	Number of very heavy rainfall days	Annual count of days when PRCP>=20mm	Days
Rnn	Number of days above nn mm	Annual count of days when PRCP>=nn mm, nn is user defined threshold	Days
CDD	Consecutive dry days	Maximum number of consecutive days with RR<1mm	Days
CWD	Consecutive wet days	Maximum number of consecutive days with RR>=1mm	Days
R95p	Very wet days	Annual total PRCP when RR>95th percentile	Mm
R99p	Extremely wet days	Annual total PRCP when RR>99th percentile	mm
PRCPTOT	Annual total wet-day rainfall	Annual total PRCP in wet days (RR>=1mm)	mm

ANNEX 6

Table A6: Distribution of BVRB soil in the SWAT model

		Area [ha]	Area[acres]	
		13500318	33359960.88	
Watershed		Area [ha]	Area[acres]	%Wat.Area
SOILS:	Qc1-1598	217000.946	536220.1885	1.61
	Ql1-1a-1614	1087540.85	2687367.819	8.06
	Re35-1a-1684	131711.628	325466.0189	0.98
	I-Re-b-1294	248117.525	613110.8111	1.84
	Re24-1665	9265.1669	22894.6908	0.07
	Re34-1a-1680	369320.956	912610.548	2.74
	Re35-1a-1685	11819.0526	29205.4699	0.09
	Re36-1a-1687	115620.819	285704.8238	0.86
	Re33-1674	365365.156	902835.5675	2.71
	Vc8-1729	67540.672	166896.3776	0.5
	Re33-1a-1677	1143927.81	2826702.812	8.47
	Lg5-2a-1515	729801.882	1803376.94	5.41
	Lg1-1495	67491.0817	166773.8374	0.5
	Vc1-3a-954	169574.344	419026.6814	1.26
	Je1-1359	55674.012	137573.2675	0.41
	Vc9-1730	65610.7041	162127.3305	0.49
	Lf18-1434	162087.09	400525.3038	1.2
	Vp9-1960	29241.9174	72258.24	0.22
	Lg3-2a-786	450080.162	1112170.585	3.33
	Lg1-3a-1496	426913.301	1054924.113	3.16
	I-Lf-1255	33689.3193	83247.9924	0.25
	Re33-1a-1676	33711.7079	83303.3158	0.25
	Lf30-1a-1450	341530.784	843939.6436	2.53
	Lf37-1463	536260.01	1325125.297	3.97
	Lp4-1532	299777.365	740764.8575	2.22
	Lp7-1541	501403.865	1238994.02	3.71
	Lg12-1501	142863.997	353024.0797	1.06
	Bv6-1145	69194.6528	170983.4469	0.51
	Lp5-1a-1536	191432.844	473040.1291	1.42
	Lp6-1a-1540	493122.552	1218530.481	3.65
	Lp8-1542	543159.067	1342173.212	4.02
	Nd1-1544	144817.64	357851.6294	1.07
	Vc11-1718	39975.6052	98781.7193	0.3
	Be25-1083	670887.617	1657796.845	4.97

	I-Rd-79	24285.7662	60011.3425	0.18
	Lf31-a-1453	1570695.52	3881267.161	11.63
	Lg11-1500	2734.1508	6756.2232	0.02
	Lg8-1520	156160.112	385879.4459	1.16
	Lf30-132	85295.0389	210768.3059	0.63
	I-Lp-1274	18989.4628	46923.912	0.14
	Lf32-1a-1457	89666.9571	221571.5343	0.66
	Lp9-1543	194098.814	479627.8745	1.44
	Lf38-1464	16177.9967	39976.6388	0.12
	Lp10-1a-1527	11860.1009	29306.9024	0.09
	Lg28-1a-1513	735697.44	1817945.159	5.45
	Lp5-1534	42881.9623	105963.4729	0.32
	Nd3-1565	41056.102	101451.6807	0.3
	Lf26-a-1442	5745.6396	14197.7627	0.04
	Ap22-2a-1074	93970.6552	232206.1876	0.7
	Be42-2-3b-1093	3210.8951	7934.2823	0.02
	Lf12-b-1431	95813.9524	236761.0671	0.71
	Ao46-a-1058	146311.616	361543.3178	1.08
	Bf5-2-3ab-1102	57658.4234	142476.8472	0.43
	Af18-1a-1024	22944.9135	56698.0286	0.17
	Be7-1b-1096	1819.834	4496.9009	0.01
	Ao59-a-1063	117710.586	290868.7425	0.87

ANNEX 7

The Mann-Kendall trend test

The Mann-Kendall test statistic (S), is calculated according to:

$$S = \sum_{i=1}^{n-1} \sum_{j=i+1}^{n} sgn(xj - xi) \quad (1)$$

Where, $x_{1,}x_{2,}x_{3\ldots,}x_n$ represent n data points and x_j represents the data point at time j.

with

$$sgn\left(x_{j-}x_i\right) = \begin{pmatrix} +1\ if\ \left(x_j - x_k\right) > 0 \\ 0\ if\ \left(x_j - x_k\right) = \quad 0 \\ -1\ if\ \left(x_j - x_k\right) < 0 \end{pmatrix} \quad (2)$$

The test statistic (S) is assumed to be approximately normal, with E(S) = 0 for sample size n ≥ 8 and variance as follows:

$$Var\ (S) = \frac{[n(n-1)(2n+5) - \sum_t t(t-1)(2t+5)}{18} \quad (3)$$

Where t represents the number of ties up to sample i. The standardized MK test statistics (Zmk) is estimated as follows:

$$Z_{mk} = \begin{matrix} \frac{S-1}{\sqrt{V(S)}}\ if\ S > 0 \\ 0\ is\ S + \ 0 \\ \frac{S+1}{\sqrt{V(S)}}\ if\ S < 0 \end{matrix} \quad (4)$$

The standardized MK test statistics (Zmk) follows the standard normal distribution with a mean of zero and variance of one. A positive (negative) value of Zmk indicates an 'upward trend' (downward) trend.

ANNEX 8

The non-parametric Sen's slope estimator

In this test, the slope Qi estimates N pairs of data values which are computed using

$$Qi = \frac{xj - xk}{j - k} \quad (5)$$

where xj and xk are data values at time j and k respectively, and j>k. The Sen's estimator of the slope is the median of these N values of Qi. The N values of Qi are ranked from the smallest to the largest and the Sen's estimator is computed by:

$$Q_{med} = Q\left[\frac{(n+1)}{2}\right], if\ N\ is\ odd \quad (6)$$

or

$$Q_{med} = \frac{1}{2}\left(Q\frac{n}{2} + Q\left[\left(\frac{n+2}{2}\right)\right]\right), if\ N\ is\ even \quad (7)$$

Q_{med} is then tested with a two-sided test which is carried out at 100(1 – α)% confidence interval to obtain the true slope for the non-parametric test in the series. The positive slope Qi is obtained as an increasing trend and the negative slope Qi as a decreasing trend.

Candidate biography

Fati Aziz (Mrs) is a Ghanaian Environmental Scientist. She received her Master's degree in Environmental Science (2011) and her Bachelor's degree in Biological Science (2007) at the Kwame Nkrumah University of Science and Technology, Ghana. Mrs. Aziz is currently an International Climate Protection Fellow Alexander von Humboldt Foundation (AvH) and a guest scientist at the Leibniz Institute for Baltic Sea Research in Rostock, Germany. She is assessing the vulnerability of Ghana's coastal areas to climate change with funds from the AvH.

Abstract:

The Black Volta River Basin (BVRB) in West Africa plays a vital role in supporting the life in and around it. The availability and use of the water resource of the basin is however threatened by population growth, changes in land use/land cover (LULC) and climate change. This study investigated the impacts of climate change on river flow and sediment yield and assessed the sensitivity of LULC changes on flow in the Basin using the Soil and Water Assessment Tool (SWAT) model. Prior to the impact study, trends in historical (1981-2010) extreme events over the basin were analyzed using the RClimDex 1.0 software package. The results of the extreme event analysis showed a warming trend in temperature, and increasing trends in amounts and intensity of rainfall events over the Basin during the historical period. The study also showed that climate change will cause changes in flow and sediment yield in the basin. Sensitivity analysis of streamflow in the basin based on a 10-year land use/land cover change showed statistically insignificant changes.

Key words: Climate Change, Land use/land cover change, streamflow, sediment yield.

PhD	**FATI AZIZ**	**Assessing the impact of climate and land use/land cover change on streamflow and sediment yield in the Black Volta River Basin using the SWAT model.**	**GRP/CCWR/INE/WASCAL – UAC APR, 18**